AN ADVANCED CONTROL OF GRID CONNECTED WIND TURBINE GENERATORS FOR ENHANCEMENT OF LOW-VOLTAGE RIDE-THROUGH CAPABILITY

PhD Dissertation

AN ADVANCED CONTROL OF GRID CONNECTED WIND TURBINE GENERATORS FOR ENHANCEMENT OF LOW-VOLTAGE RIDE-THROUGH CAPABILITY

Aung Ko Thet

ELECTRICAL AND COMMUNICATION DEPARTMENT

GRADUATE SCHOOL OF ENGINEERING

TOHOKU UNIVERSITY

SENDAI, JAPAN

January 25, 2012

Acknowledgement

First of all, I would like to express my sincere gratitude to my supervisor, Professor Dr. Hiroumi Saitoh, Graduate School of Engineering, Tohoku University, for providing dedicated guidance, qualified supervising, invaluable suggestions and kind encouragement throughout this work. I have also learned valuable lessons from his visions of the future power systems. Moreover, I wish to thank Professor Dr. Osamu Ichinokura and Professor Dr. Akio Ishiguro for helpful advice and comments.

In addition, my special thanks go to my seniors Mr. Yuichi Tobita, Mr. Yuki Hori, Mr. Daiki Satoh, Mr. Masatoki Koduki and to all of the members of laboratory, including for sharing their opinion, knowledge, numerous fruitful discussions and making pleasant study environment. I also wish to thank for all who helped me improving my knowledge of my research in Electrical Power Systems Engineering.

I am heartily thankful to the Professor Dr. Hiroumi Saitoh's family for their kind moral and personal support, especially during the recovery period of the Great Eastern Japan Earthquake at Laboratory.

Finally, it is a pleasure to show my deepest gratitude to my parents, brothers and sisters for their love, continuous encouragement and dedicated support throughout my life; without which I would not have been able to continue my study.

Last, certainly but not least, the financial support of the Monbukagakusho Committee is gratefully acknowledged.

Contents

CHAPTER 1

INTRODUCTION

The worldwide concern about global warming and the possible energy shortage lead to increasing interest in electricity generation from renewable energy sources. Among various renewable energy sources, electricity generation from wind power has become the fastest-growing in many industrial nations and interconnections of large-scale wind farms are increasing every year. If the capacity of wind turbine generators (WTGs) interconnected to existing power systems increases significantly, the sudden disconnection of WTGs will cause abnormal change in system frequency.

Up to now, WTGs have been treated in a similar manner to that of the other types of distributed generators and thus have been required to trip following even minor disturbances. To improve the stability of the power systems with large-scale wind farms, it would be desired that the wind farms continue the power injection without their disconnection due to the event of a fault occurring in the transmission network. In this regard, one of the concerns in large number of WTGs interconnection to power systems is the issue of Low-Voltage Ride-Through (LVRT).

The main objective of this doctoral dissertation is to improve the LVRT of wind power generation; i.e. continuity of the wind turbine generators under faulted condition of electric power transmission network in order to mitigate the impact on the operation and stability of the power grids they feed. A new control method is proposed for LVRT capability improvement of the fixed-speed and variable-speed WTGs. The main concept of proposed control method is to adjust the generated output power according to the

voltage dip. The voltage dip detection in proposed method is done by under voltage relay and then releases part of wind power. The proposed method adjusts the pitch angle in the fixed-speed WTG and, adjusts the pitch angle and modulation of converter in variable-speed WTG. The effectiveness of the proposed method is confirmed by simulation studies in which the analysis of the LVRT capability of wind farm is carried out based on the fixed-speed and variable-speed WTGs. With the use of proposed control method, wind farm can contribute the LVRT capability for improvement in short-term stability of interconnected power systems.

1.1 BACKGROUND OF WIND POWER INTEGRATION IN POWER SYSTEMS

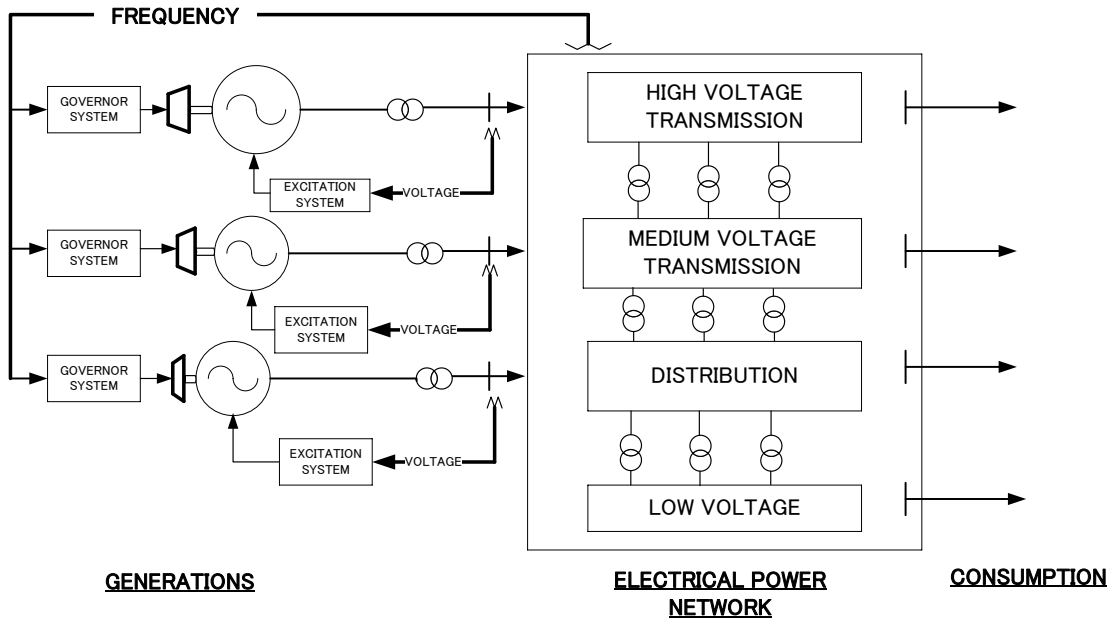

Figure 1.1: A schematic diagram of power systems

The major task in operation of power systems is to maintain the balance between the generations and consumption all the time. A schematic diagram of power systems is shown in Figure 1.1. Although the modern electric power systems in all over the world vary in size and structural components, they all have the same basic characteristics [1]:

A) They are comprised of three-phase ac systems operating essentially at almost constant voltage.

B) They transmit electrical energy over significant distances to consumers spread over a wide area. This requires a transmission network system comprising subsystems operating at different voltage levels.

C) For electricity generation, prime movers convert the primary sources of energy

(fossil, nuclear, and hydraulic) to mechanical energy and then convert to electrical energy.

Basically, the stability, the reliability and the secure operation of modern power systems depend on the network configuration, protection relay system, and the operation and control of conventional power plants. The conventional power plants produce electric energy with synchronous generators from the energy resources such as fossil fuels and uranium. By controlling the energy feed into the prime movers, those power plants can control the balancing between the total generation and system load so that the desired frequency and power interchange with neighboring systems can be maintained. When the power system is subject to a short-circuit fault, the excitation control of synchronous generators in conventional power plants contributes to the voltage re-establishment in the power grid, and their frequency control ensures the systems frequency during such events. Therefore, the operation and control of synchronous generators in conventional power plants contribute the reliable and secure operation of modern power systems [1].

According to the World Wind Energy Association (WWEA), 35,652 MW of new wind energy capacity were added summing up to a global installed capacity of 194,390 MW by the end of December 2010. The currently installed wind power capacity generates 430 TWh per year, equaling 2.3% of the global electricity demand. Wind power has already contributed 36% and more of the electricity consumption in some countries and regions. The northern Germany state of Schleswig-Holstein has over 2500 MW of installed wind capacity which is enough to meet 36% of the region's total electricity demand, while in Navarra, Spain, some 50% of consumption is met by wind power. Moreover, according to the expectations of WWEA, the global installed wind

power capacity can be reached at least 1,500,000 MW by the end of year 2020 [2].

At low penetration level of wind power, the impact of wind farms is not the system wide concerns. At high penetration level, if a large numbers of wind power generators replace the conventional power plants, the concerns about the power system stability increase; such as the deviations in power system frequency and voltage due to the unscheduled disconnection of a large numbers of WTGs following the disturbance. Therefore, the impacts of wind power in power systems have been studied and experiences in power systems operation with large amounts of wind power plants have been reported in many literatures.

According to the reference [3], several power systems and control areas coping with the large amounts of wind power have been operated. The experiences from Denmark, Spain, Portugal and Ireland; which have integrated the wind power equal to the 9-20% of yearly electricity demand, show that wind power production will only have to be regulated at some rare instances, and Transmission Systems Operators (TSOs) need on-line information of both the production and demand levels as well as respective forecasts in their control rooms. Spain and Portugal have launched centers for distributed energy that convey data to TSOs and even can react to control needs.

The experiences from Northern Germany show that the unscheduled disconnection of wind farms in the event of grid fault jeopardizes not only problem for system reserve but also the voltage collapse in the grid [4]. To avoid such unscheduled disconnection, it is desired to keep the wind turbine operation during and after the momentary voltage dip or fault. Therefore, TSOs of most industrial countries have been revised their grid codes (Requirements and Standards for Grid Connection) by adding “Low-Voltage Ride-Through” (LVRT) requirements in large-scaled wind farm interconnection to

power systems. Without the fulfillment of grid codes, the penetration level of wind power generation cannot be increased further, according to the experiences and practices of European countries [5].

In this regard, one of the concerns in the interconnection of large amounts of the wind power generator is the issue of “Low-Voltage Ride-Through” (LVRT) capability (in some literatures or grid codes, the terms of “Fault-Ride-Through” (FRT) is used). The characteristic of LVRT requirement varies according to the TSOs, due to the differences in voltage level at Point of Common Coupling (PCC), voltage and frequency controllability, and generation mix of the existing systems that they operate.

As shown in Figure 1.2, Germany, Denmark, Spain, Portugal, France, Sweden, Belgium, Poland, Ireland, Romania, Italy and UK have implemented Fault-Ride-Through (FRT)/Low-Voltage Ride-Through (LVRT) requirements for wind power plants in order to keep a certain level of security of supply [3, 4, 5, 6]. LVRT does not necessarily presuppose voltage control. In grid codes, time-voltage diagrams are used to define a dip profile area where disconnection is not allowed. Depending on specific requirements and experiences in wind power integration, the European countries have defined different LVRT characteristics up to now, as shown in figure 1.2. Most of LVRT requirements address only symmetrical three-phase grid fault. The voltages refer to the voltage level at the point of connection and the diagrams describe border lines, and tripping is not allowed above the lines. According to the common interpretation of the expected wind turbine behavior below the border line, a wind turbine can be tripped by the circuit breaker [5].

In Japan, according to the Tohoku Electric Power Company news on 2011-09-30 (http://www.tohoku-epco.co.jp/news/normal/1183529_1049.html), installed capacity of

wind power integration will be expected to reach about 2000 MW in year 2020. Therefore, in near future, similar grid codes as shown in figure 1.2 will be necessary in Japanese power systems to avoid the system frequency deviation (appendix B).

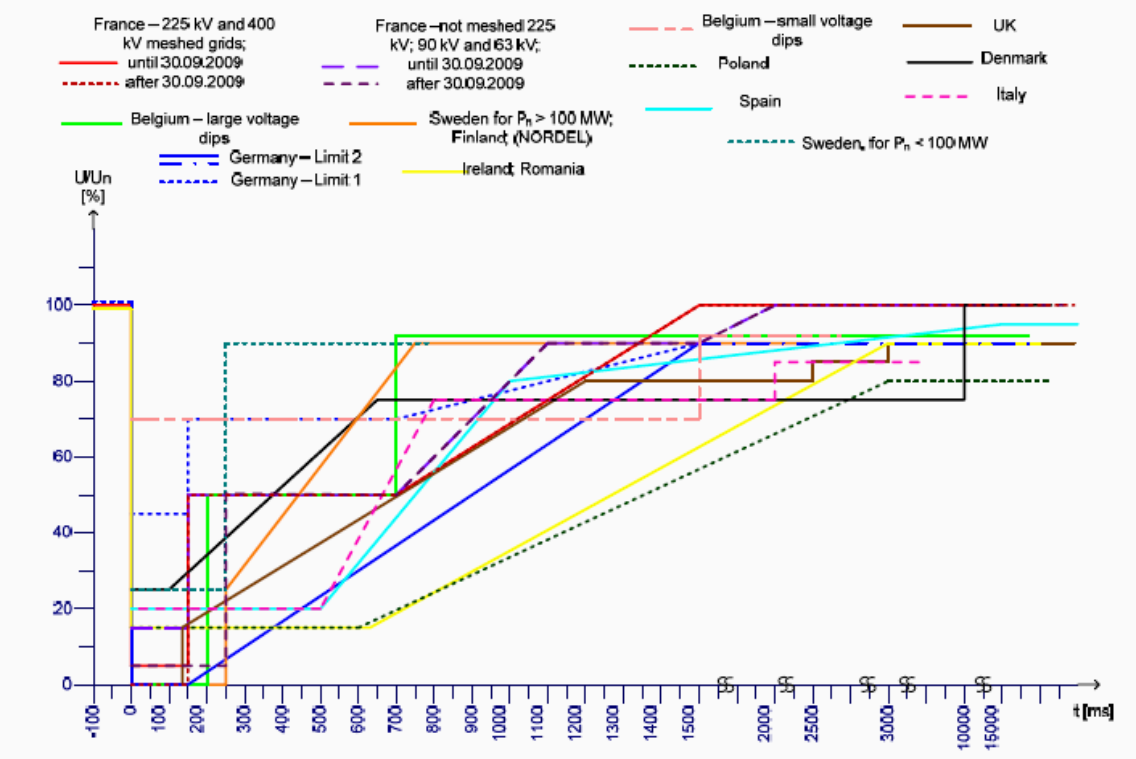

Figure 1.2: Comparison among the LVRT requirements for wind power plants [5, 6]

Nowadays, LVRT incompatible wind power plants are not accepted by most of TSOs to connect their transmission networks. In this regard, to meet the LVRT requirements is now the most challenging issue in wind power industry. In other words, to strengthen the stability, reliability and secure operation of the power systems with large amount of wind power integration, it is necessary to develop the methods and competences for LVRT capability improvement of wind power plants. This opens up the new research area in the scope of large-scaled integration of wind power plants in power system.

1.2 MOTIVATION

Historically, wind turbines have not been designed to react rapidly to a voltage dip. They have been traditionally treated in a similar manner to that of distributed generation. Wind turbine generators have been required to trip following even minor disturbances, as described in reference [7]. If wind power integration into power systems is high, the sudden disconnection of wind farms due to the voltage dip can affect significantly the power balance in the power systems. Hence, for the stability improvement of the wind farm connected power system, it would be desired that the wind farm continues the power injection without disconnecting. In this regard, one of the concerns in large amounts of wind power integration is the issue of low-voltage ride-through (LVRT); remaining connected and supplying power during and after the voltage dip, which contributes to mitigate the impact of wind farm connected power system stability.

In order to contribute the LVRT capability to wind farms, there are two approaches;

1) Improvement in power systems network side and
2) Improvement in wind power generation side.

The former one is to improve or reinforce the voltage stability of power systems by the application of extra devices such as Flexible AC Transmission Systems (FACTS) devices. The later one is to improve the controllers or re-design the wind generation systems in wind farms. The response time of FACTS devices is in the range of some ten milliseconds. In case of critical events within the power system, e.g. faults or instantaneous voltage drop, FACTS devices react immediately to these events due to their short response time. However, it is obvious that usage of FACTS devices increases the wind power integration and operation costs. This will cause the cost distribution to

non-wind-power related stakeholders; such as electric transmission network operator, consumers, etc. Therefore, WTGs are demanded more controllability to fulfill the LVRT requirements. On the other hand, to achieve the LVRT ability by improvement in wind power generation, there are many challenges such as fast response time to the voltage dip.

In this dissertation, we have paid a special attention to “Low-Voltage Ride-Through” capability of wind farm to mitigate the wind generation impact on electric power systems during and after the instantaneous low voltage condition. We propose the advanced control systems for LVRT capability improvement of fixed-speed wind turbine (FSWT) and the variable-speed wind turbine (VSWT) in wind farm, which is based on the voltage dip detection to contribute the LVRT capability of the wind power generator to remain connected to the grid during and after the fault.

1.3 OUTLINE OF DISSERTATION

The dissertation is organized as follows:

Chapter 2 describes the large wind farms impact on power system balancing, transient stability, and the requirement of Low-Voltage Ride-Through.

Chapter 3 addresses the concept of proposed generic pitch-angle control. The main concept of the proposal is to release the active power extracted from wind by adjusting the pitch angle when the momentary voltage dip is occurred. The proposed pitch angle control is based on the fast-response under voltage relay and the use of voltage as an input of PI controller. The effectiveness of the proposed pitch angle control is confirmed by comparing with base case.

Chapter 4 discusses the effectiveness of the proposal as well as power systems modeling in fault study and voltage stabilization of wind farm connected bus by Static Var Compensator Systems (SVS or alternately SVC). This chapter also deals with the short-term voltage stability phenomena of wind farm with respect to the 3 phase ground fault. The relation of active power injection and voltage stability of power systems is explained. Influence on the voltage recovery by the reactive power requirement of the induction generator is also described. The effectiveness of proposed pitch angle control is confirmed with different voltage controllability of network, grid stiffness, location of SVC, and fault locations. The range of proportional gain in a proposal with respect to the response time of under voltage relay is presented. Moreover, performance of the proposed pitch control is compared with feedback approach.

Chapter 5 discusses the improvement of LVRT capability of Permanent Magnet Synchronous Generator (PMSG) typed wind power generation systems. The analysis of

PMSG behavior under different grid stiffness shows that the proposed control method is effective for LVRT improvement.

Chapter 6 summarizes the dissertation main points and contributions. Moreover, future aspects of research are proposed.

Finally, this dissertation is ended with appendixes.

CHAPTER 2

STATE-OF-THE-ART IN MITIGATING THE IMPACTS OF WIND POWER INTEGRATION IN POWER SYSTEMS

2.1 INTRODUCTION

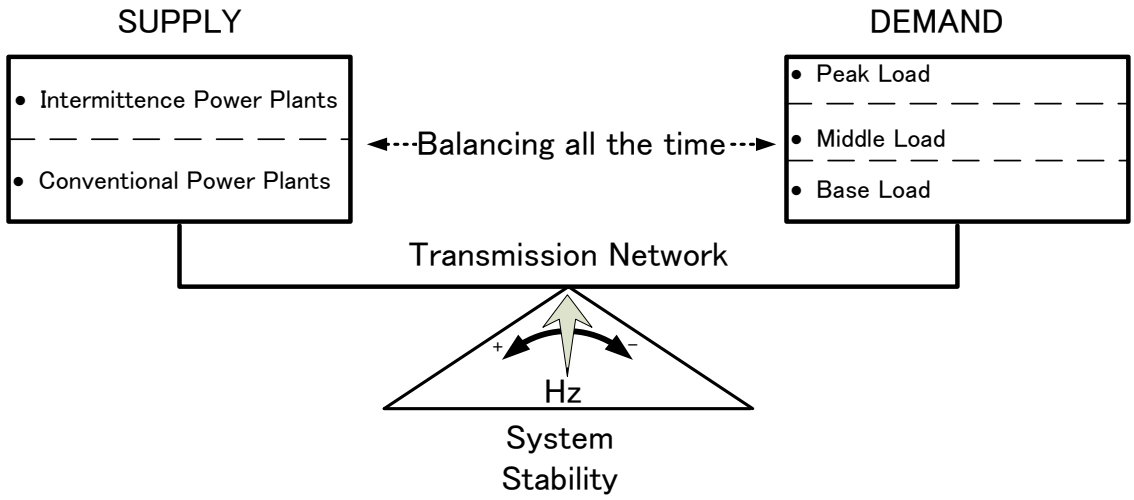

Figure 2.1: Conceptual diagram of power system operation

Wind power interconnection has influence on the power system operation. Figure 2.1 shows the conceptual diagram of power system operation. Electrical energy is transported by transmission network from power plants to load, and the system operator has to maintain the stability by balancing between supply and varying demand at all times. According to literature [2], a properly designed and operated power system should meet the following fundamental requirements:

1. The system must be able to meet the continually changing demand for active and reactive power. As the electricity cannot be stored conveniently in sufficient quantities, adequate "spinning reserve" of active and reactive power should be maintained and appropriately controlled all the time.
2. The system should supply energy at minimum cost and with minimum ecological impact.
3. The quality of power supply must meet certain minimum standards with regards to the constancy of frequency and voltage, and level of reliability.

From the standing point of those fundamental requirements, the integration of wind energy generation systems has impacts on the power quality and operation of power systems. The impacts of wind power integration on power systems depend to a large extent on the:

1) Level of wind power penetration
2) Grid size, and
3) Generation mix in the system.

Wind power integration at low to moderate levels is a matter of cost. For low integration levels of wind power, system operation will hardly be affected. If the amount of wind power generation increases, the power generation from conventional power plants must be reduced in order to balance power generation and consumption. Presently, conventional power plants are kept in operation to provide voltage and frequency control through the grid. The increase in large amount of wind power generation introduces a challenge with regard to controlling the voltage and balancing the power in the grid, thus affecting the system stability. Therefore, several studies are reported related to the wind impact on power system stability. The findings of these studies are

related to a superposition of different aspects of wind power, such as the fluctuating nature, distributed location of wind farms, generator technologies, generator control and prediction of network reinforcements and additional reserve requirements [8].

Generally, the impacts of wind power on the power system can be categorized into short-term effects and long-term effects. In literature [9], as shown in Figure 2.2, the studies of wind power impact on the power system are presented in terms of time scale and area relevant for impact studies.

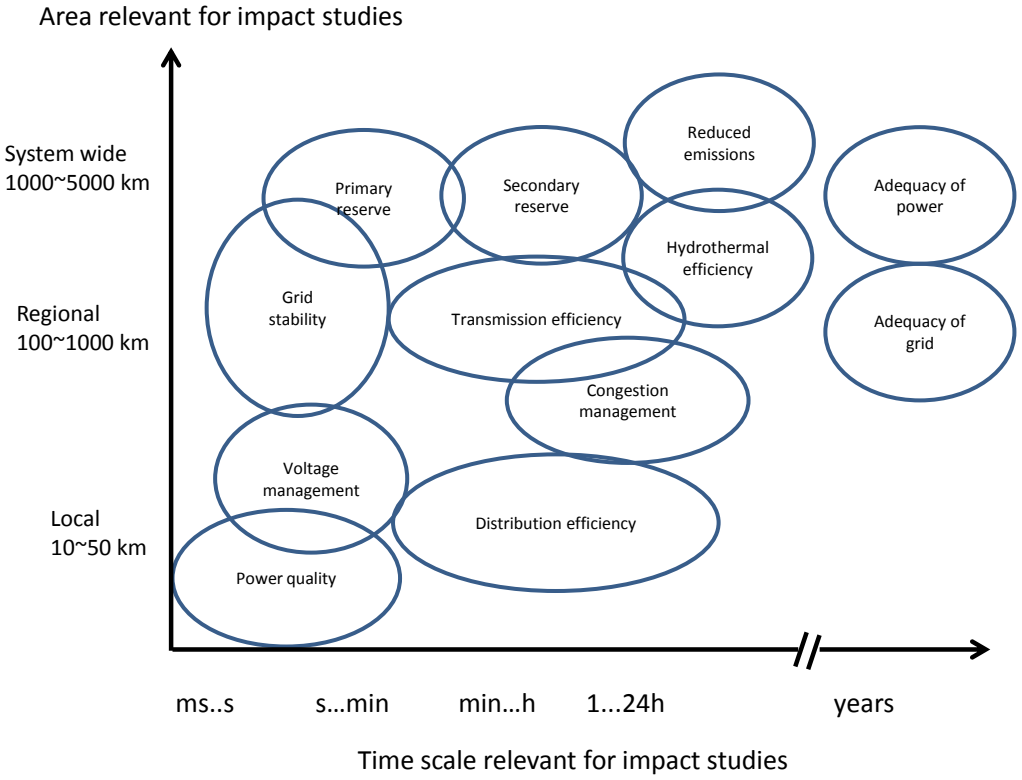

Figure 2.2 Impacts of wind power on power systems; divided in different time scales and width of area relevant for the studies [9]

For the time scale of milliseconds to a minute, power quality problem is the local area issue of grid connection, ranging from 10km to 50km. Voltage management problem

is concerned with local and regional area, ranging from 50km to 100km. Grid stability and primary reserve (frequency activated reserve) concerns are dealt with the system-wide perspective, ranging from 1000km to 5000km.

For the time scale of minutes to an hour, distribution efficiency and congestion management problems are concerned with local and regional area. Transmission efficiency is related to the regional and system-wide perspective. Regulating the secondary reserve (load following reserve) is the issue of system-wide concerns. For the time scale of day to years, adequacy of power and grid problems are concerned with the regional and system-wide area.

The scope of this thesis is mainly related to the wind power impacts **on short-term effects of power system**; based on the time scale of milliseconds to a minute.

2.2 IMPACT ON POWER BALANCING

The impacts of wind power on the power system operational security, reliability and efficiency are mainly related to the balancing capability of power systems.

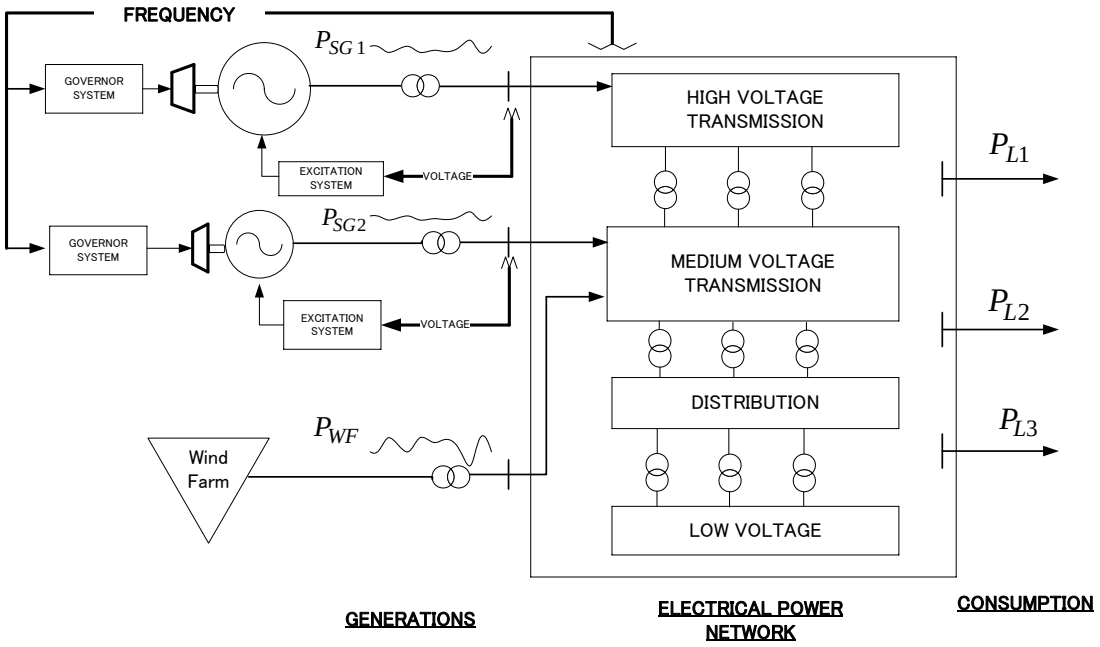

Figure 2.3: Conceptual diagram of power system operation with wind farm

Figure 2.3 shows the conceptual diagram of power system operation with wind farm. The frequency in a power system is controlled by adjusting the active power of the generators with respect to the load. Large wind farms can contribute to frequency control, if the wind turbines are capable of controlling their pitch angles from a power system operator. The impact of large wind power generation (exceeding 50% of the overall power) on frequency stability and voltage profile during a contingency situation was explored in literature [10]. Taking the existing control systems for wind generators

as the baseline case, it was found out that at the conceptual level, there are indeed a range of options which would place wind generating plants in a position to support system frequency in an emergency situation.

For both fixed-and variable-speed wind turbines, load-frequency control can be obtained by slightly increasing the nominal blade pitch angle, reloading the wind turbine by a corresponding amount. Fixed-speed wind turbine tends to be more sensitive to changes in pitch angle compared with variable-speed wind turbine due to their constant speed operation. Thus, the wind turbine output can be adjusted in sympathy with frequency variations, akin to governor control on a conventional generator [8].

To reduce the frequency fluctuation which cannot be absorbed by power systems, the causing wind power generators with the maximum turbulence degree for frequency fluctuation can be searched and frequency stability can be improved by appropriately disconnection of wind farm [11]. In the literature [12], frequency fluctuation by wind power can be improved by using the kinetic energy stored in the inertia of variable-speed wind turbine. Therefore, the wind power generation can contribute in primary and secondary frequency control.

Frequency deviations from nominal can happen not only under normal operation, but also in the wake of transient faults. To assist the generation after transient faults, power system operators require wind turbines to be able to operate in a wide range of frequencies, which can be problematic for fixed speed wind turbines [13]. In the literature [14], a PID pitch angle controller is presented for damping of grid frequency oscillations in most of the wind speeds of the wind turbine operating range. Therefore, the pitch angle control enables a wind turbine to perform power system stabilization similar to conventional power plants.

In the literature [15], a system of wind power forecasting has developed to predict the total wind power output in the power system of Tohoku Electric Power Co., Inc, Japan. The weather forecasting data from Japan Meteorological Agency is used to stimulate the wind speed at tower height of every wind farm in control area of Tohoku Electric Power Co., Inc. Then, this system forecasts and provides the estimated output of wind power in every 10 minutes, and the forecasting errors are improved by using statistical methods with several steps. This system has accuracy of about 8% (current day forecast) and 10% (next day forecast), which can contribute the power balancing control in system.

According to the literatures discussed in above, wind energy generation systems can contribute to mitigate the impacts on short-term power balancing. Moreover, by forecasting the wind power output in power system, the operation of generators can be scheduled to maintain the balance between the demand and supply.

2.3 IMPACT ON TRANSIENT STABILITY

One of the major concerns in power system operation is the stability which deals with the behavior of the power system to remain in a state of operating equilibrium under normal operating conditions and to regain an acceptable state of equilibrium after being subjected to disturbances such as,

1) continual gradually load changes and the system adjusts itself to the changing conditions,
2) sudden changes in load or generation, loss of a tie between two subsystems, or short circuits on transmission lines.

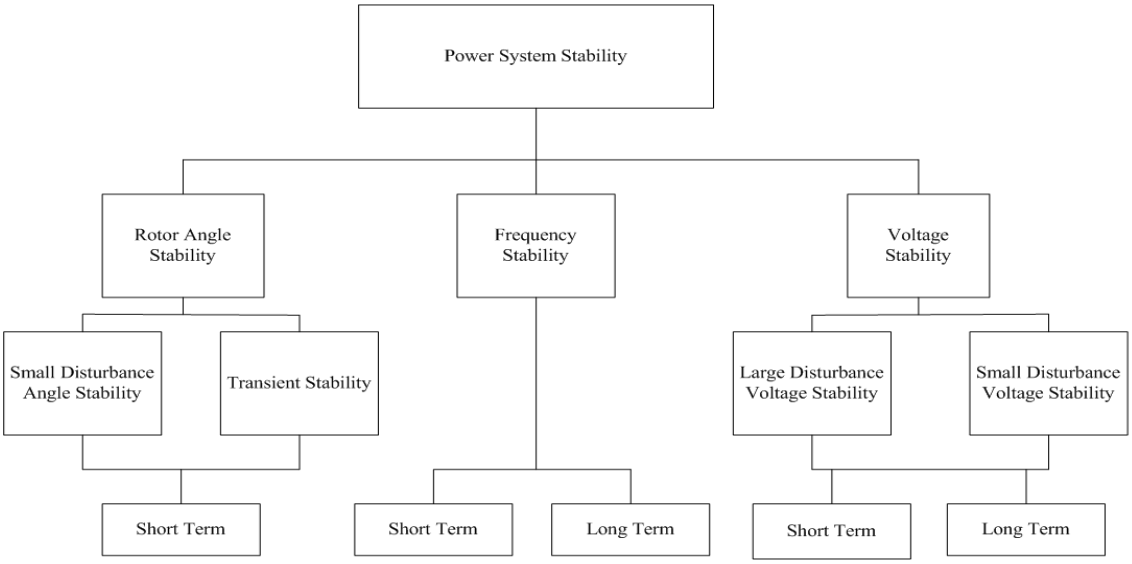

Figure 2.4: IEEE/CIGRE Power system stability diagram

It is impractical to study by considering all the aspects into a single problem. Power system's stability can be classified according to time scale and interests of ability to maintain in equilibrium regarding to the disturbance. Figure 2.4 presents the general

classification of power system stability [16].

If the amount of wind power generation increases, the power generation from conventional power plants must be reduced in order to balance power generation and consumption. Presently, conventional power plants are kept in operation to provide voltage and frequency control through the grid. Therefore, the large amount of increasing wind power generation introduces the challenges with regard to controlling the voltage and balancing the power in a grid, thus affecting systems stability.

The impacts of wind turbine on the stability of power systems have been discussed in many publications. The main aspects of wind power having a possible impact on stability issues are:

1) Wind energy generators are usually connected to lower voltage levels than conventional power stations. Most wind farms are connected to sub-transmission (110kV, 66kV) or even to distribution levels (20kV, 10kV) and not directly to transmission levels (>110kV) via big step-up transformers as in case of conventional power stations.
2) Wind resources are usually scattered in locations than conventional power stations. Hence, power flows are considerable different in the presence of a high amount of wind power and power systems are typically not optimized for wind power transport and to be vulnerable to fault. This aspect can be more or less severe according to the geographical location.
3) Because of the fluctuating nature of wind power and limited predictability of wind speed, power systems with a high amount of wind power usually require higher spinning reserve than conventional power systems, which adds inertia to the system.
4) Wind generators are usually based on different generator technologies so that the

impacts on power system stability depend on their characteristic accordingly.

The impacts of voltage quality, power characteristic and grid frequency depend on the turbine type considered [17]. Such findings are not only based on theoretical considerations, but have been confirmed by measurements [18]. The inherent variability of wind power causes wind turbines to exhibit power fluctuations and causes flicker in the grid [19]. In more critical operating conditions, wind turbines can even compromise voltage stability in the grid [20]. It has been found though, that the operation of wind turbines itself is also affected by variations in grid voltage, voltage imbalance, variation in system frequency and voltage distortion [13].

The effect of large-scale wind power generation on power system oscillation was investigated and presented the results qualitatively, in literature [21], in which the power generated by the two synchronous generators in the test system is gradually replacing by power from either constant or variable-speed wind turbines, while observing the movement of the eigenvalues through the complex plane. From the results, an increase in frequency and damping of power system oscillations was observed. Furthermore, it was shown that constant-speed wind turbines damp the power system oscillations more than variable-speed turbines because of the damping effect of the squirrel cage induction generator used in constant-speed wind turbines.

However, the above mentioned studies did not consider the protective disconnection due to the voltage dip at the wind turbine generator terminals. Even simple grid problem such as a two-phase line fault occurred in the 220kV grid in the Oldenburg region, Northern Germany, resulted in split second-long voltage dips in the region concerned, which caused a sudden loss of around 1,100MW of wind power feed-in [4]. Furthermore, in literature [22], significant power loss caused by a factitious short-circuit

fault in Western Denmark grid was explained. According to the study for the value of Low-Voltage Ride-Through (LVRT) capability of wind generation in the UK [23], the lack of LVRT capability will lead to increasing in fuel cost because of the wind energy loss which will need to be compensated by an equivalent increase in the output from convention plant. For LVRT capability improvement, use of Flexible AC Transmission Systems (FACTS) devices is reported in literature [24] and the use of series dynamic barking resistors is reported in literature [25]. In literature [26], the issue of voltage stability at a short-circuit fault in the grid and associated control strategies for induction generator based wind turbines are presented. However, it is not included how to achieve the fast control action for LVRT of constant-speed wind turbine rather that the use of command from power system control center.

The representative previous works related to the LVRT of wind turbine generator based on Doubly Fed Induction Generator (DFIG) are as follows. In the literature [27], the effect of protection devices such as a crowbar is investigated. Analyzing the reasons of a DFIG system with series grid-side converter for LVRT and control scheme for operation under unbalanced grid faults conditions are presented in literature [28]. The dynamic behavior of variable- speed wind turbines and their interaction with the power systems are discussed in literature [29].

Due to the grid connection via a full-scale converter, the Permanent Magnet Synchronous Generator (PMSG) based wind turbine can easier accomplish LVRT and provide a higher amount of reactive power to the grid than DFIG wind turbines. In contrast to full converter connected wind turbines, the reactive power supply of a DFIG wind turbine is limited due to the limited size of the converter. Because of direct grid connection, DFIG wind turbines are directly subjected of using a partial scale converter

turns into a technical disadvantage in cause of grid faults. Nevertheless, with an appropriate control and protection system, DFIG can also ride-through the grid faults and contribute to power system support in a satisfactory manner.

The previous works with respect to the countermeasures for voltage dip on PMSG are described as follows. In the literature [30], the Braking Resistor (BR) is used in parallel with DC capacitor to dissipate the extra energy. The advantage of this approach is simple in control performance although the additional cost is added. In the literature [31], the use of diode rectifier and DC-DC chopper, DC-DC boost-converter, and PWM rectifier with battery for storing the extra wind energy are suggested. In the literature [32], the use of Energy Storage System (ESS) and Braking Chopper (BC) is suggested to handle the DC-link voltage. Although the extra cost is inevitable, this results the improvement of overall performance for both fault ride-through and power smoothening so as to the overall performance of PMSG. In the literature [33], a control scheme is suggested to store the excessive kinetic energy in the large rotating masses of wind turbine and generator. However, the phenomenon of reactive power injection and over speeding of rotor during the voltage dip are not shown in this literature. According to the study in the appendix D, this method cannot inject reactive power during fault period.

2.4 LOW-VOLTAGE RIDE-THROUGH REQUIREMENTS IN WIND ENERGY GENERATION INTERCONNECTION

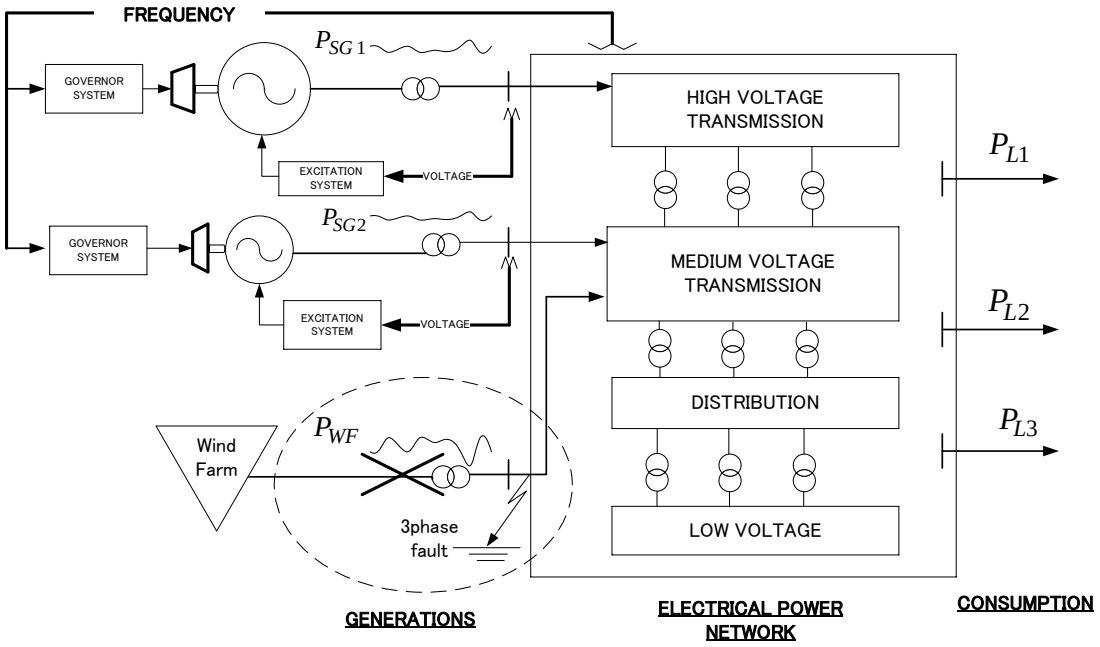

Figure 2.5: Conceptual diagram of low-voltage ride-through requirement

The term "Low-Voltage Ride-Through" of wind turbine stems from the desire to remain connected to the grid during a momentary voltage dip. In the Figure 2.5, a conceptual diagram which shows the necessity of wind farms' low-voltage ride-through capability for stable power system operation. As shown in the Figure 2.5, the dotted circle represents the generated power loss, P_{WF}, from wind farm due to the unscheduled disconnection by fault occurring. In the event of a fault in the transmission network, the voltage over the network will be depressed as a result of the current flowing into the fault point. When the fault is cleared by the operation of the protection system, the

voltage recovers to system voltage. The voltage dip duration time is related to the length of time to clear a transmission line fault, usually 10 to 20 cycles, and the magnitude of the voltage dip is determined by the location and type of fault. The rate of recovery likely depends on the strength of the interconnection and reactive power support. Many wind turbine generators are based on asynchronous machines, directly connected squirrel cage machine which cannot control reactive power and terminal voltage themselves. Being the lack of voltage and reactive power self-controllability, the terminal voltage of wind turbine generators are strongly related to the voltage at the point of interconnection and, of course, also in the case of voltage depressed by the fault.

Wind turbine generators have traditionally been treated in a similar manner to that of distributed generation. They have been required to trip following even minor disturbances, as in literature [7]. In this regards, the generated wind power capacity will be lost when the event of voltage dip continues until the fault clearing. The ability of the generation capacity to remain connected to the network during and after the voltage dip is vital to the stability of the network, and hence the premature tripping of wind turbine generators due to voltage dip can further risk the short-term voltage stability of the power systems and the amplification of the effect to the transient and frequency stability. Especially, when there is a high generating capacity from wind power, LVRT is seen to be particularly important in terms of maintaining the short-term stability of power systems relates to large disturbance. Therefore, to prevent the sudden loss of large amounts of wind power due to voltage dip in the grid, power system operators in most industrial countries have been revised their grid codes of LVRT requirement of wind power generator for interconnection to grid. It becomes clear that “Low-Voltage

Ride-Through" capability has been an essential requirement in wind power generation to mitigate the impacts on power systems.

The most important stipulations of Low-Voltage Ride-Through (LVRT) requirements which are introduced in most countries with high penetration of wind power generation are twofold, namely that;

1) wind turbines have to stay connected to the grid during voltage dips and,
2) they have to initiate forced reactive current injection for supporting the grid voltage.

The second requirement implies that wind turbine has to implement a fast voltage controller [4]. In other words, wind turbine must response quickly with respect to the voltage dip in order to remain connected with grid.

In the previous studies, there is still lack of considering how to get fast response in controlling for LVRT improvement. Moreover, consideration of the network stiffness is not included in developing their methods. Since the short circuit current depends on the network stiffness, the amount of power injected by Wind Turbine Generator (WTG) during and after a fault is strongly related to the stiffness. In this regard, the network stiffness in terms of Short Circuit Capacity (SCC) should be considered. Therefore, this thesis presents the new control method for fixed-speed wind turbine (FSWT) and permanent magnet synchronous generator (PMSG) for mitigating the impact of voltage dip under various SCC. The effectiveness of the proposed control method is compared with the use of conventional approaches.

2.5 CONCLUSIONS

Wind energy integration to power systems has impacts on frequency stability. According to the experience from European countries, the unscheduled disconnection of wind energy generation is not undesirable to maintain the demand-supply balance. Therefore, LVRT requirement becomes one of the essential grid codes in interconnection of wind farm. The terminology of Fault-Ride-Through (FRT) is also used in some literatures although the essence is the same with LVRT. The characteristics of LVRT requirements of each country are different according to their network structure, voltage level of interconnection, size of wind farm, generation mix and so on.

CHAPTER 3

PROPOSAL OF PITCH ANGLE CONTROL BASED ON FAST-RESPONSE VOLTAGE DIP DETECTION

3.1 INTRODUCTION

In the case of conventional power stations such as hydro, gas or steam, diesel power stations, etc., the delivery of energy can be regulated and adjusted to match demand by users (Figure 3.1(a)). In contrast, the wind power generation system is subject to the delivery of wind energy which cannot be demanded by end users (Figure 3.1 (b, c)). Moreover, as shown in the Figure 3.1 (b, c)), the control strategies applied on generators are different which depend on the types of wind power generation systems. Generally, wind power generation systems can be classified into variable speed wind turbine and fixed speed turbine, according to the nature of rotor operation. However, turbine-blade angle controlling is a common to any wind turbine generation systems regardless of fixed or variable speed operation. Wind turbine blade-angle control can be achieved by the pitch control of wind turbine. Pitch control is the most common means of controlling the aerodynamic power generated by the turbine rotor.

This study proposes the pitch angle control and Power Curtailment (PC) control for FSWT with a directly grid-coupled squirrel-cage induction-generator (SCIG) model [34] and the variable-speed wind turbine (VSWT) with a PMSG model [35], as shown in the Figure 3.1 (b) and (c), respectively.

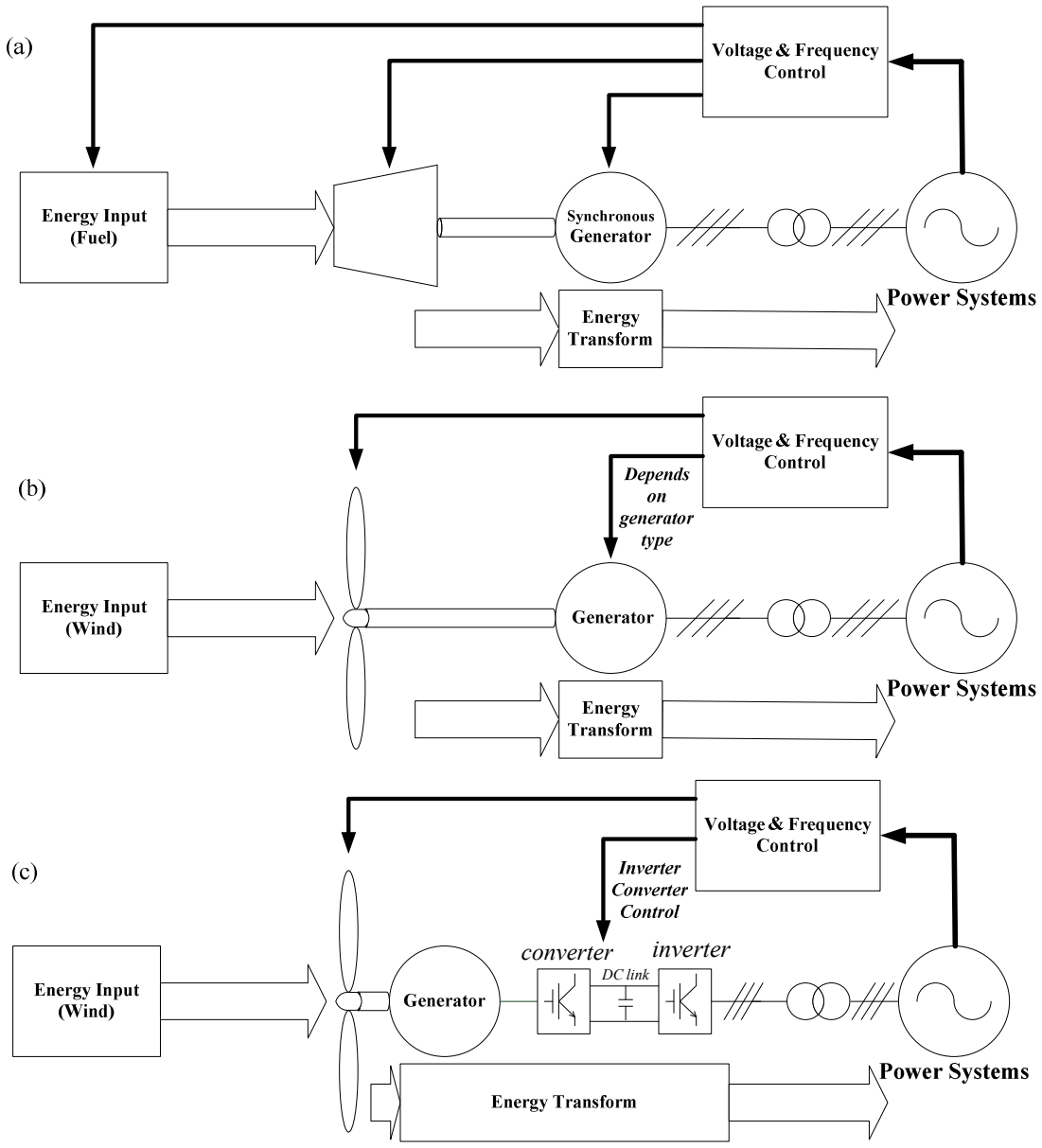

Figure 3.1: Energy delivery and control of electrical supply systems in (a) Conventional power generation (b) Wind power generation with direct grid connection (c) Wind power generation with back-to-back frequency converter

Chapter 3. Proposal of Pitch Angle Control based on Fast-Response Voltage Dip Detection

In this chapter, the detail of proposed pitch control for LVRT capability improvement is explained. In FSWT, LVRT behavior is related to the sudden disconnection of wind turbine in the wake of fault. The difficulty with the LVRT issue in FSWT is the capability of controlling active and reactive power output to ensure the proper response to the faults.

3.2 PROPOSAL OF PITCH ANGLE CONTROL IN FIXED-SPEED WIND TURBINE

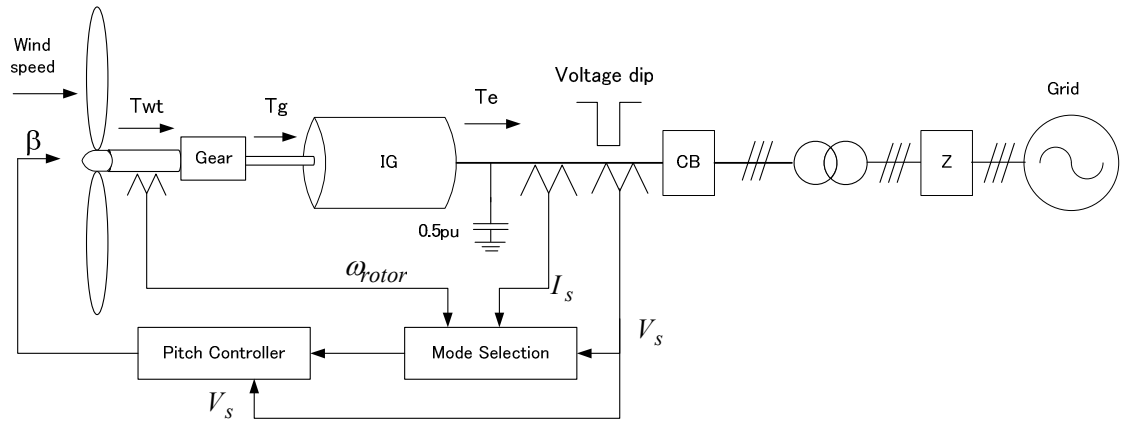

Figure 3.2: A Proposed pitch controller for LVRT capability of FSWT

In the FSWT, a directly grid-coupled SCIG is used mostly for wind power generation which absorbs reactive power from the power grid. This implies that the conventional induction generators are excited from the power grid. Such induction generators cannot control their excitation by themselves. Due to the lacks of self-excitation control, the SCIG consumes reactive power and therefore, it is usually equipped with capacitors for reactive power compensation. However, the use of these capacitors is not enough to enhance the LVRT.

Therefore, during the voltage depression caused by a fault, the wind turbine is only able to deliver real power to the network in proportion to the retained voltage. The difference between mechanical power supplied by the rotor and electrical power of the generator will appear as acceleration power, speeding up the rotor and drive train (gear box) and accumulating stored energy in inertia. If this situation is allowed to continue,

1) the wind turbine will over speed which can damage to the drive train (gear box),

and

2) the accumulated energy stored in inertia after recovering the generator terminal voltage will produce over current which can damage the induction generator.

To avoid these occurrences, the following action must be either done;

1) to control the rotor speed to reduce the incoming wind power or

2) to separate the generator from the grid and introduce a dump load to dissipate the power that cannot be absorbed by the grid.

In order to continue the power supply during the voltage dip, the second approach is not desirable. The control of wind turbine speed by reducing the extracted wind power is the only way to achieve the LVRT for the fixed-speed wind turbine. So the pitch control action to balance the mechanical and electromagnetic torque is necessary for the LVRT.

In the FSWT, squirrel -cage induction-generator typed WTGs are implemented. These types of generators absorb reactive power from a power network to supply real power, so that they cannot control their terminal voltage by themselves. This implies that, during the voltage depression caused by a fault occurred in the network, the wind turbine is only able to deliver real power to the network in proportion to the retained voltage. Therefore, as shown in Figure 3.2, the power imbalance between mechanical input power, $\boldsymbol{T_{wt}}$, to the generator and electrical output, $\boldsymbol{T_e}$, accelerates the generator rotor. If this situation is allowed to continue, the WTG will reach to over speed limit or over current limit in the wake of the fault and then eventually, the generator will be disconnected by protection systems. So it is vital to balance between the mechanical input power, $\boldsymbol{T_{wt}}$, and the electrical output, $\boldsymbol{T_e}$, for enhancing the LVRT capability of FSWT. If the turbine rotor speed, ω_{rotor}, can be reduced quickly during voltage dip so as

not to rise over the maximum speed, then the sudden disconnection of WTG can be avoided.

The main concept of the proposed pitch angle control is based on the voltage dip detection by fast response of under voltage relay and a feedback PI control of terminal voltage, V_s, during voltage dip. A sudden voltage dip is detected by the under voltage relay to initiate the pitch angle control in LVRT mode. Then, the pitch angle of blades is changed according to the depth of voltage dip so as to suppress the rapid increase of rotor speed by the release of blowing wind power. By this way, the mechanical input power, T_{wt}, can be controlled in order to balance the retarding electrical torque, T_e, of the generator during and after the fault.

3.3 CONFIGURATION OF PROPOSED PITCH CONTROL

The configuration of pitch angle control system consists of three parts: (1) wind turbine protection and pitch angle controller selection, (2) LVRT mode controller, and (3) normal mode controller, as shown in Figure 3.3. In the first part, the protection relays for the rotor over speed and induction generator over current are included. The protection system detects the rotor speed, ω_{rotor}, and generator current, I_s, whether in LVRT pitch control mode or normal mode. If the protection system detects over speeding limit or over current limit [26], wind turbine is disconnected for the safety purpose, and the pitch angle is set to 90°.

The second part is designed to control the pitch angle according to the WTG behavior during voltage dip. The proposed pitch controller for LVRT is illustrated in the part of Figure 3.3 enclosed by the dotted lines. The pitch angle β_{LVRT} for LVRT is the output of proportional integral (PI) controller which is very widely used for many kinds of control systems. The parameters are shown in Appendix A.1. The input of the PI controller is the difference between reference voltage, V_{ref}, and the measurement of generator terminal voltage, V_s. When the generator terminal voltage drops below the 0.7 (p.u.) of nominal voltage, the LVRT pitch control mode is activated by the under voltage relay with the total delay time of 100ms. It is assumed that this delay time includes the relay pickup time, T_{uvr}<100ms, communication and switching delay. After the monitored voltage, V_s, has recovered for more than 5s, LVRT pitch control mode is deactivated. These under voltage relay time settings used in this study are taken from the reference [36].

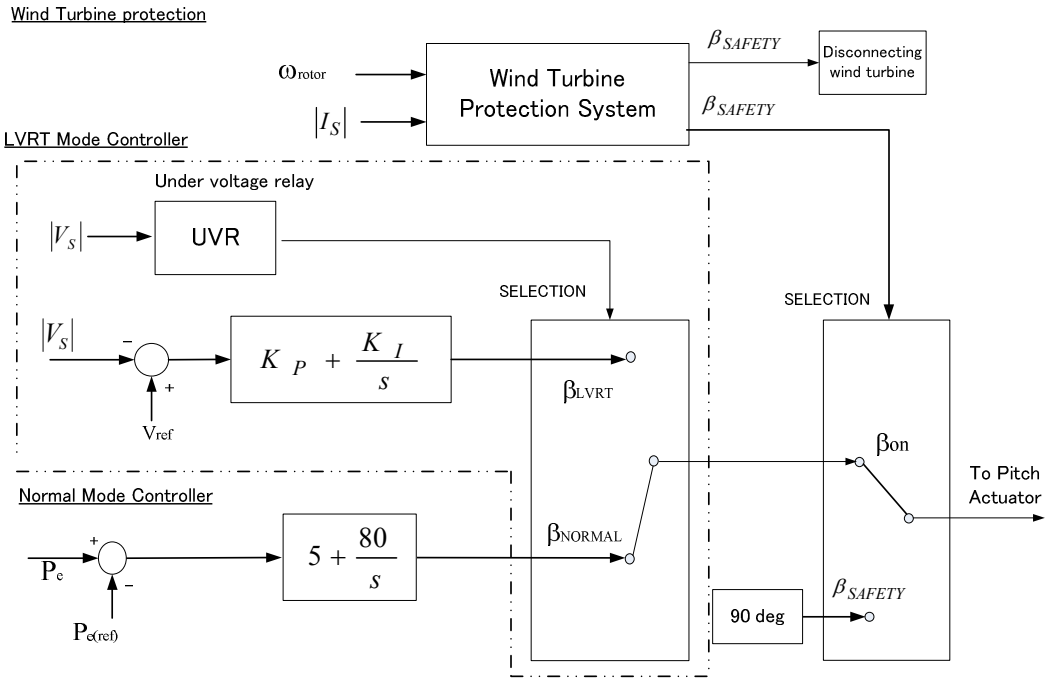

Figure 3.3: A block diagram of the proposed pitch control

The pitch angle control in wind turbine is the most common means of controlling the generated power. Therefore, the pitch controller in normal mode operation is also included as a third part. During the normal mode operation which is determined by the protection system switching logic, the pitch angle is controlled by conventional controller in which generated active power, P_e, is used as an input parameter. When the generated active power is above the rated power, 2MW, the blades are pitched by β_{NORMAL} to reduce the extracted wind power. The explanation of the pitch control mode selection scheme is done in the next section.

3.3.1 PITCH CONTROL MODE SELECTION LOGIC

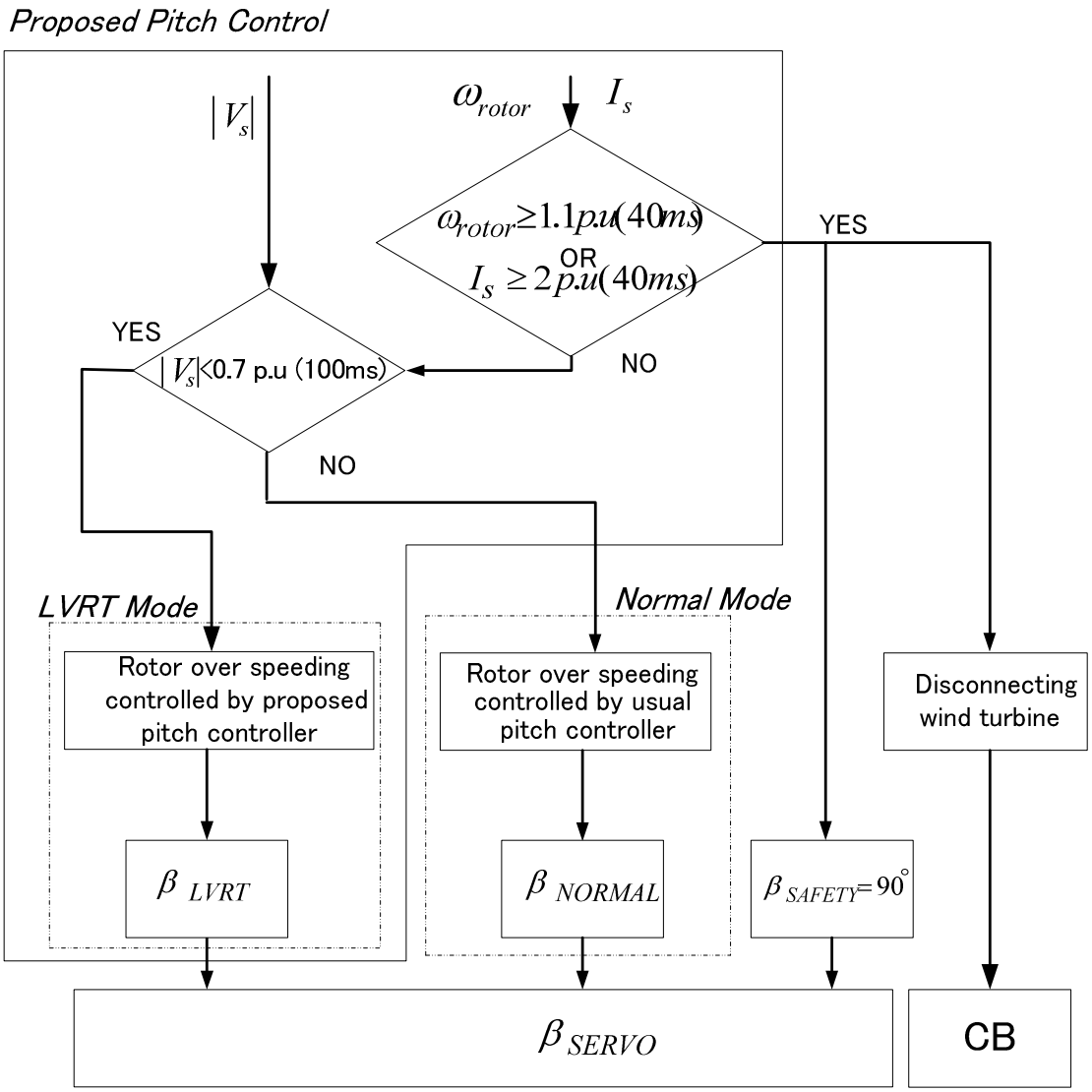

Figure 3.4: Flow chart of pitch control mode selection

The pitch control mode selection is done by the coordination of wind turbine protection system. The selection between the two control modes in section 3.2 is based on monitoring the magnitude of terminal voltage, Vs, the stator current, I_s, of SCIG, and wind turbine rotor speed, ω_{rotor}. The selection logic for pitch control modes is explained

here by using Figure. 3.4. Firstly, checking of whether the stator current, I_s, or the rotor speed of wind turbine, ω_{rotor}, exceeding the specified limit parameters [26] is carried out. If, at least one of these parameters is exceeded for 40 *ms*, the safety stop command is sent to pitch controller to set the maximum pitch angle (β_{SAFETY}=90°) and, at the same time, the WTG is disconnected from power network by the operation of circuit breaker (CB). Otherwise, pitch angle, β_{NORMAL}, is set by the normal mode pitch control with the input signal of generated active power unless a voltage dip is detected. If the voltage dip inception is detected, the protection system switches the LVRT mode pitch control action and sets pitch angle, β_{LVRT}.

3.4 DESCRIPTION OF FIXED-SPEED WIND TURBINE

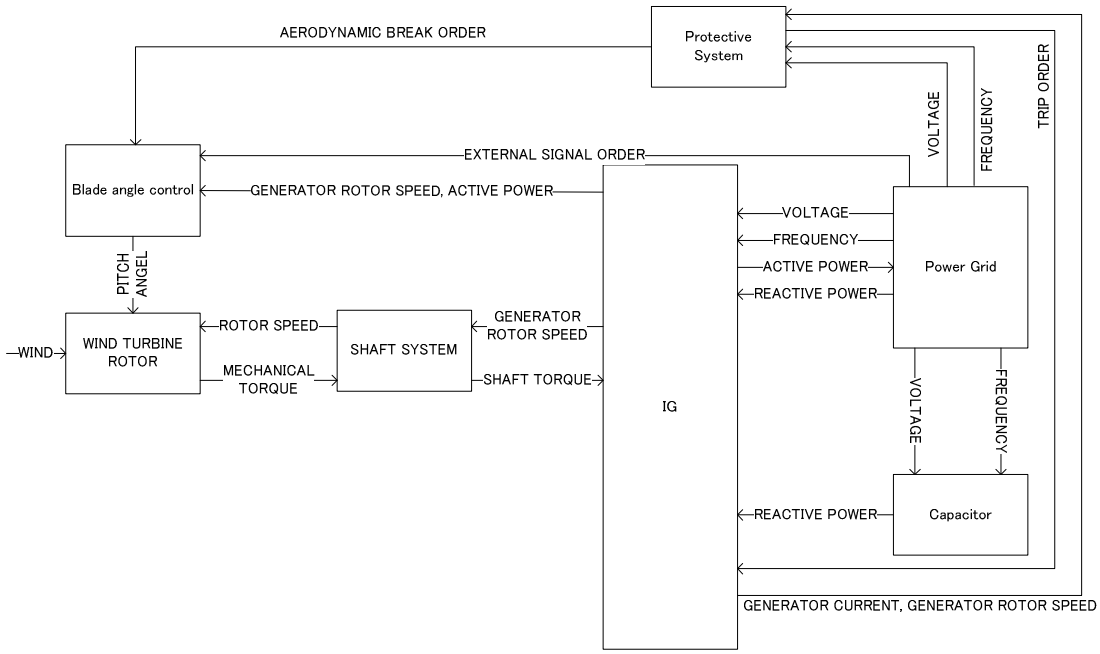

Figure 3.5: Generic block diagram of wind turbine with FSWT [26]

Figure 3.5 shows the generic block diagram of FSWT used in this study. An induction generator in FSWT is connected directly to the AC network, and therefore the turbine rotates at a nearly constant speed. As the wind speed varies, the power produced will vary roughly as the cube of the wind speed. At rated wind speed, the electrical power generated becomes equal to the rating of the turbine, and the blades are then pitch in order to reduce the aerodynamic efficiency of the rotor and limit the power to the rated value. The usual strategy is to pitch the blades in response to the power error, defined as the difference between the rated power and the actual power being generated, as measured by a power transducer. The primary objective of the pitch control is then to maintain the output power at the rated level when the wind speed is higher than the rated speed. In emergency condition, pitch angle adjustment can be done not only by the

supervisory control for active power control but also by the protection systems as an aerodynamic break for safety.

3.4.1 AERODYNAMIC MODEL

The power extracted from the blowing wind can be expressed by the following equation [34]:

$$P_m(\lambda,\beta,u) = \omega_{wt} T_m = C_p P_w = \frac{\rho}{2} A_{wt} C_p(\lambda,\beta) v_{wind}^{\ 3} \tag{3.1}$$

where ρ is the air density, λ is the tip speed ratio $\lambda = \frac{\omega R}{V_w}$, β is the pitch angle, A_{wt} is the area covered by the wind turbine rotor, ω_{wt} is the wind turbine rotor angular frequency, T_m is the torque from blowing wind and v_{wind} is the wind speed. The power coefficient, C_p, is approximated by the following equation [34]:

$$C_p(\lambda,\beta) = c_1(\frac{c_2}{\lambda_i} - c_3\beta - c_4\beta^{c5} - c_6)e^{-\frac{c7}{\lambda_i}} \tag{3.2}$$

$$\lambda_i = 1/(\frac{1}{\lambda + c_8\beta} - \frac{c_9}{\beta^3 + 1}) \tag{3.3}$$

Equation 3.1 can be normalized at the certain based condition. In the per unit (pu) system, we have:

$$P_{m\_pu} = k_p C_{p\_pu} v_{wind\_pu}^3 \tag{3.4}$$

where

P_{m_pu} =Power in pu of nominal power for particular values of ρ and A

C_{p_pu} =Performance coefficient in pu of the maximum value of C_p

v_{wind_pu} =Wind speed in pu of the base wind speed.

The parameters c_1~c_9 in equation (3.2) and (3.3) used in the simulation study are

shown in Appendix A.3. By adjusting the pitch angle, β, the power extracted from the blowing wind can be effectively controlled.

3.4.2 PITCH SERVO ACTUATOR MODEL

A pitch servo actuator model is shown in Figure 3.6. The pitch servo actuator system actually has non-linear characteristics, but it can be approximately expressed as a first-order servo model. Usually, a first-order servo model is sufficient in investigations of phenomenon related to power system stability [26]. In this model, a servo time constant and a limitation of both the pitch angle and its rate of change are taken into account, as the pitch angle cannot be changed immediately. The rate of change limitation decides how fast the extracted wind power can be reduced. In this study, the pitch angle changes, Δβ/Δt, is limited by a possible pitch rate for a modern wind turbine, i.e., dβ/dt MAX and dβ/dt MIN at ±15 [deg/s] respectively [37]. Then, the pitch angle is limited between β_{MAX}=90° and β_{MIN}=0°. The servo time constant is set at T_{SERVO}=0.25s [24].

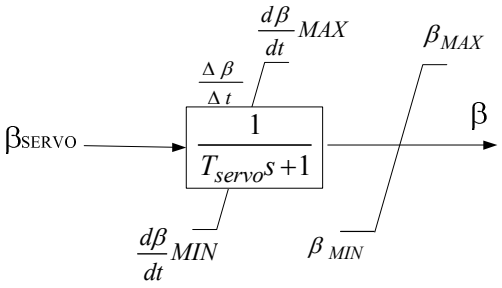

Figure 3.6: Pitch actuator model

3.4.3 INDUCTION GENERATOR AND SHAFT SYSTEM MODEL

In SCIG model, we take into account the transients in the rotor circuit as well as the fundamental-frequency transients components of stator circuit [38]. It implies that the magnetic saturation and any losses apart from the copper losses are neglected, and flux distribution, stator voltages and currents can be assumed as sinusoidal at the fundamental frequency [1, 26, 38, 39]. The model equations of SCIG in per unit (p.u.) systems [38] can be expressed by equations 3.5 to 3.9. The electrical part of the machine is represented by a fourth-order state-space model and the mechanical part is represented by a second-order system. The electrical output torque, T_e, can be expressed by equations 3.9. All electrical variables and parameters shown in Appendix A.4 are referred to the stator.

$$v_{qs} = R_s i_{qs} + \frac{d}{dt}\psi_{qs} + \omega\psi_{ds} \tag{3.5}$$

$$v_{ds} = R_s i_{ds} + \frac{d}{dt}\psi_{ds} - \omega\psi_{qs} \tag{3.6}$$

$$v'_{qr} = R_r i_{qr} + \frac{d}{dt}\psi_{qr} + (\omega - \omega_r)\psi_{dr} \tag{3.7}$$

$$v'_{dr} = R_r i_{dr} + \frac{d}{dt}\psi_{dr} - (\omega - \omega_r)\psi_{qr} \tag{3.8}$$

$$T_e = 1.5\,p(\psi_{ds} i_{ds} - \psi_{qs} i_{qs}) \tag{3.9}$$

The subscript definitions are as follows: *d* is d axis quantity, *q* is q axis quantity, *r* is rotor quantity, *s* is stator quantity, *l* is leakage inductance, *m* is Magnetizing inductance *a* is the phase a of AC three phase and *b* is the phase b of AC three phase.

The parameter definitions are as follows: ψ is electromagnetic flux, R is resistance, L is inductance, *i* is current, *v* is voltage. Those parameters have the following relations:

$\psi_{qs} = L_s i_{qs} + L_m i_{qr}$, $\psi_{ds} = L_s i_{ds} + L_m i_{dr}$, $\psi_{dr} = L_r i_{dr} + L_m i_{ds}$ $\psi_{qr} = L_r i_{qr} + L_m i_{qs}$,

$L_s = L_{ls} + L_m$, $L_r = L_{lr} + L_m$

The equations of motion are as follows:

$$\frac{d}{dt}\omega_m = \frac{1}{2H}(T_e - F\omega_m - T_{wt}) \tag{3.10}$$

$$\frac{d}{dt}\theta_m = \omega_m \tag{3.11}$$

$$\begin{bmatrix} i_{as} \\ i_{bs} \end{bmatrix} = \frac{1}{2}\begin{bmatrix} 2\cos\theta & 2\sin\theta \\ -\cos\theta + \sqrt{3}\sin\theta & -\sin\theta - \sqrt{3}\cos\theta \end{bmatrix}\begin{bmatrix} i_{qs} \\ i_{ds} \end{bmatrix} \tag{3.12}$$

$$\begin{bmatrix} i_{ar} \\ i_{br} \end{bmatrix} = \frac{1}{2}\begin{bmatrix} 2\cos\beta & 2\sin\beta \\ -\cos\beta + \sqrt{3}\sin\beta & -\sin\beta - \sqrt{3}\cos\beta \end{bmatrix}\begin{bmatrix} i_{qr} \\ i_{dr} \end{bmatrix} \tag{3.13}$$

$$i_{cs} = -i_{as} - i_{bs} \tag{3.14}$$

$$i_{cr} = -i_{ar} - i_{br} \tag{3.15}$$

$$\begin{bmatrix} V_{qs} \\ V_{ds} \end{bmatrix} = \frac{1}{3}\begin{bmatrix} 2\cos\theta & \cos\theta + \sqrt{3}\sin\theta \\ 2\sin\theta & \sin\theta - \sqrt{3}\cos\theta \end{bmatrix}\begin{bmatrix} V_{ab(s)} \\ V_{bc(s)} \end{bmatrix} \tag{3.16}$$

$$\begin{bmatrix} V_{qr} \\ V_{dr} \end{bmatrix} = \frac{1}{3}\begin{bmatrix} 2\cos\beta & \cos\beta + \sqrt{3}\sin\beta \\ 2\sin\beta & \sin\beta - \sqrt{3}\cos\beta \end{bmatrix}\begin{bmatrix} V_{ab(r)} \\ V_{bc(r)} \end{bmatrix} \tag{3.17}$$

where $\beta = \theta - \theta_r$, β =the difference between the position of reference frame and rotor, θ_r =position (electrical) of the rotor, θ=angular position of the reference frame, θ_m is the rotor angular position, ω_m is rotational speed, H is a lumped inertia constant, F is damping coefficient, and T_{wt} is the mechanical input torque.

3.4.4 PROTECTION SYSTEMS MODEL

It is helpful to consider the protection system as quite distinct from the main or ‘normal’ control system of the turbine. Its function is to bring the turbine to a safe condition in the event of serious or potentially serious problem. It means that the turbine with the applied brakes is brought to be at rest.

The normal wind-turbine supervisory controller should be capable of starting and stopping the turbine safely in all foreseeable ‘normal’ conditions, including extreme winds, loss of the electrical network, and most fault conditions which are detected by the controller. The protection system acts as a back-up to the main control system, and takes over if the main system appears to be failing to do this. It may also be activated by an operator-controlled emergency stop button.

Therefore, the protection system must be independent from the main control system as far as possible, and must be designed to be fail-safe and highly reliable. Rather than utilizing any form of computer or micro-processor based logic, the safety system would normally consist of a hard-wired fail-safe circuit linking a number of normally open relay contacts. The protective relay system of a fixed-speed wind turbine watches and checks several electrical and mechanical parameters such as the terminal voltage, the stator current and the rotor speed. The protective relay system orders disconnection of the wind turbines when at least one of the monitored parameters exceeded its relay settings. The induction generator is rigid and not usually harmed by delivering over of its rated power for some period of time as long as its rated temperature is not exceeded. Especially in the application of wind turbine generation system, the blowing wind can reduce the temperature of generator. According to the typical relay settings for

fixed-speed wind turbines manufactured and commissioned in Denmark, the over current relay will be tripped if the generated current above 2 (p.u.) for 40ms [26]. In this study, in addition to the monitoring of over current above 2 (p.u.) for 40ms, the rotor speed which is not more than 18.7 rpm (110% of rated speed) is also used as a monitored parameter. If any one of those contacts is lost, the protection system trips, causing the appropriate fail-safe actions to operate. This might include disconnecting all electrical systems from the supply, allowing fail-safe pitching to the feather position, and allowing the spring-applied shaft brake to come on.

The protection system might, for example, be tripped by any one of the following:

- Rotor over-speed, i.e., reaching the hardware over-speed limit- this is set higher than the software over-speed limit which would cause the normal supervisory controller to initiate a shut-down (typical arrangement of rotor speed sensing equipment on low-speed shaft);
- Emergency stop button pressed by an operator;
- Other faults indicating that the main controller might not be able to control the turbine such as generator over current.

The wind turbine may also trip by under voltage, over voltage, under frequency, and over frequency relay. These relay settings can be found in [26]. However, when wind turbines disconnect in operation situations without any risk of voltage instability or damage to the equipment, this can be defined as unnecessary disconnection. In this study, wind turbine tripping by over and under frequency conditions is not included as the frequency fluctuation is not considered. Moreover, as the main goal of this study is not to disconnect by voltage dip, the tripping by under voltage relay is not desired. Although the protective tripping by under voltage relay is not included, the proposed

control method adjusts the pitch angle according to the voltage dip.

3.5 WIND FARM CONNECTED POWER SYSTEM MODEL

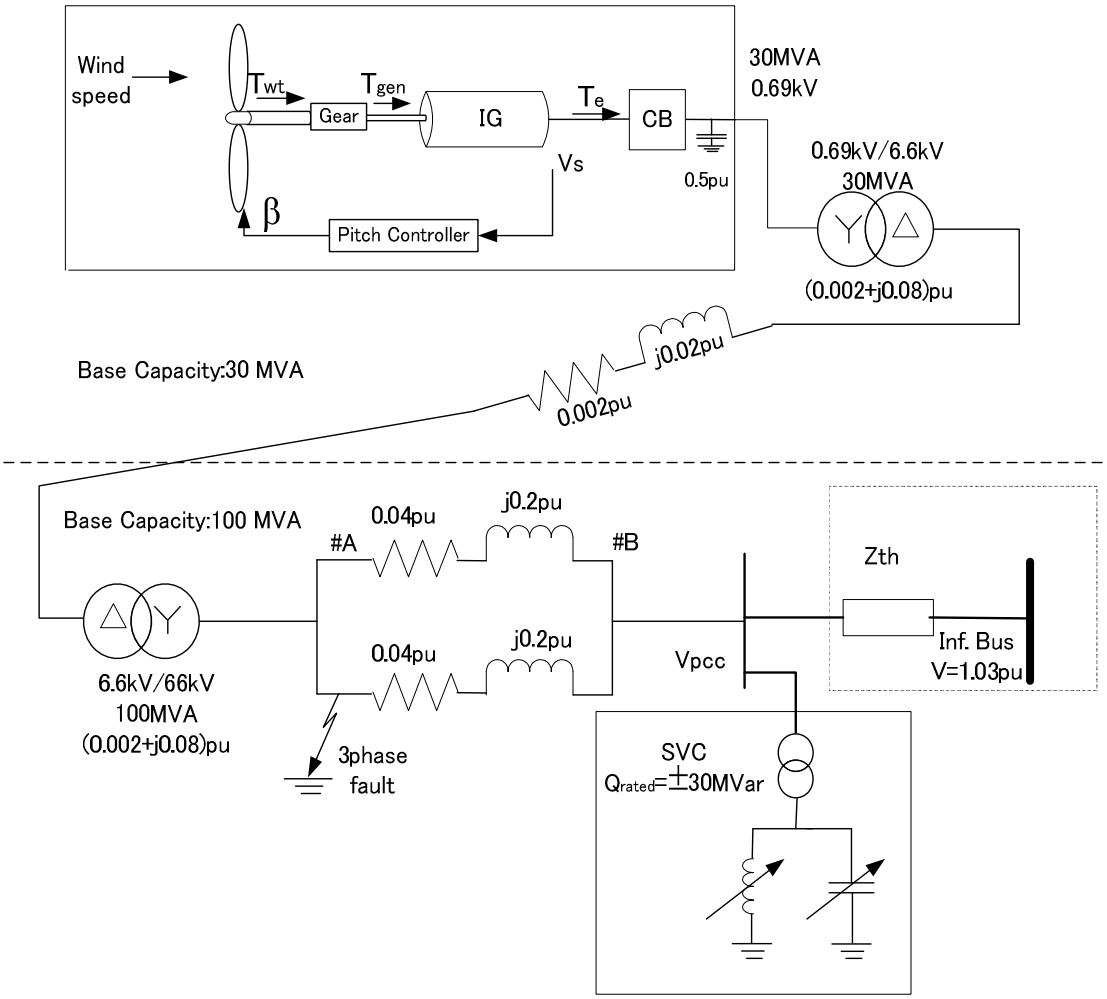

Figure 3.7: A model of power systems including wind farm and SVC

The power system model including a wind farm shown in Figure 3.7 is used. The wind farm consists of 15 FSWTs of which each has 2MW rated power capacity [34]. The wind farm is connected to 66kV bus at which Static Var Compensator System (SVC) of 30 Mvar capacity is installed for bus voltage stabilization.

The turbulence nature of wind speed can be neglected because the voltage dip duration is relatively short in LVRT studies. During the normal operation, even the wind blows up to 25 m/s, the maximum possible rotor speed will be around the rated rotor speed. Therefore, it can be considered that the maximum power generation conditions are the worst-cases performance for evaluating LVRT. In this regard, the complicated wind speed model is omitted in the simulation studies, and the rated wind speed of 14m/s is mainly used as the worst-case condition for LVRT.

Moreover, the internal wind farm network and any interactions between the turbines themselves are neglected in this study. This implies that, it is not necessary to model individual wind turbines in the wind farm as far as they are in same type and connected to the same bus. Instead, an aggregated wind farm model is used to evaluate the interaction with power systems. The aggregated model is developed by lumping of 15 WTGs into a single equivalent wind turbine. These WTGs are assumed to have the identical system parameters and same wind speed are exerting on each WTGs. The fixed shunt capacitor of (0.5p.u.) [34] is assumed to be connected to each WTG throughout the LVRT.

The power system is represented by the infinite bus with an equivalent impedance, Z_{th}. The Z_{th} has X/R ratio of 10 and the value is set according to the short circuit capacity (SCC) of power systems, i.e. (4.356+j43.56)Ωat100MVA, (0.8712+j8.712)Ω at 500MVA, and (0.4356+j4.356)Ω at 1000MVA respectively. The FSWT, CB, wind turbine transformers, SVC, cables and grid transformers [35] are modeled by using the simulation tool of MATLAB/Simulink environment.

3.5.1 STATIC VAR COMPENSATOR SYSTEM MODEL

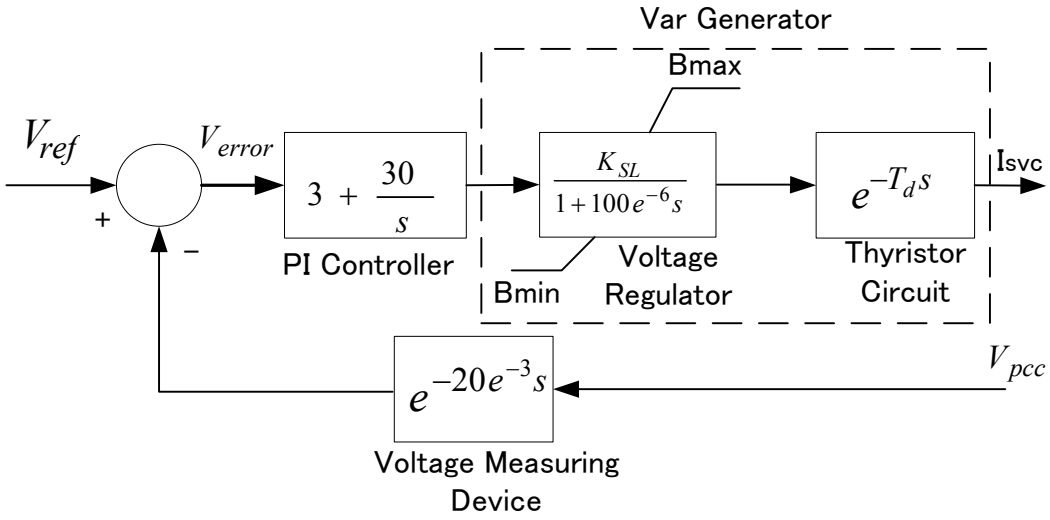

Figure 3.8: Block diagram of SVC

When a wind farm is connected to the power systems, the impedance between wind farm and systems will be dominated by reactance. Therefore, the reactive power flow dominates any voltage variation at the point of wind farm connection. In general, it would be expected that the fast response reactive power compensation device is implemented at the point of wind farm connection to control the voltage variation due to fluctuated nature of wind speed causing the variation in reactive power absorption by SCIG. Therefore, to verify the effectiveness of the proposed pitch control method, the voltage control ability at the point of wind farm connection is considered by using SVC.

The SVC is modeled as an equivalent current source, I_{svc}. The current, I_{svc}, is assumed to be regulated by the control system indicated in Figure 3.8. This model only considers for observing the impact on voltage stability at fundamental frequency [38, 40]. It implies that the details of power electronics, the measurement system, and the

synchronization system are represented by simple transfer functions at the system's fundamental frequency. The SVC has the dynamic performance of ±30 Mvar, with the average thyristor valves firing time delay, T_d, of 4ms and the V-I characteristics slope or droop reactance, K_{SL}, of 0.03 p.u. at 30 MVA base. The reference voltage (V_{ref}) of the voltage regulator with PI controller is set at 1.03 p.u. to stabilize the voltage at the Point of Common Coupling (Vpcc).

3.5.2 FAULT MODEL

Three-phase-to-ground fault model [38] is used in this study. The fault in the transmission network depresses the network voltage and thereby weakens the power transfer capacity of the wind farm to power system across the network. Then the WTGs are in over speeding and trip from the network in consequence. Therefore, one of the serious network faults, three-phase-to-ground fault, is used as a worst-case for evaluating the proposed pitch control for LVRT.

3.6 VERIFICATION THE EFFECTIVENESS OF PROPOSED PITCH CONTROL

The effectiveness of the proposed pitch control is checked by simulation studies. By assuming the different fault points between node #A and #B (at 1km, 8km, 18 km of 19km long sub-transmission line from the node #A respectively) in Figure 3.7, the voltage along the sub-transmission lines is depressed until the faulted line is isolated. The fault sequence used in the simulation is the three-phase-to-ground fault occurred in one of the 66kV sub-transmission lines. The fault is occurred at 500 *ms* and the faulted line is isolated at 700 *ms* from the start point of simulation.

3.6.1 COMPARISON WITH BASE CASE

Base Case (Without pitch control scenario of SCC=500MVA, SVC at node #B, fault point of 1 km from node #A between node A and B)

The LVRT of wind farm cannot be achieved in base case. The associated LVRT behavior of wind farm is shown in Figure 3.9 and 3.10. After isolating the faulted line, the generated active power of wind farm is lost at 2098 ms from the start point of simulation, as WTG is disconnected. When the fault is occurred at the distance of 1km from node #A at 500 ms, the generator terminal voltage is depressed suddenly to 0.5p.u. Although the wind turbines are not designed to be disconnected by the under voltage relay, both mechanical parts and electrical parts of wind turbine generator are protected by means of the over current relay and over speed protection systems. The generator terminal voltage continues depressing to the 0.03 p.u. until the faulted line is isolated at

700ms. During the voltage dip, as explained in section 3.2, the electrical output of WTG proportionally decreases to the magnitude of terminal voltage. As a result, as shown in Figure 3.9, the turbine rotor speed increases because of the imbalance between mechanical input and electrical output.

Once the faulted line is isolated at 700 *ms*, the terminal voltage tends to recover back. Consequently, SCIG absorbs more reactive power due to over speeding (not reached to the protection system limit of 1.1 p.u. at that instance) and this causes over current in the stator of SCIG (not reached to the protection system limit of 2 p.u. for 40*ms* at that instance) as shown in Figure 3.9 and Figure 3.10. However, the terminal voltage of SCIG is collapsed due to the continuous over speeding of rotor and unfortunately reached to the over speed protective relay limits for 40 *ms* at the time of 2098 ms from the start point of simulation. Therefore, WTG is disconnected from the grid by over speed protection in order to avoid the damaging.

The behavior of SVC which explained in section 3.5.1 is shown in Figure 3.11. Due to the fault, the bus voltage controlled by SVC at node #B is depressed to the 0.4 p.u. until the fault is isolated. According to the reference voltage setting of voltage regulator, SVC injected the reactive power of 30Mvar once the voltage at node #B is recovered back. Although the SVC fed the reactive power absorbed by the wind farm during and after the fault, the continuous power supply of wind farm is cannot be achieved in this case.

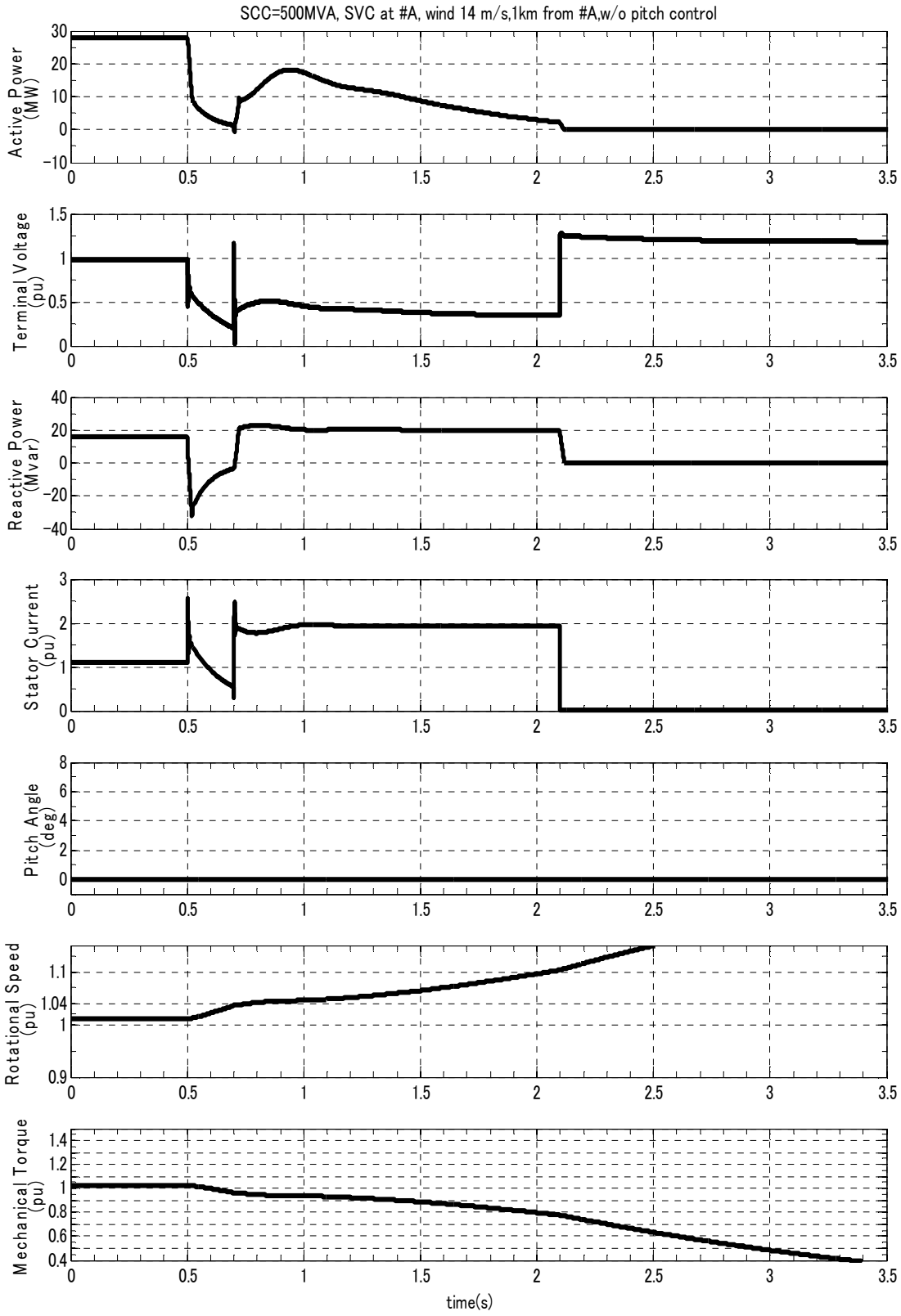

Figure. 3.9: Wind Farm Behavior (Base Case: without pitch control)

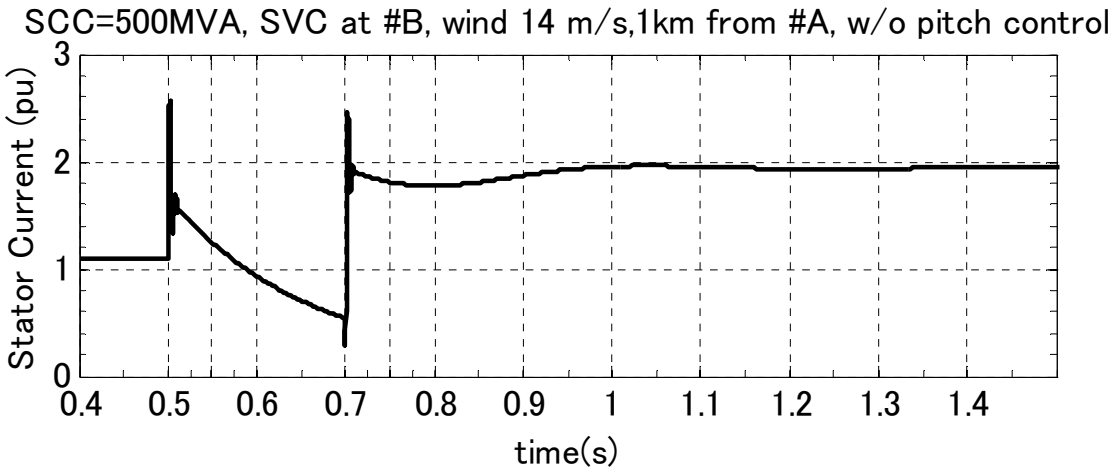

Figure 3.10: Stator current (Base Case: without pitch control)

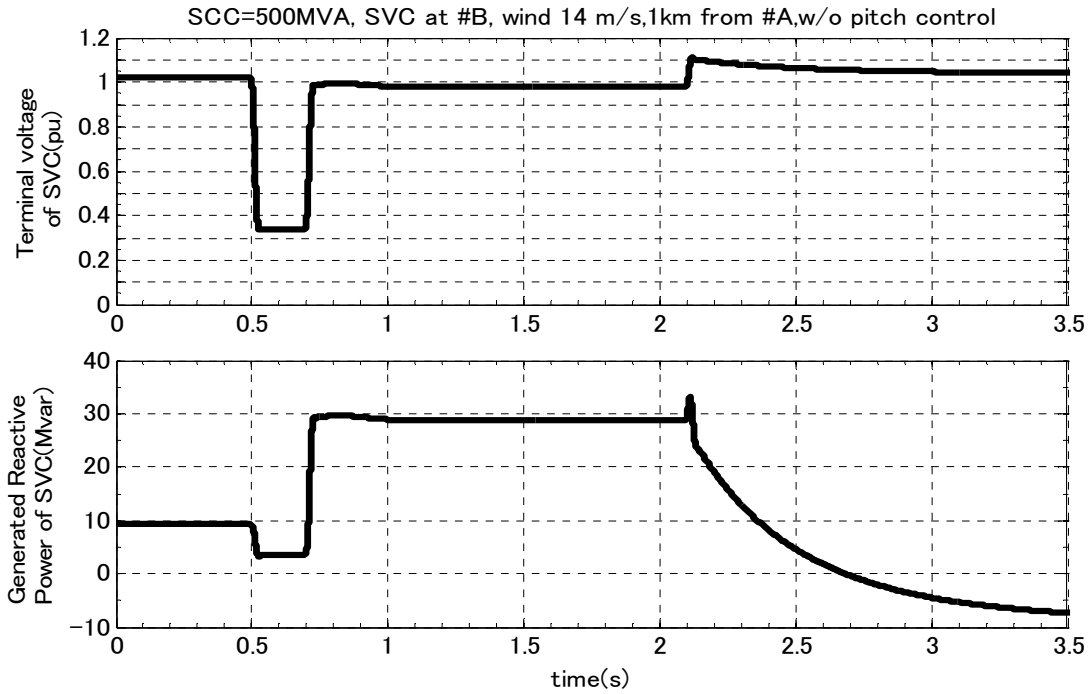

Figure 3.11: SVC behavior (Base Case: without pitch control)

Proposal Case (With pitch control scenario of SCC=500MVA, SVC at node #B, fault point of 1 km from node #A between node A and B)

The LVRT of wind farm can be achieved in proposal case. The associated LVRT behavior of wind farm in proposal case is shown in Figure 3.12 and 3.13. In comparison with the case 1, the generated power from wind farm can continue to supply after the fault is isolated although the behavior of wind farm during the voltage dip (except the pitch angle) in proposal case is almost the same as base case. The pitch angle is started to adjust by proposed pitch control at 600*ms* (100*ms* after the fault) from the start point of simulation so as to reduce the torque and rotor over speeding.

By comparing Figure 3.9 with 3.12, the over speeding of rotor can be reduced during the post-fault period in proposal case. The rotor speed recovers back to pre-fault level (around 1 p.u.) at 1500*ms*. Consequently, the proposed pitch control contributes to voltage recovery and reduction of the over current in the stator of SCIG after the fault is isolated as shown in Figure 3.12 and 3.13 respectively.

The behavior of SVC in proposal case is shown in Figure 3.14. Due to the fault, the bus voltage controlled by SVC at node #B is depressed to the 0.4 p.u. until the fault is isolated. According to the reference voltage setting of voltage regulator, SVC injected the reactive power of 30Mvar once the voltage at node #B is recovered back. The SVC fed the reactive power absorbed by the wind farm during and after the fault until the terminal voltage recovers back to the nominal voltage of 1 p.u.

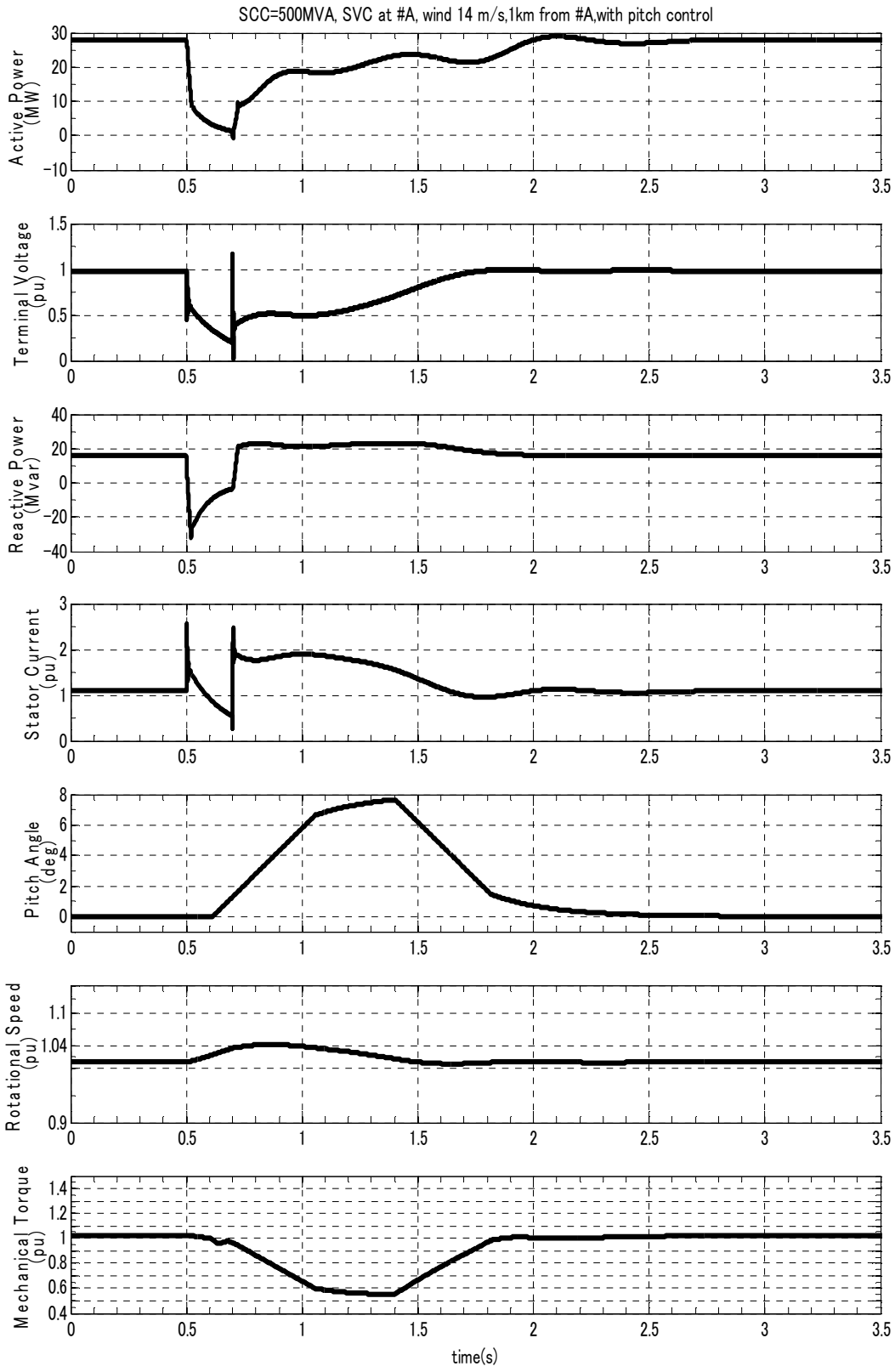

Figure. 3.12: Wind Farm Behavior (Proposal Case: with pitch control)

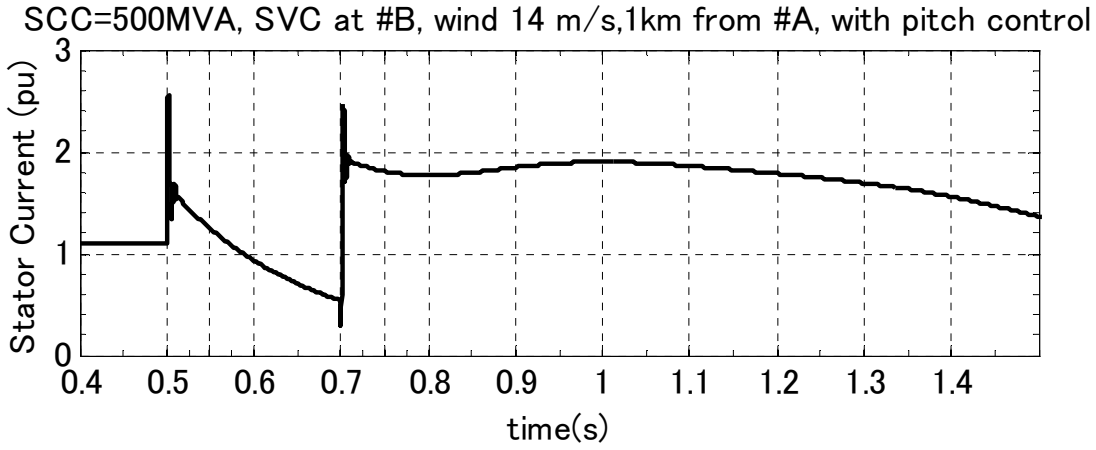

Figure 3.13: Stator current (Proposal Case: with pitch control)

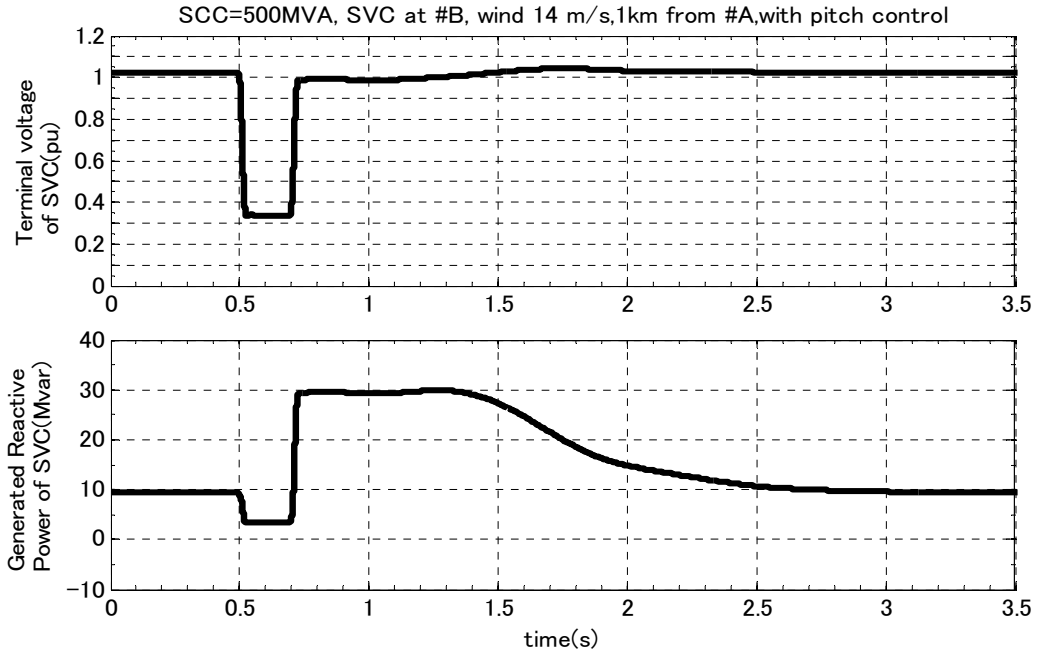

Figure 3.14: SVC behavior (Proposal Case: with pitch control)

3.7 CONCLUSIONS

This chapter described the concept and detailed description of the proposed pitch control. The effectiveness of this method is also shown. The kernel of the proposed pitch control is to release the active power extracted from the wind by adjusting the pitch angle of wind turbine blade according to the magnitude of voltage dip. Due to the use of disturbance as a control systems input, the proposed method is fallen into the group of feed-forward approach. The proposed control systems can modify the pitch angle in the short response time by the coordination of protective relay. Then the pitch angle is adjusted by PI controller based on the measurement of induction generator terminal voltage.

CHAPTER 4

PERFORMANCE OF PROPOSED PITCH CONTROL IN FIXED-SPEED WIND-TURBINE GENERATOR WITH INDUCTION GENERATOR

4.1 INTRODUCTION

In this chapter, the effectiveness of the proposed pitch control method for LVRT is confirmed by means of simulation studies. The objective of this study is related to the electromechanical dynamic behavior of WTG and hence, only the fundamental frequency component of voltages and currents is taken into account in all the simulation models. The simulation models in this chapter are explained in Chapter 3.

The performance of proposed pitch control is discussed under different grid stiffness with the consideration of

1) Different fault locations.
2) Different locations of Static Var Compensation System (SVC).

Moreover, the effectiveness of the proposed method is confirmed under several wind speeds condition. Design consideration is included by quantitative study in which the influence of sensitivity of control parameters on LVRT behavior is examined. As the proposed control method is based on the feed-forward approach, the comparison with feedback approach is done for clear understanding.

4.2 EVALUATION BY DIFFERENT SHORT CIRCUIT CAPACITY AND FAULT POINT

The effectiveness of the proposed pitch control is checked by simulation studies. By assuming the different fault points between node #A and #B (at 1km, 8km, 18 km of 19km long sub-transmission line from the node #A respectively) in Figure 3.7, the voltage along the sub-transmission lines is depressed until the faulted line is isolated. The fault sequence used in the simulation is the three-phase-to-ground fault occurred in one of the 66kV sub-transmission lines. The fault is occurred at 500 *ms* and the faulted line is isolated at 700 *ms* from the start point of simulation. In addition to these, LVRT behaviors of wind farm are explored by considering the two different locations (whether at node #A or node #B) of SVC and the three different stiffness (100MVA, 500MVA, 1000MVA of SCC respectively) of power systems.

4.2.1 SCENARIO 1 (SVC AT NODE #B, 1000MVA SCC, FAULT AT 1KM FROM NODE #A, WITHOUT PITCH CONTROL)

The LVRT behavior of wind farm for this scenario is shown in Figure 4.1 and Figure 4.2. The associated SVC behavior is also shown in Figure 4.3. In Figure 4.1, the generated active power of wind farm is lost at 2338 ms from the start point of simulation due to the wind farm disconnection after isolating the faulted line. When the fault is occurred at the distance of 1km from node #A, the generated terminal voltage is depressed suddenly to 0.5 p.u at the 500 ms. The generator terminal voltage continues depressing to the 0.03 p.u. until the faulted line is isolated at 700 ms. As explained in section 3.2, the imbalance between mechanical input and electrical output is occurred

which causes the rotor over speeding.

Once the faulted line is isolated at 700 ms, the terminal voltage tends to recover back. Consequently, SCIG absorbs more reactive power due to over speeding (not reached to the protection system limit of 1.1 p.u. at that instance) and this causes over current in the stator of SCIG (not reached to the protection system limit of 2 p.u. for 40ms at that instance) as shown in Figure 4.1 and Figure 4.2. However, the terminal voltage of SCIG is collapsed due to the continuous over speeding of rotor and unfortunately reached to the over speed protective relay limits for 40 ms at the time of 2338 ms from the start point of simulation. Therefore, WTG is disconnected from the grid by over speed protection in order to avoid the damaging.

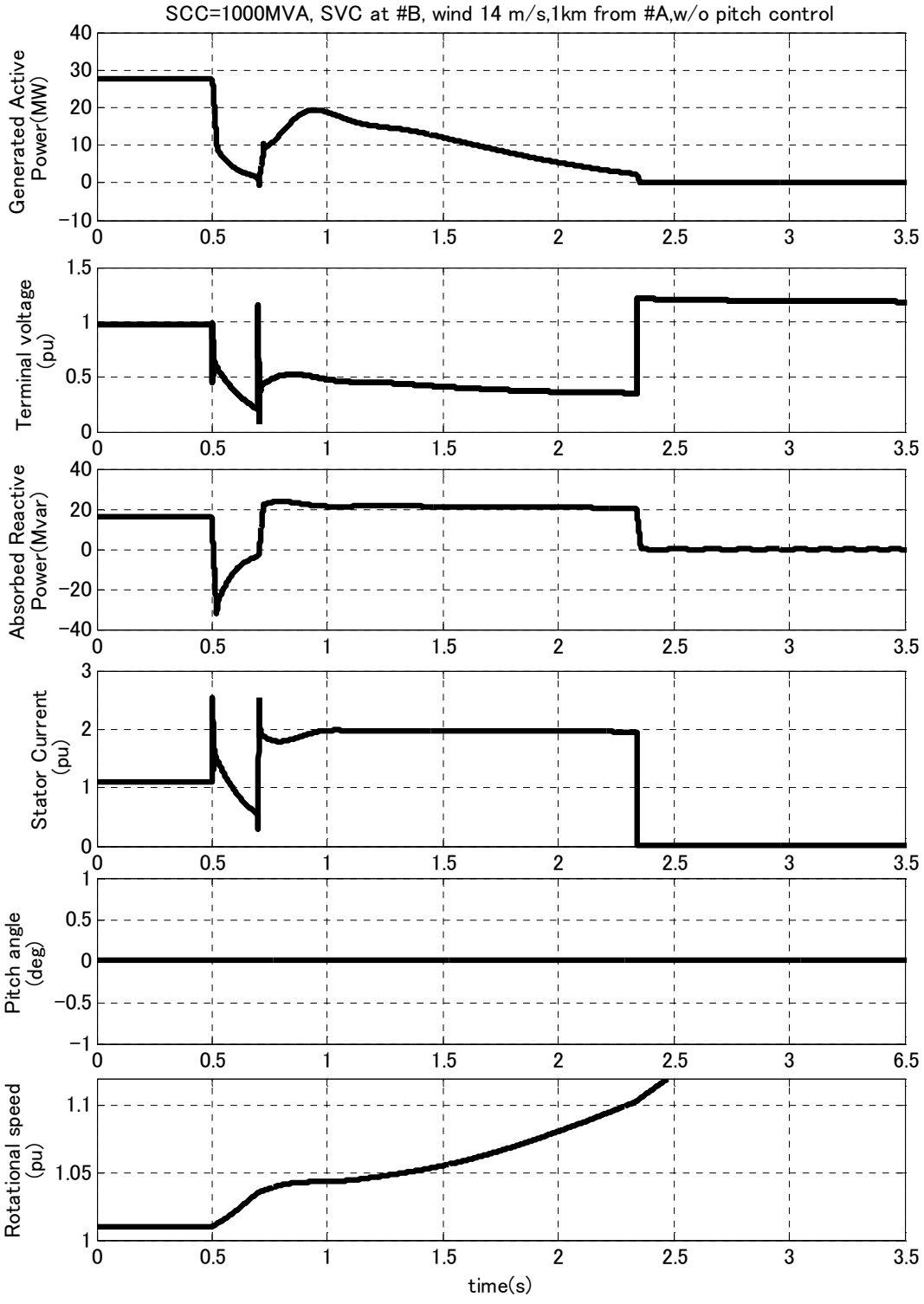

Figure 4.1: Wind Farm Behavior (scenario1: without pitch control)

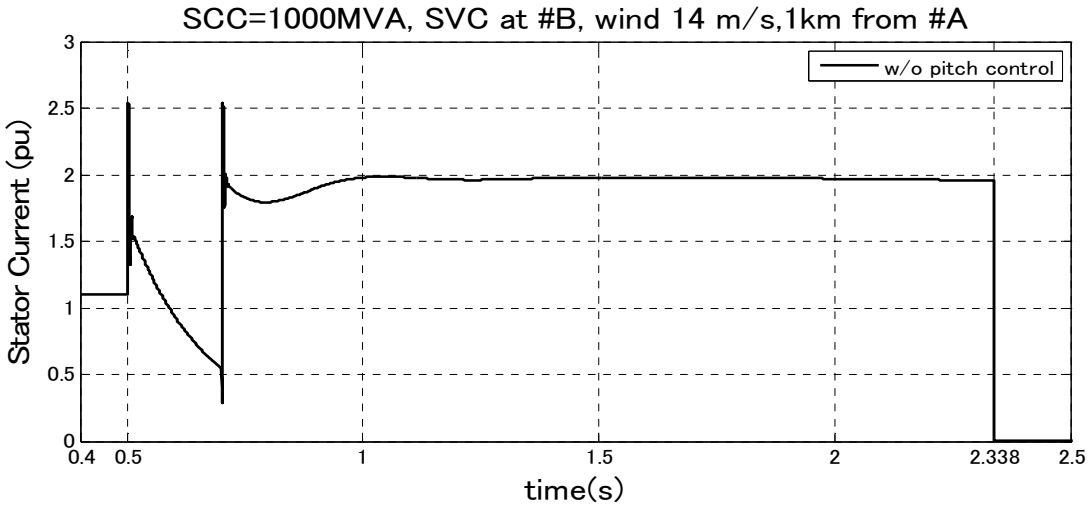

Figure 4.2: Stator current (scenario1: without pitch control)

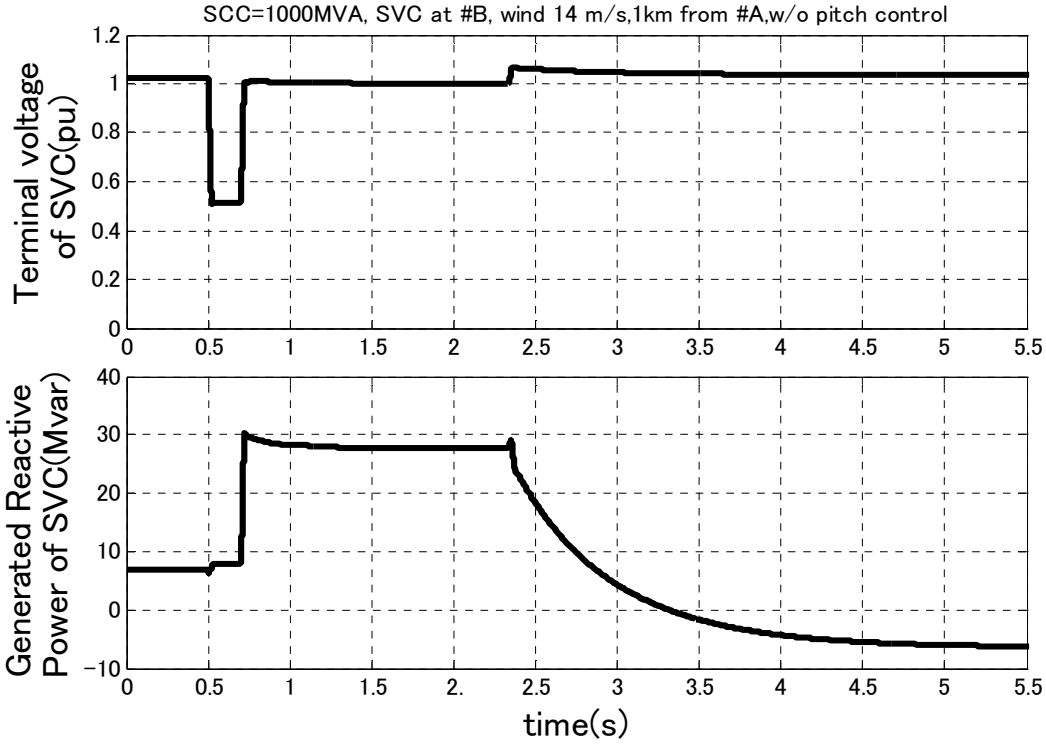

Figure 4.3: SVC Behavior (scenario1: without pitch control)

The behavior of SVC is shown in Figure 4.3. Due to the fault, the bus voltage controlled by SVC at node #B is depressed to the 0.5 p.u. until the fault is isolated. According to the reference voltage setting of voltage regulator, SVC injected the reactive power of 30Mvar once the voltage at node #B is recovered back. Although the SVC fed the reactive power absorbed by the wind farm during and after the fault, the continuous power supply of wind farm cannot be achieved in this case.

4.2.2 SCENARIO 2 (SVC AT NODE #B, 1000MVA SCC, FAULT AT 1KM FROM NODE #A, WITH PITCH CONTROL)

The LVRT behavior of wind farm for this scenario is shown in Figure 4.4 and Figure 4.5. The associated SVC behavior is also shown in Figure 4.6. With the use of proposed pitch control, the LVRT can be improved. By comparing Figure 4.1 with Figure 4.4, the over speeding of rotor can be reduced during the post-fault period in scenario 2. The rotor speed recovers back to pre-fault level (around 1 p.u.) at 1500ms. Consequently, the proposed pitch control contributes to voltage recovery and reduction of the over current in the stator of SCIG after the fault is isolated as shown in Figure 4.4 and Figure 4.5 respectively.

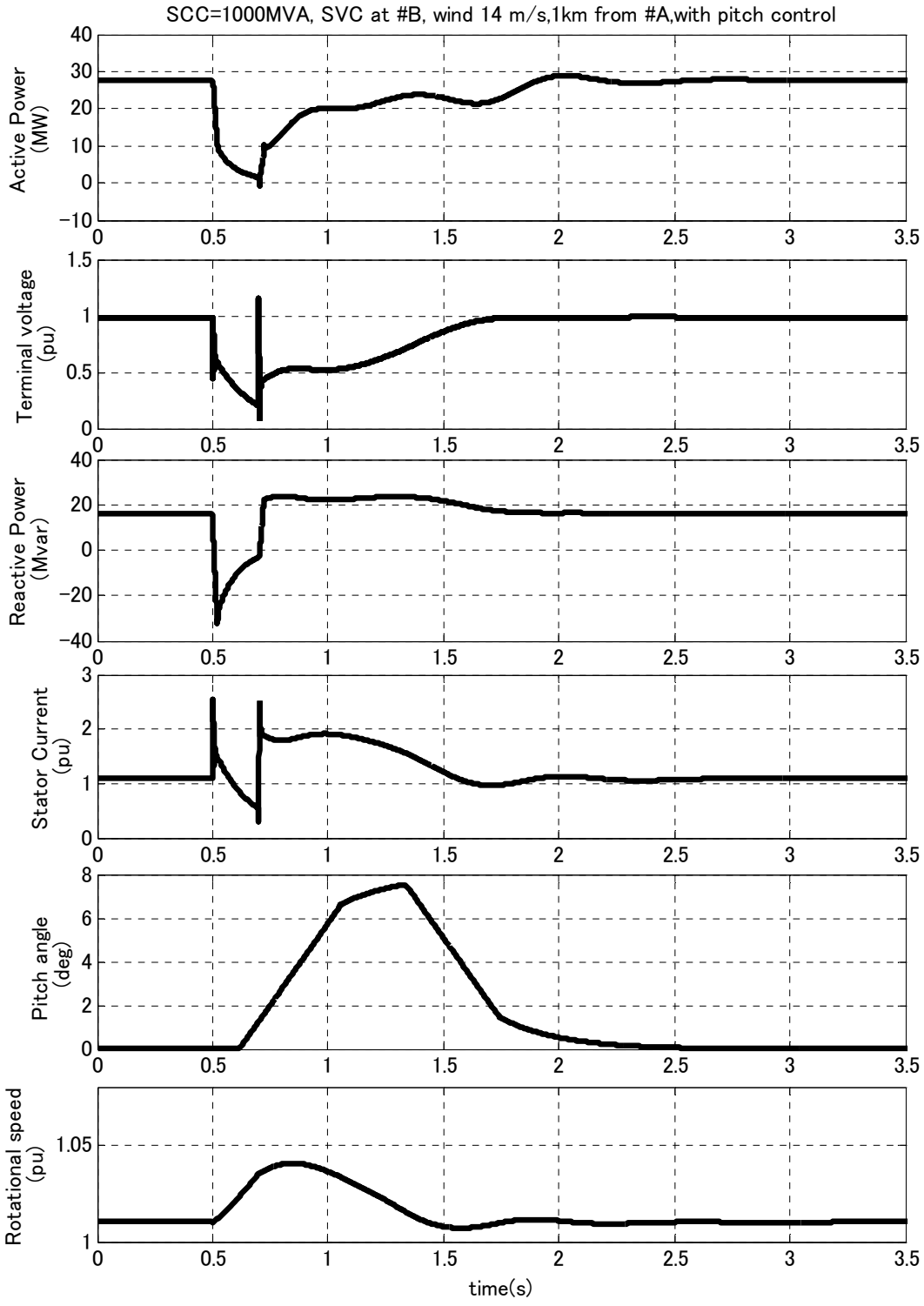

Figure 4.4: Wind Farm Behavior (scenario2: with pitch control)

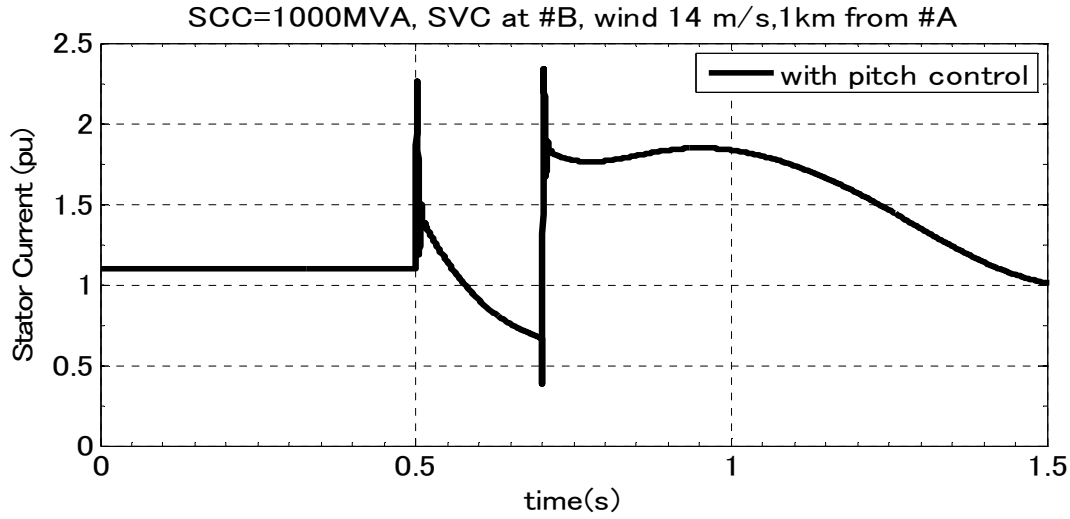

Figure 4.5: Stator current (scenario2: without pitch control)

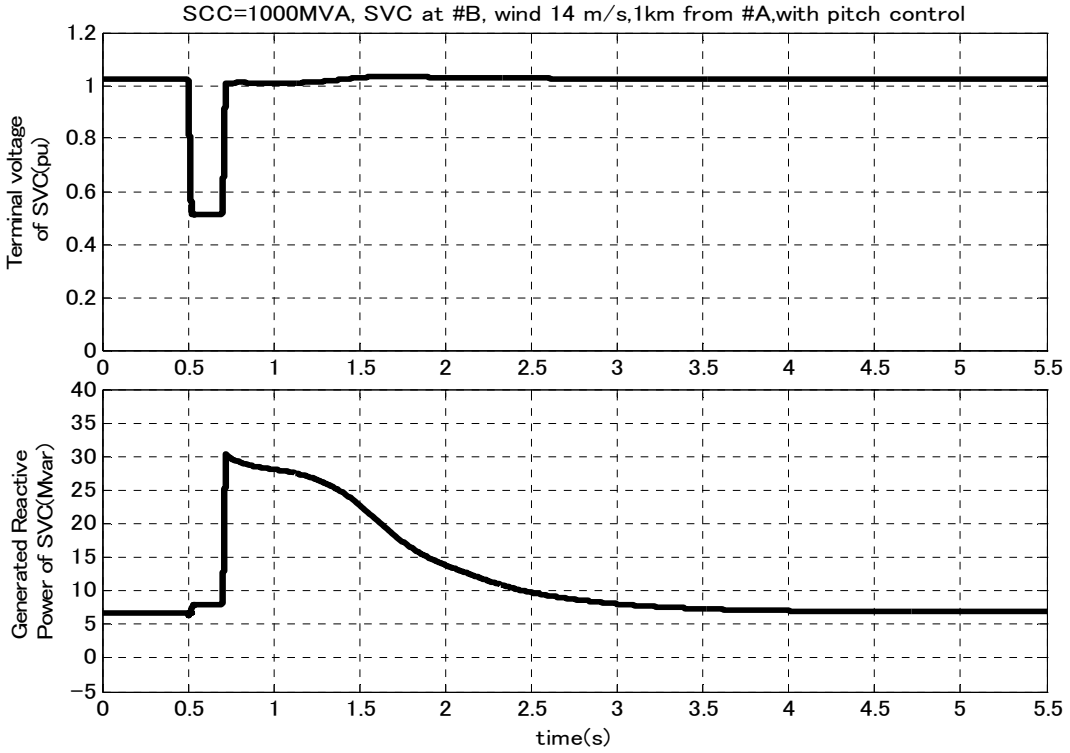

Figure 4.6: SVC Behavior (scenario2: without pitch control)

4.2.3 SCENARIO 3 (SVC AT NODE #A, 1000MVA SCC, FAULT AT 1KM FROM NODE #A WITHOUT PITCH CONTROL)

The LVRT behavior of wind farm in this scenario is shown in Figure 4.7 and Figure 4.8. The associated SVC behavior is also shown in Figure 4.9. In Figure 4.7, the generated active power of wind farm is lost at 1023 ms from the start point of simulation due to the wind farm disconnection after isolating the faulted line. As shown in Figure 4.8, wind farm is disconnected by over current protection.

The behavior of SVC in scenario 3 is shown in Figure 4.9. Due to the fault, the bus voltage controlled by SVC at node #B is depressed to the around 0 p.u. until the fault is isolated. According to the reference voltage setting of voltage regulator, SVC injected the reactive power of 30Mvar once the voltage at node #B is recovered back. The SVC fed the reactive power absorbed by the wind farm after the fault until the terminal voltage recovers back to the nominal voltage of 1 p.u. Due to the close location to fault, SVC cannot fed reactive power during the voltage dip.

By comparing scenario 1 and 3, the location of SVC with respect to the fault point will affect the reactive power injection during the voltage dip. This will cause the different phenomenon in disconnection of wind farm.

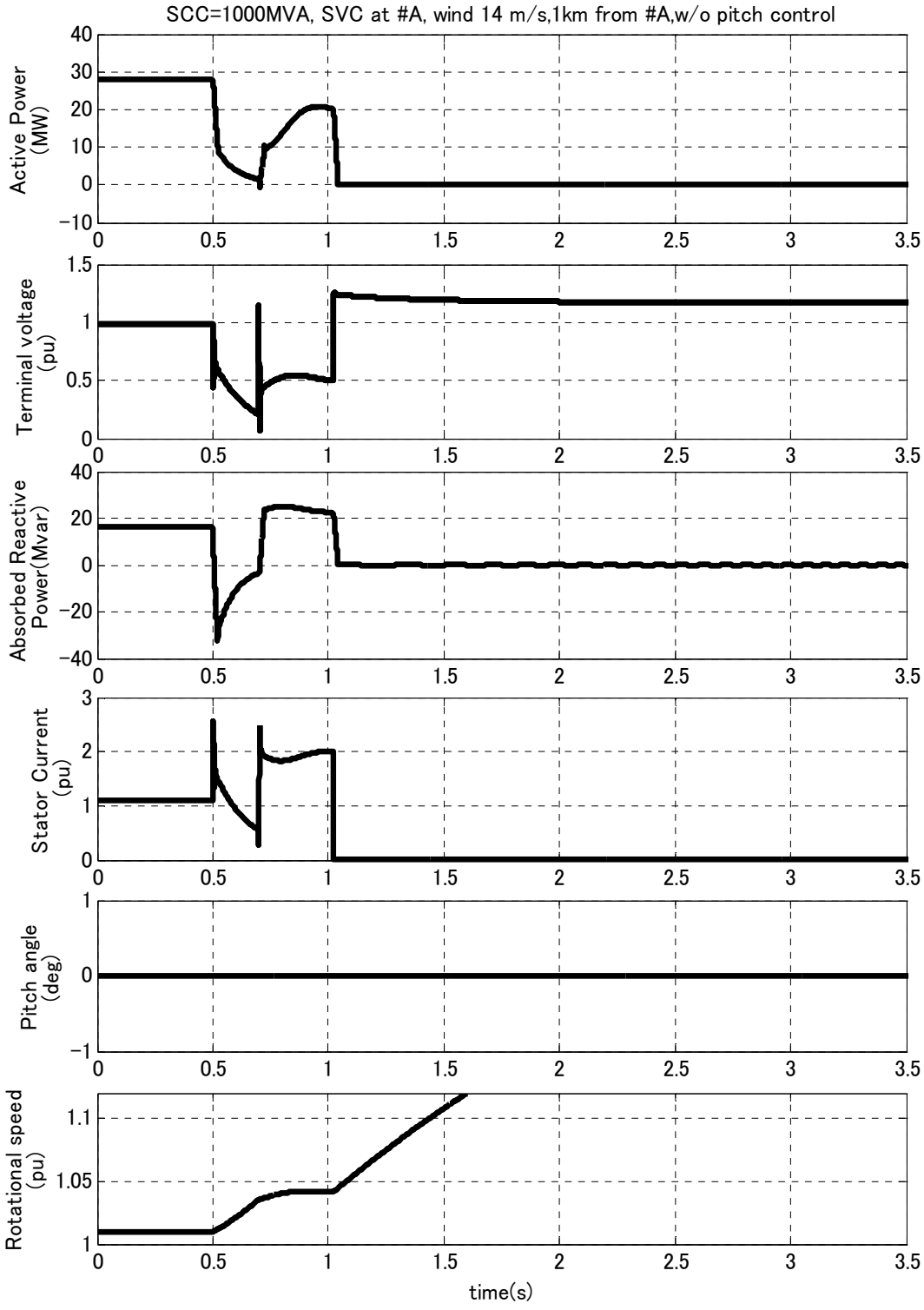

Figure 4.7: Wind Farm Behavior (scenario3: without pitch control)

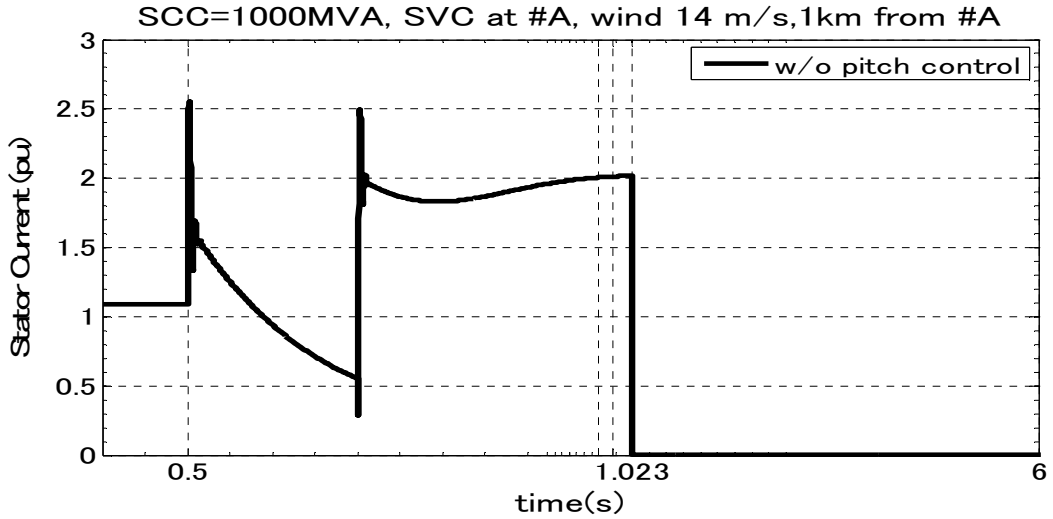

Figure 4.8: Stator current (scenario3: without pitch control)

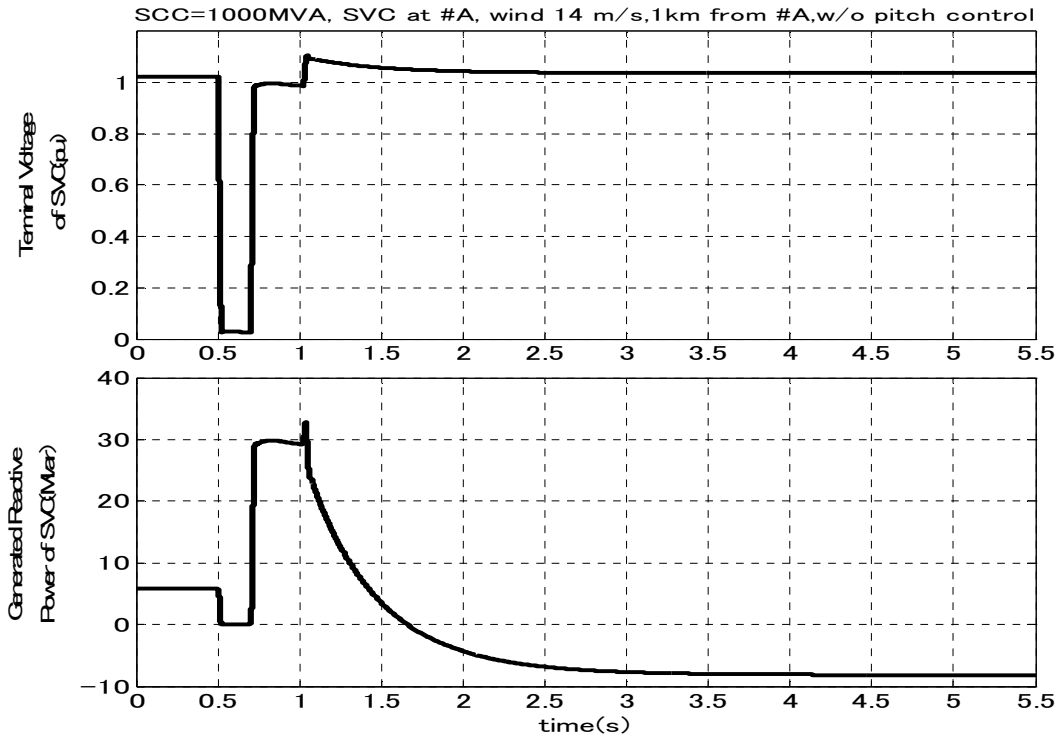

Figure 4.9: SVC Behavior (scenario3: without pitch control)

4.2.4 LVRT BEHAVIORS UNDER DIFFERENT SHORT CIRCUIT CAPACITY AND FAULT POINT (SVC AT NODE #B CASE)

Table 4.1. LVRT Behaviors for SVC at node #B (far from wind farm)

(SCC)	with pitch control	without pitch control	fault pt. from #A
100 MVA	Over Speed (5.59s)	Over Speed (1.534s)	1km
	Succeed	Over Speed (1.552s)	8km
	Over Speed (5.62s)	Over Speed (1.535s)	18km
500 MVA	Succeed	Over Speed (2.098s)	1km
	Succeed	Over Speed (2.392s)	8km
	Succeed	Over Speed (2.131s)	18km
1000 MVA	Succeed	Over Speed (2.338s)	1km
	Succeed	Succeed	8km
	Succeed	Over Speed (2.472s)	18km

The LVRT behaviors of wind farm are evaluated under different SCC and fault points. Table 4.1 summarizes the LVRT behaviors of wind farm for these cases in which the SVC is supposed to be connected at the node #B. In this table, the disconnection reason with corresponding time, and fault points are shown according to the SCC. The proposed pitch control is effective for all the cases of 500 MVA SCC and 1000 MVA SCC, as explained in previous sections.

In the 100 MVA SCC case, the proposed pitch control is only effective for the 8 km fault point case. LVRT cannot be achieved for 1 km fault point and 18 km fault point cases. For the 1 km fault point case, the voltage recovery capability of WTG is reduced due to the close fault location. Similarly, the fault at 18 km from node #A reduces the voltage support ability of SVC. Therefore, in the section 4.2.5, we considered the close

location of SVC to the wind farm in evaluation of LVRT.

The stiffness of power systems influences on LVRT behavior. LVRT can be achieved with the use of only SVC for the 8km fault point in 1000MVA SCC case. This is because the impact of fault on voltage support ability of SVC is less.

4.2.5 LVRT BEHAVIORS UNDER DIFFERENT SHORT CIRCUIT CAPACITY AND FAULT POINT (SVC AT NODE#A CASE)

Table 4.2. LVRT Behaviors for SVC at node #A (close to wind farm)

(SCC)	with pitch control	without pitch control	fault pt. from #A
100 MVA	Succeed	Over Speed (1.552s)	1km
	Succeed	Over Speed (1.572s)	8km
	Succeed	Over Speed (1.555s)	18km
500 MVA	Succeed	Over Speed (2.315s)	1km
	Succeed	Over Speed (2.998s)	8km
	Succeed	Over Speed (2.382s)	18km
1000 MVA	Succeed	Over current (1.023s)	1km
	Succeed	Succeed	8km
	Succeed	Over current (1.071s)	18km

Table 4.2 summarizes the LVRT behaviors of wind farm for the cases in which the SVC is supposed to be connected at the node #A. With the proposed pitch control, the disconnection of wind farm by over speed and over current can be avoided in all conditions.

For the only SVC cases in the 100 MVA SCC and the 500 MVA SCC, as mentioned before, the LVRT cannot be improved as wind farm is disconnected by over speed

protection. For 1 km fault point and 18 km fault point cases in 1000MVA, although the continuous connection can be achieved for the 8 km fault point, the wind farm is disconnected by over current protection of WTG. This phenomenon may be related to the close location of reactive power injection.

By comparing the Table 4.1 and Table 4.2, especially in SCC of 100 MVA case, the closed location of SVC to wind farm (at node #A) gives better LVRT performance than the far location of SVC from wind farm (at node #B). Two factors influence on LVRT behavior of wind farm. One is the location of SVC and the other is the SCC of power systems.

The voltage variation of network depends on the location of SVC. In the case of SVC at node #A (close to wind farm), the voltage variation at wind farm terminal is less than that of SVC at node #B (far from the wind farm). In consequence, the wind farm can inject more power during the terminal voltage recovery after isolating the fault. Therefore, in the case of SVC at node #A, the rotational speed increases slowly up to over speed limit compared with the case of SVC at node #B.

In addition, the larger in SCC results smaller voltage variation of network due to the smaller equivalent impedance. Therefore, except for the 1000MVA case in Table 4.2 (disconnection due to over current), it takes longer time for the rotor speed to reach the upper limit when the SCC becomes larger.

4.3 INVESTIGATION WITH DIFFERENT WIND SPEED

(SCC=500MVA, SVC at node #B, fault points of 1 km and 8km from node #A; between node A and B)

Due to the varying nature of wind, we also investigate the effectiveness of proposed pitch control under the different wind speed conditions from 7 m/s to 25 m/s.

Table 4.3 summarizes the LVRT behaviors of wind farm for the fault point of 1km from node #A. The proposed pitch control can improve LVRT at all wind speed range. For SVC only case, LVRT cannot be achieved for wind speed of 14~16 m/s and 21 m/s. The reason of disconnection in those wind speeds is related to the magnitude of terminal voltage recovery. In those wind speeds, the terminal voltage of WTG cannot recover back to nominal voltage from the 0.5 p.u. level during the post-fault period and this leads to continuation of over speeding. Except for those wind speeds, the use of SVC improves the terminal voltage to recover higher than 0.5 p.u. level during the post-fault period. This phenomenon seems to be related to the voltage regulation characteristic of network with respect to the WTG operation state and performance of SVC.

The similar investigations are also performed for the fault point of 18km from node #A. The simulation results are summarized in Table 4.4. The proposed pitch control can improve LVRT at all wind speed range. For SVC only case, LVRT cannot be achieved for wind speed of 14 m/s, 15 m/s, 16 m/s, due to the disconnection by over speed protection, as mentioned above.

Table 4.3. LVRT Behaviors for fault point of 1km from node #A; between node A and B

wind speed(m/s)	7-13	14- 16	17-20	21	22-25
Only SVC	Succeed	Fail	Succeed	Fail	Succeed
SVC&Pitch	Succeed				

Table 4.4. LVRT Behaviors for fault point of 18km from node #A between node A and B

wind speed(m/s)	7-13	14- 16	17-20	21	22-25
Only SVC	Succeed	Fail	Succeed	Succeed	Succeed
SVC&Pitch	Succeed				

4.4 INVESTIGATION BY SLOWER PITCH ACTUATOR CHARACTERISTICS

(With pitch control scenario of SCC=500MVA, SVC at node #B, fault point of 1 km from node #A between node A and B)

We also checked the effectiveness of the proposed pitch control with respect to the servo time constant and rate of change of pitch angle, dβ/dt. Figure 4.10 is the simulation results with pitch control scenario of the same as simulation conditions mentioned in section 3.6.1 except the difference in pitch actuator model parameters. The servo time constant, T_{SERVO}=1s and dβ/dt=±10 [deg/s] are used as a slower pitch actuator. According to Figure 4.10, the proposed pitch control method is effective with the slower pitch actuator condition of up to T_{SERVO} =1s and dβ/dt=±10 [deg/s]. Due to the slow response in pitch angle, the slower voltage recovery occurs comparing with the proposal case in section 3.6.1.

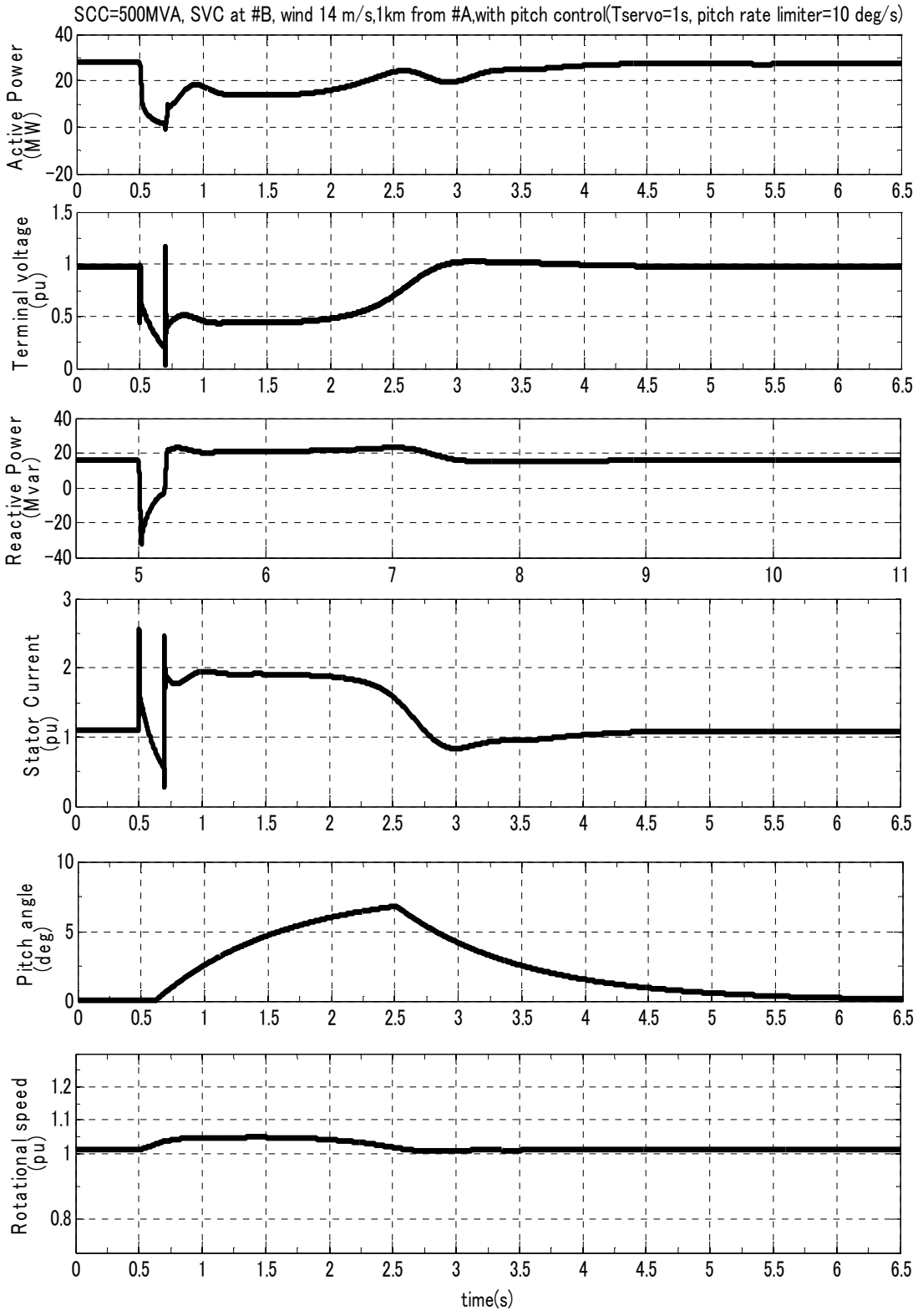

Figure 4.10: Wind farm behavior (with T_{servo}=1s and dβ/dt=±10 [deg/s])

4.5 DESIGN CONSIDERATION IN SENSITIVITY OF CONTROL PARAMETERS ON LVRT BEHAVIOR

In this section, the influence on LVRT behavior by sensitivity of control parameters is explored. The proposed pitch control includes Proportional Integral (PI) controller, as explained in section 3.3, which has influence on the LVRT behavior. Therefore, by simulation study, the quantitative analysis is carried out to find out the influence of PI parameters on LVRT with respect to response time of control action. According to this study, we can say that the range of the proportional gain parameter in PI controller should be between 8 and 15 to get the appropriate LVRT behavior for various conditions. The range of integral gain parameter is satisfied between 0 and 50 accordingly.

The simulation results can be divided into 2 groups according to the delay time setting, T_{uvr} in section 3.3, to active pitch control with respect to the specific range of proportional and integral gains. The following two cases are studied under the condition of SCC=500MVA, T_{servo}=0.25s, SVC at #A, wind speed=14m/s, fault at 1 km from #A, 200ms of 3phase short circuit fault duration from 2s of simulation starting time.

Case (1) Fast Response Time Case [T_{uvr} =0.1s]

(a) 0=<K_p =<15

(b) 0=<K_i =<50

Case (2) Slower Response Time Case [T_{uvr} =1s]

(a) 0=<K_p =<15

(b) 0=<K_i =<50

4.5.1 FAST RESPONSE TIME CASE

[T_{uvr}=0.1s]

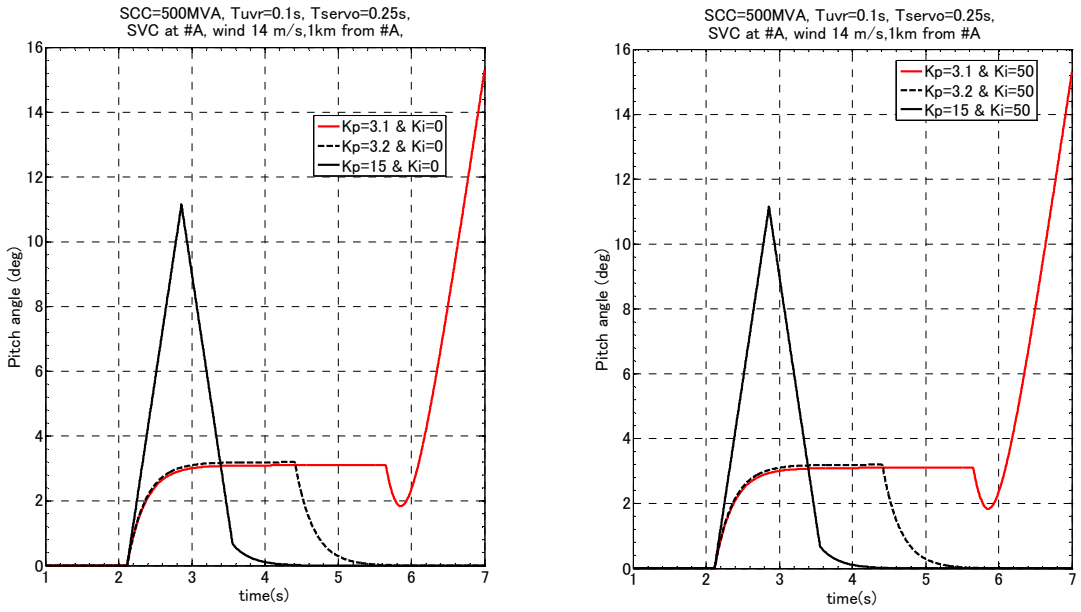

(a) K_i=0 (b) K_i =50

Figure 4.11: Pitch Angle

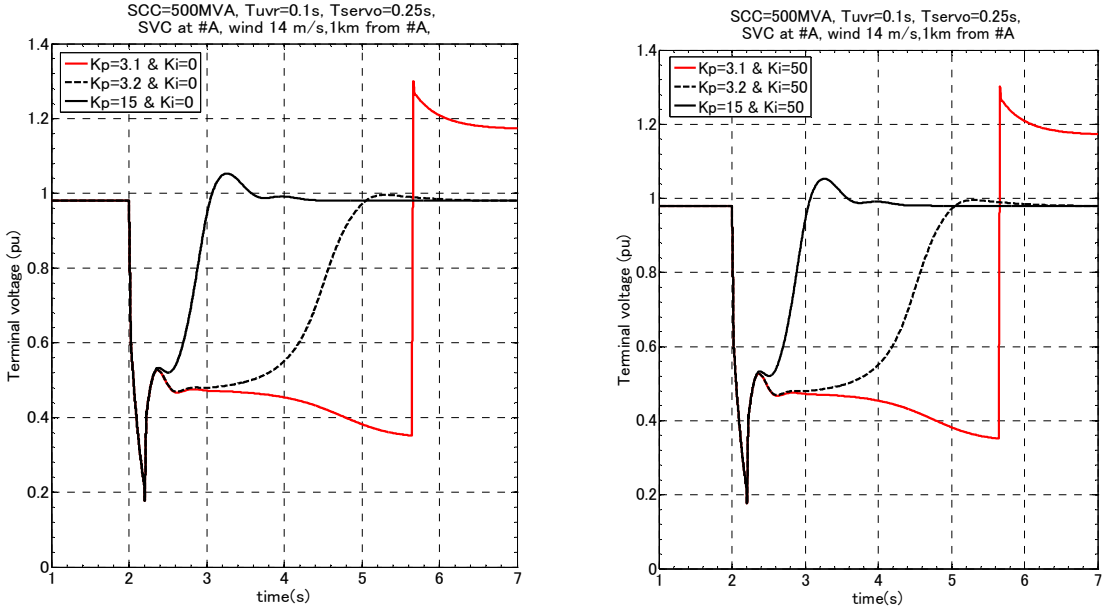

(a) K_i=0 (b) K_i =50

Figure 4.12: Terminal Voltage

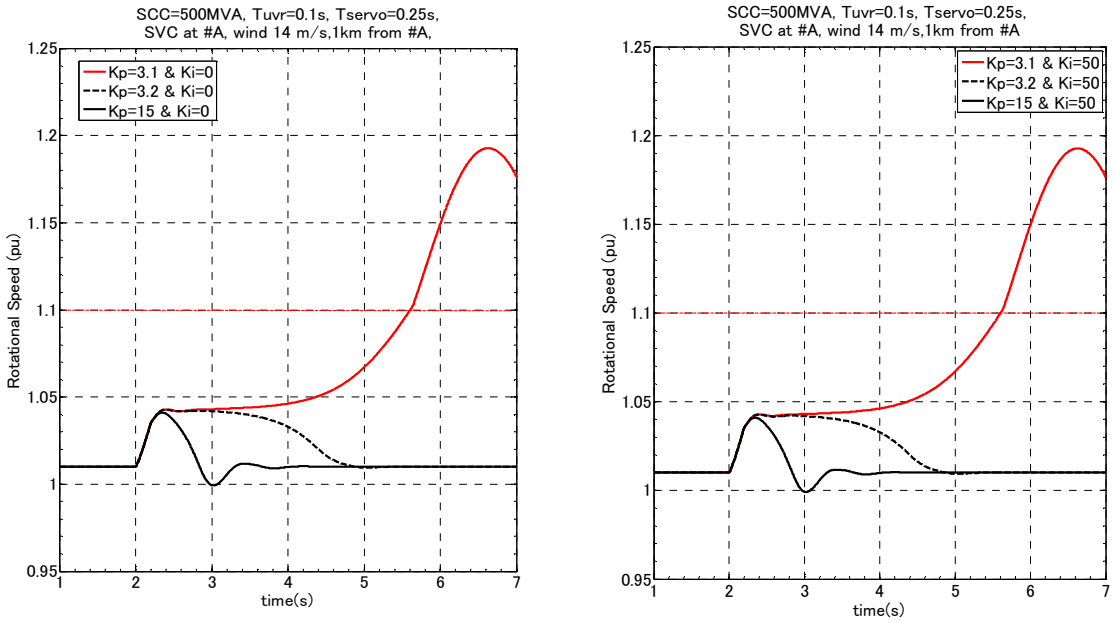

(a) K_i=0 (b) K_i =50

Figure 4.13: Rotational Speed

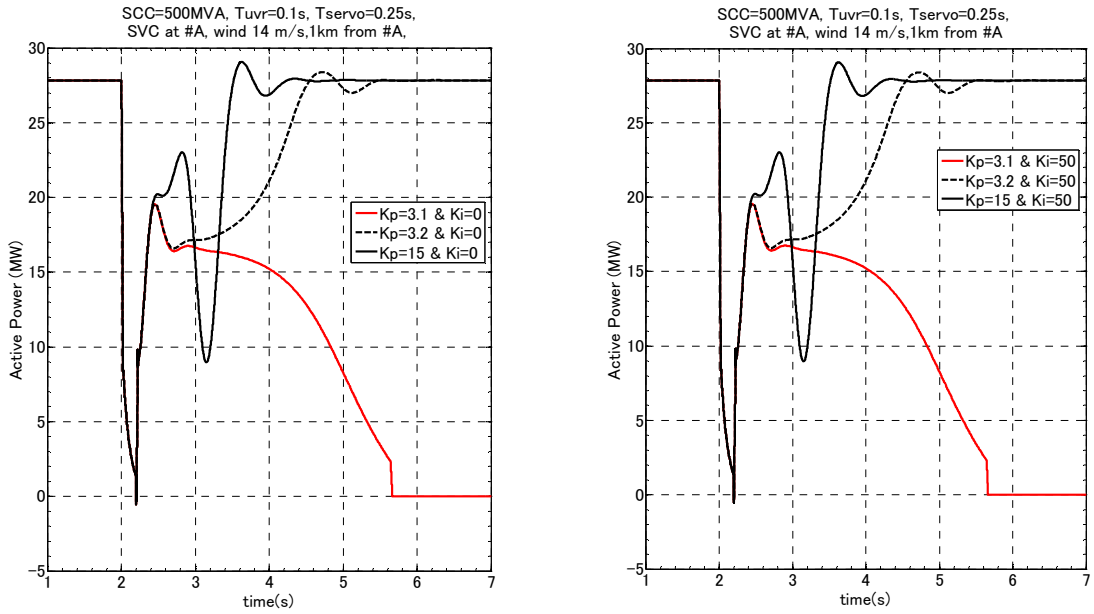

(a) K_i=0 (b) K_i =50

Figure 4.14: Active Power

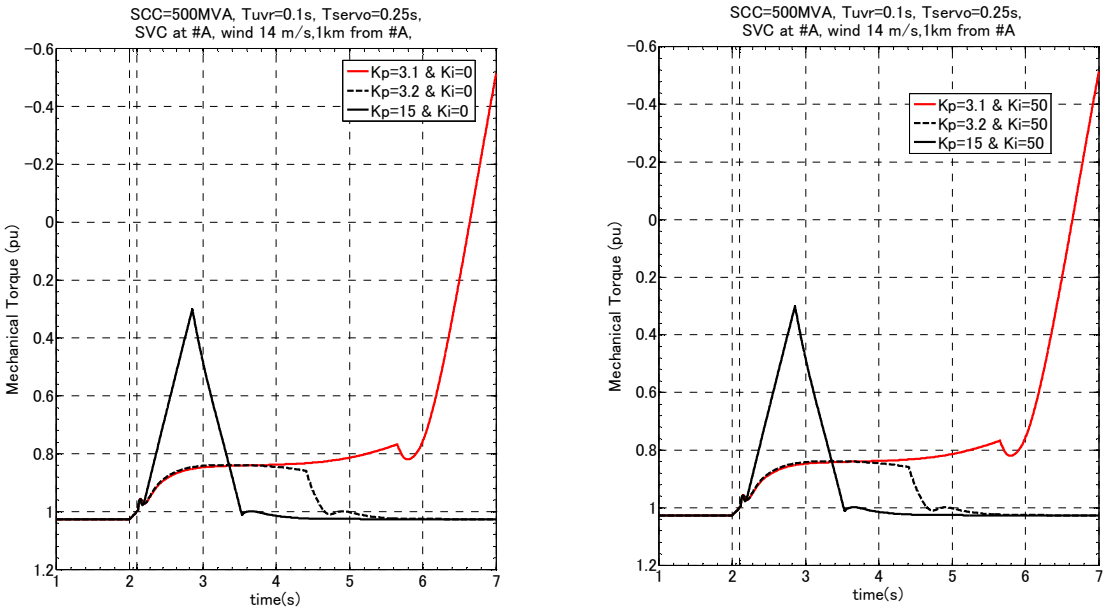

(a) K_i=0 (b) K_i =50

Figure 4.15: Mechanical Torque of WTG

In the case of delay time, T_{uvr}=0.1s, the wind farm fails to satisfy LVRT with the range of 0 ≤K_p <3.2 and 0≤K_i ≤50, and achieves to satisfy LVRT with the range of 3.2 ≤K_p <15 and 0≤K_i ≤50. The selected results are shown in Figure 4.11~ Figure 4.15. The pitch angles with PI parameters (K_p =3.1 & K_i =0), (K_p =3.2 & K_i =0), (K_p =15 & K_i =0) are shown in Figure 4.11. The pitch angles start to change with 100ms delay after detecting the voltage dip (at 2.1s). Increasing proportional gain parameter results in more pitch angle changing during the post fault period (>2.2s).

As shown in Figure 4.12, we can check that wind farm (with parameter of K_p =3.1 & K_i =0) is disconnected at 5.644s by over speed (see Figure 4.13). The WTG voltage dip behavior in all PI parameters (K_p =3.1 & K_i =0), (K_p =3.2 & K_i =0), (K_p =15 & K_i =0) are almost the same. The behavior of voltage recovery is different according to the PI parameters. The increase in K_p , the voltage recovery becomes faster. For the K_p =15, the over-shoot in voltage recovery is found although the fast voltage recovery is

achieved.

The results of associated rotational speeds are plotted in Figure 4.13. We can see that the ability to return to nominal speed is related to proportional gain. For the K_p =15, the rotational speed oscillation is found.

By comparing with the Figure 4.14 and Figure 4.15, the proportional gain, K_p =15, results in more power oscillation during voltage recovery period comparing to that of K_p =3.2 although mechanical torque oscillation is not found.

The influence of integral gain is not found in this case.

4.5.2 SLOWER RESPONSE TIME CASE

[T_{uvr}=1s]

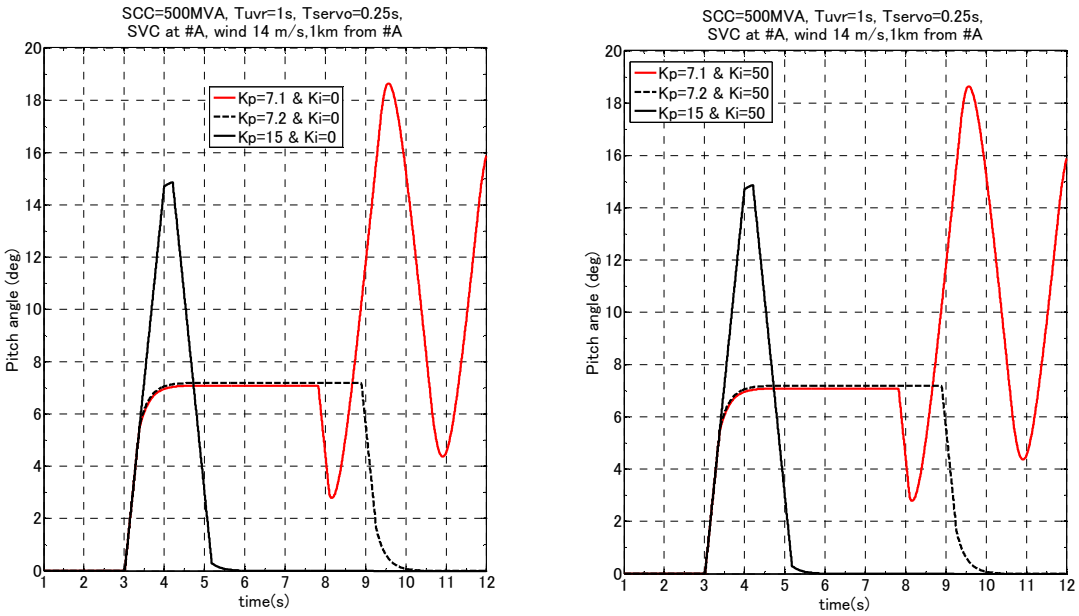

(a) K_i=0 (b) K_i =50

Figure 4.16: Pitch Angle

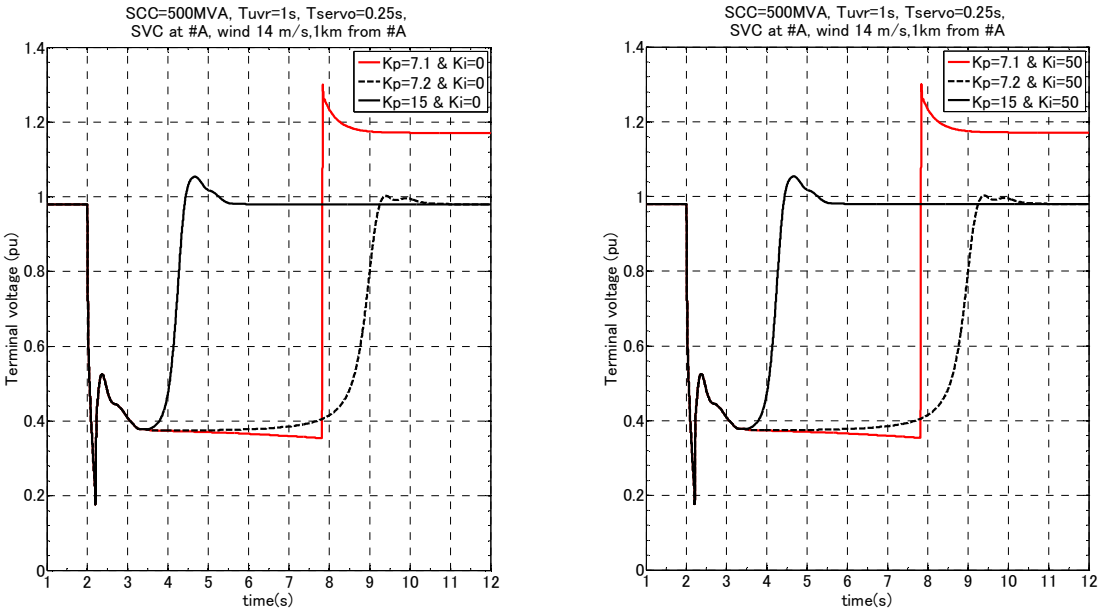

(a) K_i=0 (b) K_i =50

Figure 4.17: Terminal Voltage

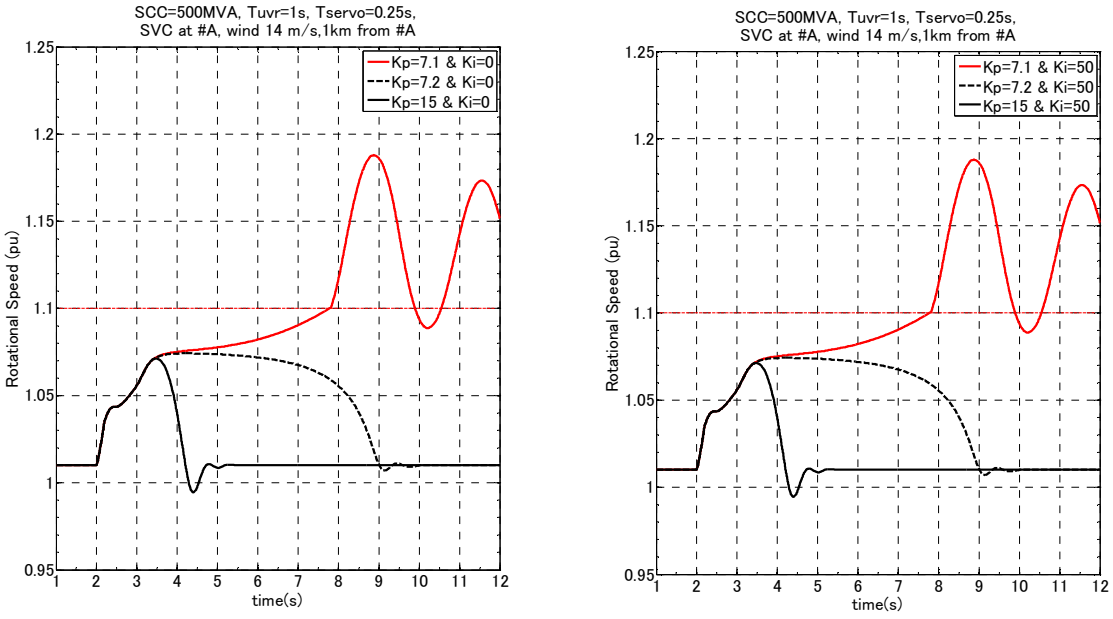

(a) K_i=0 (b) K_i =50

Figure 4.18: Rotational Speed

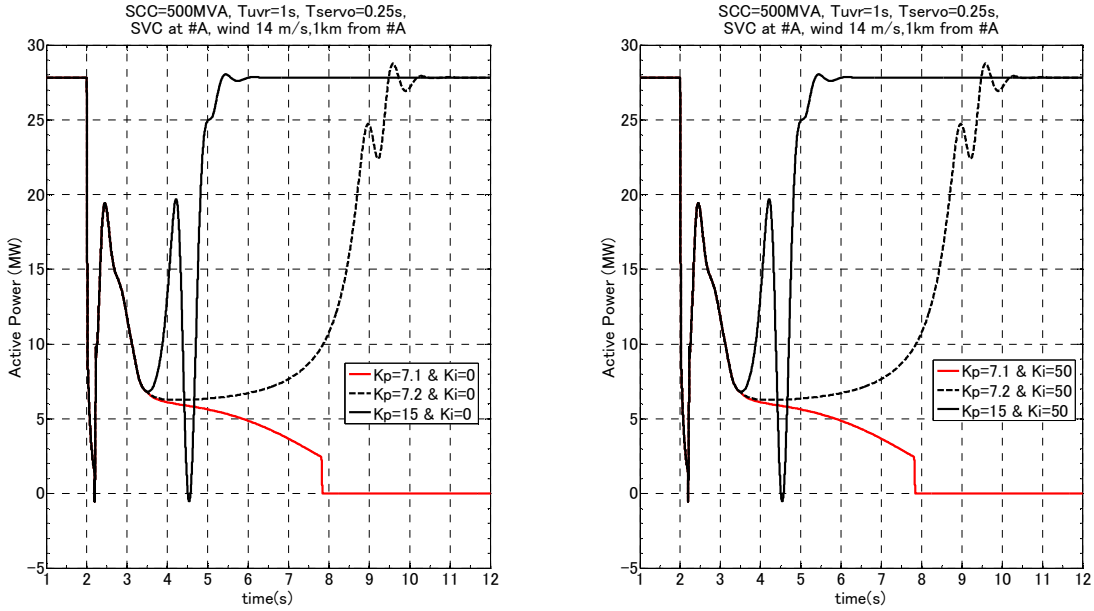

(a) K_i=0 (b) K_i =50

Figure 4.19: Active Power

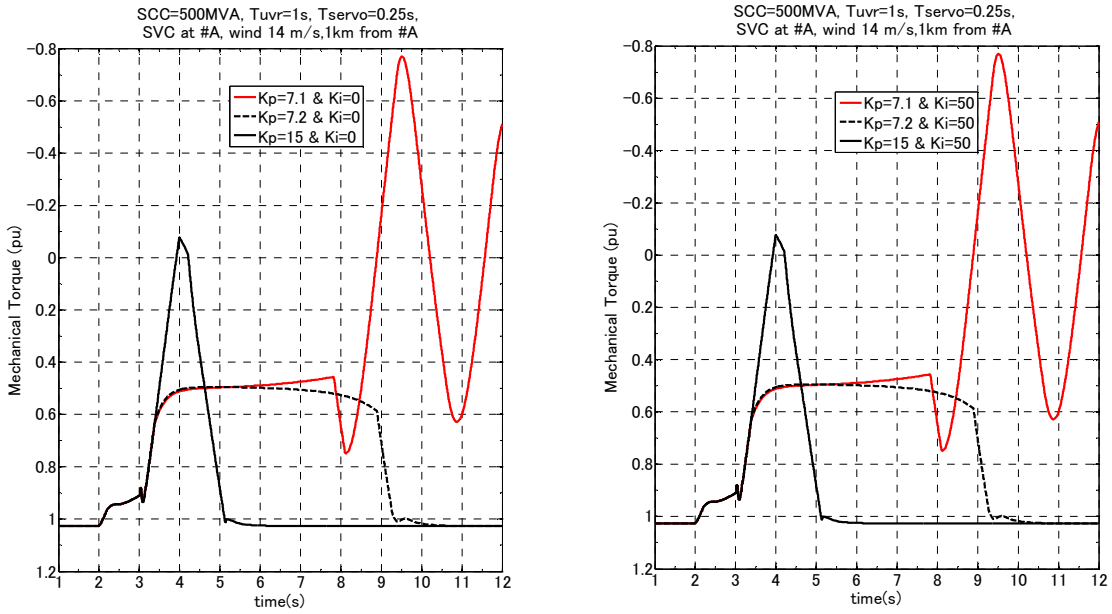

(a) K_i=0 (b) K_i =50

Figure 4.20: Mechanical Torque of WTG

In the case of delay time, T_{uvr}=1s, the wind farm fails to satisfy LVRT with the range of $0 \le K_p < 7.2$ and $0 \le K_i \le 50$, and achieves to satisfy LVRT with the range of $7.2 \le K_p < 15$ and $0 \le K_i \le 50$. The selected results are shown in Figure 4.16~ Figure 4.20. The pitch angles with PI parameters (K_p =7.1 & K_i =0), (K_p =7.2 & K_i =0), (K_p =15 & K_i =0) are shown in Figure 4.16. The pitch angles start to change with 1s delay after detecting the voltage dip (at 3s). Increasing proportional gain parameter results in more pitch angle changing during the post fault period (>2.2s). For (K_p =7.1 & K_i =0) case, the oscillation of pitch angle occurred due the hunting of normal mode pitch controller after disconnection. The more study is needed to explain.

As shown in Figure 4.17, we can check that wind farm (with parameter of K_p =7.1 & K_i =0) is disconnected at 7.82s by over speed (see Figure 4.18). The WTG voltage dip behavior in all PI parameters (K_p =7.1 & K_i =0), (K_p =7.2 & K_i =0), (K_p =15 & K_i =0)

are almost the same. The behavior of voltage recovery is different according to the PI parameters. The increase in K_p , the voltage recovery becomes faster. For the K_p =15, the over-shoot in voltage recovery is also found although the fast voltage recovery is achieved.

The results of associated rotational speeds are plotted in Figure 4.18. We can see that the ability to return to nominal speed is related to proportional gain. For the K_p =15, the rotational speed oscillation is also found.

By comparing with the Figure 4.19 & Figure 4.20, the proportional gain, K_p =15, results in more power oscillation during voltage recovery period comparing to that of K_p =7.2.

The influence of integral gain is not also found in this case.

4.5.3 APPLICABLE RANGES OF PROPORTIONAL GAIN

Figure 4.21 and Figure 4.22 show the relationship between the proportional gain value and UVR relay pickup time delay in the case of 500 MVA SCC when the SVC is connected at node #A and #B, respectively. For the fastest response time, 0.1s, the LVRT can be achieved with the proportional gain value between 3.2 and 15 in the case of SVC at node #A, and between 3.9 and 15 in case of SVC at node #B. Beyond the gain value of 15, the active power oscillation is observed during the voltage recovery period. The integral gain value can be applied up to 50 with respect to those proportional gains. The trend of narrowing the range of gain value can be found in increasing time delay to initiate the pitch control.

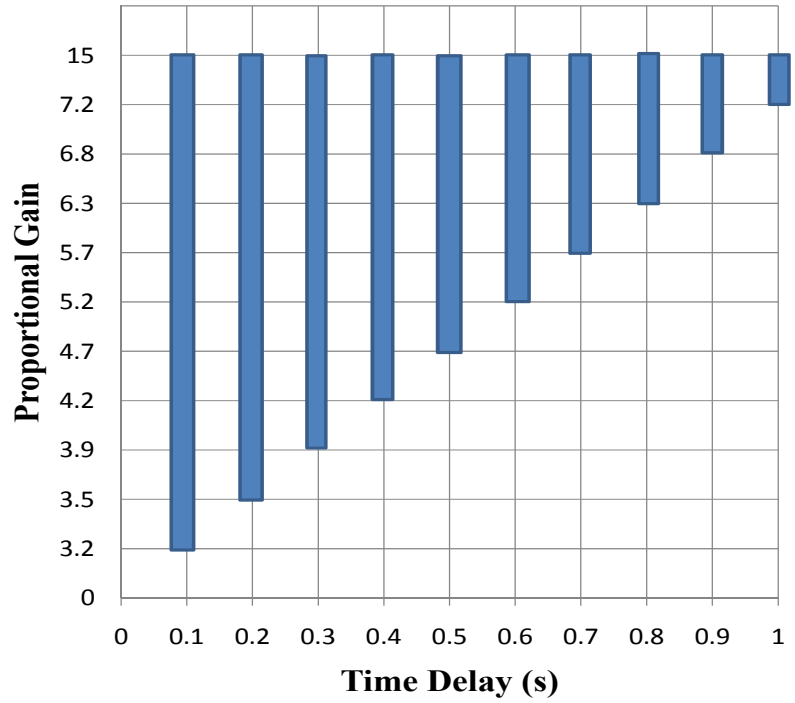

Figure 4.21 Applicable gain ranges vs. delay time (SVC at node #A case)

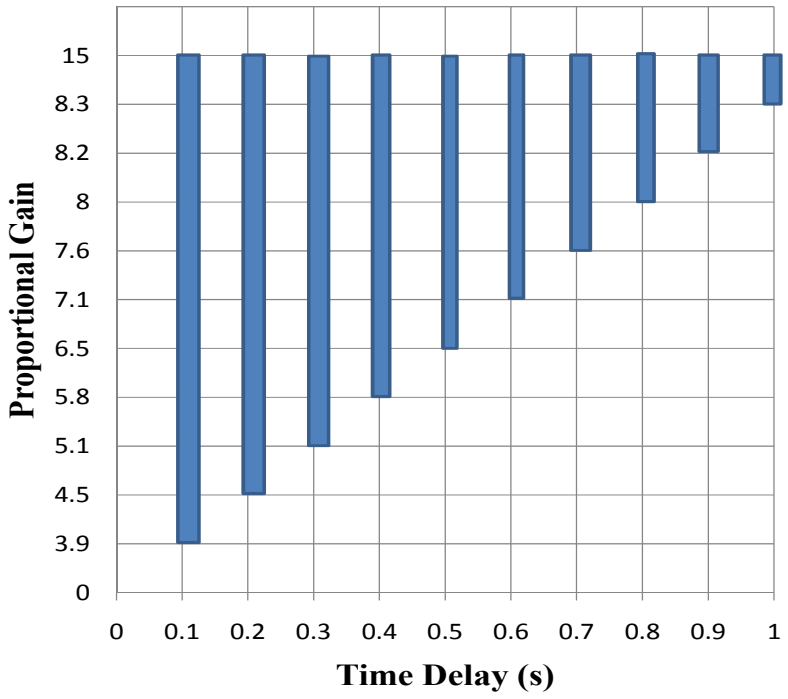

Figure 4.22 Applicable gain ranges vs. delay time (SVC at node #B case)

As shown in the Figure 4.23 and Figure 4.24, the adjustment of proportional gain can improve the voltage recovery at the terminal of WTG. Increasing the proportional gain parameter results less active power generation of WTG. This will cause the less reactive power absorption from the power systems for voltage recovery during the post fault period. Therefore, the performance of proposed method can be improved in the case of slower response time of UVR.

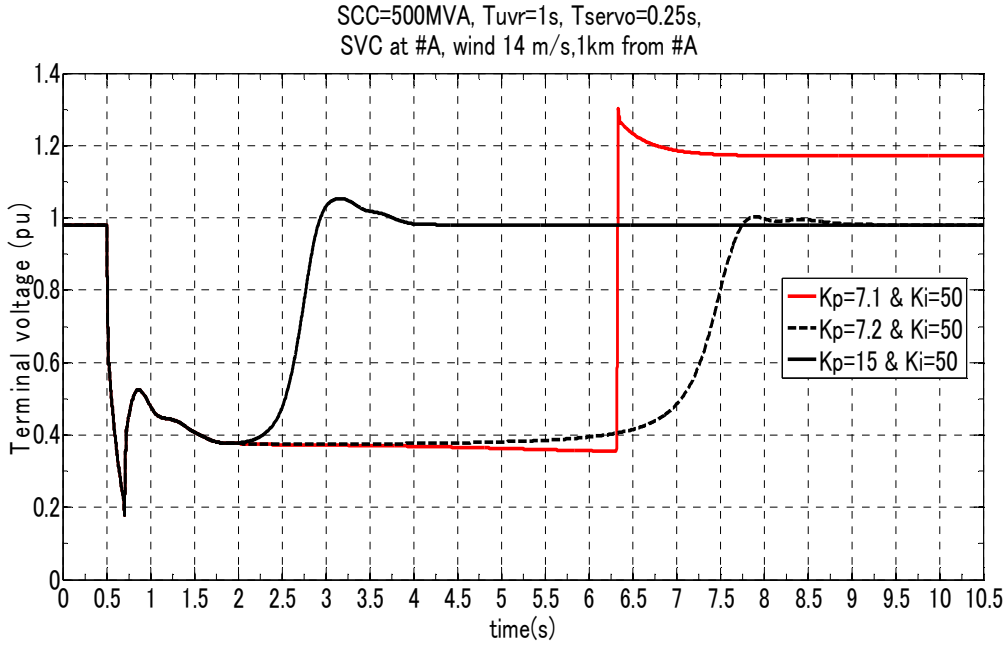

Figure 4.23: Voltage recovery with respect to the proportional gain and delay time (SVC at node #A case)

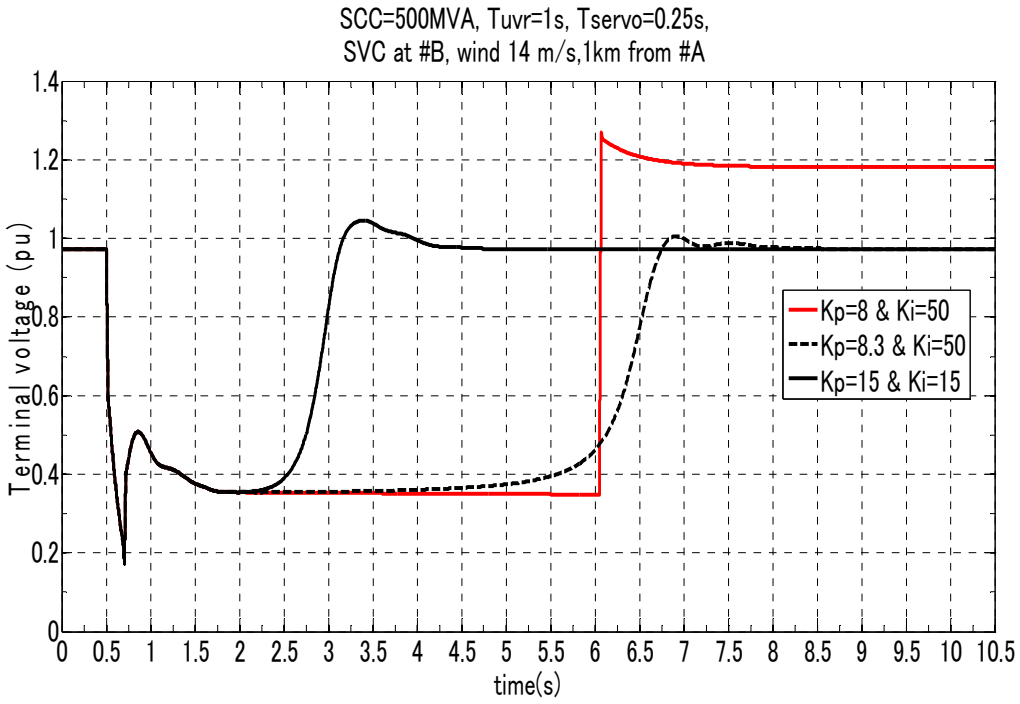

Figure 4.24: Voltage recovery with respect to the proportional gain and delay time

(SVC at node #B case)

4.6 COMPARISON STUDY WITH FEEDBACK CONTROL APPROACH

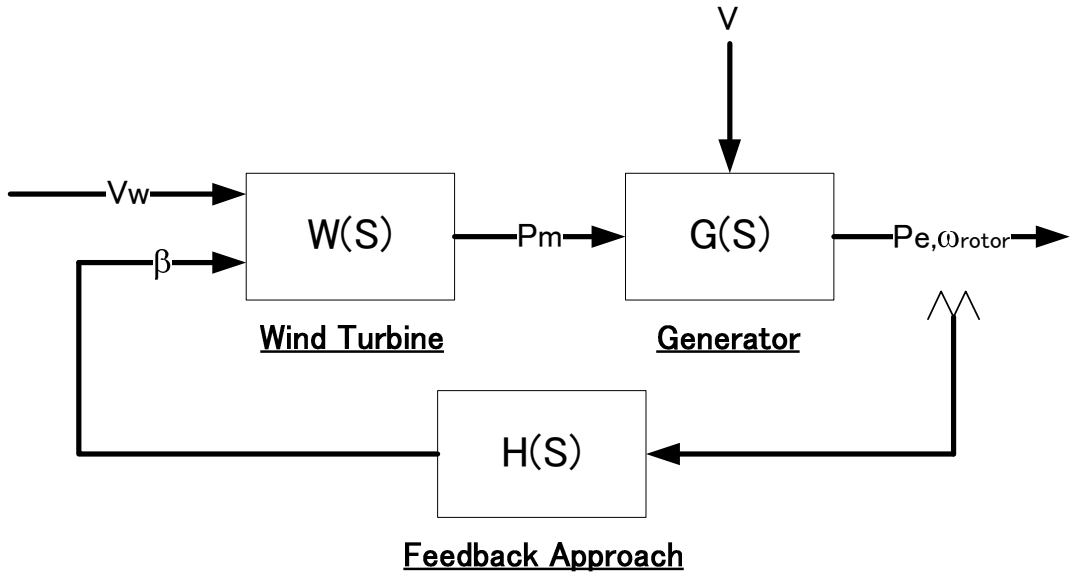

Figure 4.25: Outline of pitch angle control in feedback approach

The aim of pitch angle (β) control in conventional way is to regulate the mechanical power (Pm) extracted from the wind (V_w) to operate the WTG at desired active power (Pe) or rotor speed (ω_{rotor}). It is usually done by the supervisory control or by means of the feedback control approach in WTG, as shown in Figure 4.25. In FSWT, pitch control is used to limit the generated active power at rated capacity in the case of the rated wind speed and above. In VSWT, pitch control is used to get the maximum output generation power at the associated rotational speed with respect to the wind speed.

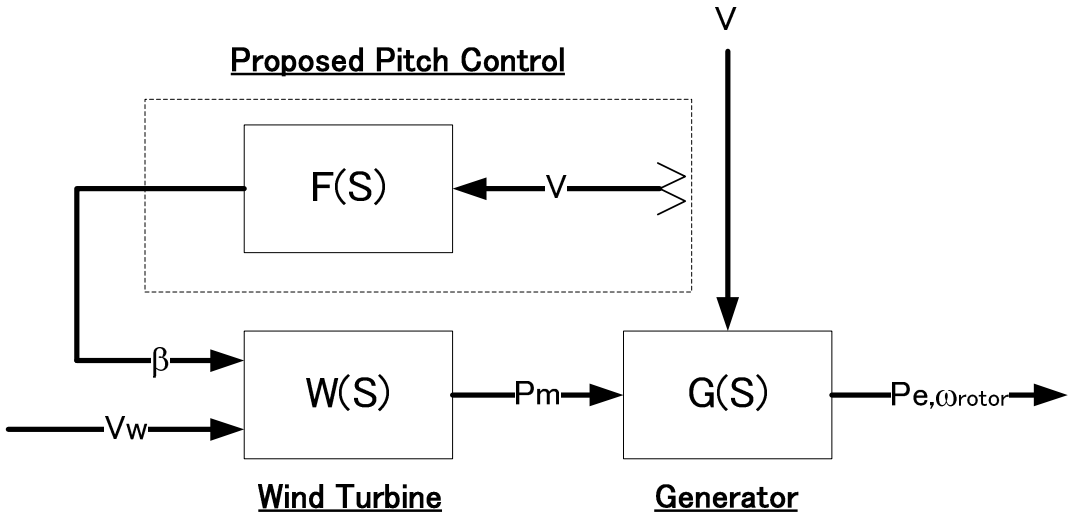

Figure 4.26: Outline of pitch angle control in proposal

The Figure 4.26 shows the outline of pitch angle control in proposed approach. The proposed pitch control is based on the feed-forward approach. If the disturbance can be measured and known in advance; even approximately or statistically, a correcting control action can be added for the compensation of disturbance. This is known as feed-forward control. The proposed control method uses the terminal voltage of wind turbine (V) for initiating the control action and using as input to LVRT mode controller. As shown in Figure 4.26, the terminal voltage is a disturbance to the WTG; i.e. G(s) and W(s). Therefore, the proposed pitch control method is fallen into the group of the feed-forward control method.

The LVRT requirement is specified by the power system operators; based on their experiences in wind energy integration and the practices of the systems operation. Therefore, the effect of the disturbance can be predicted and the use of feed-forward control approach is possible.

From the perspective of classical control theory, comparison regarding to the stability and response of controller can be done between the feed-forward approach and feedback approach as in the following Table 4.5.

Table 4.5 Comparison between feedback and feed-forward approach

	Feedback Approach	Feed-forward Approach
Stability	Characteristics of controller have influence on the stability of WTG all the time.	Characteristics of controller have influence on the stability of WTG only during the period of disturbance.
Response	Starts to response after the effect of disturbance is happening.	Starts to response once the occurring of disturbance is detected.

Therefore, from the view point of the stability and response time, the proposed pitch control has advantages and disadvantages over the conventional feedback control approach, as follows.

Advantages:

1) Comparing to the active power (Pe) feedback control, the proposed pitch control can contribute LVRT capability which cannot be achieved in conventional approach. The reason is that the proposed method uses feed-forward control approach in which the voltage dip is measured and accounted for before the occurring of voltage

dip affect; i.e. reaching to the protection system limits of WTG which cause the lack of LVRT capability.

2) Comparing to the rotor speed (ω_{rotor}) feedback control, the proposed pitch control can contribute the faster rate of voltage recovery after the wake of fault. The reason is that the proposed method uses the voltage as a control input to adjust the active power generation while the conventional rotor speed control only aims to maintain at the rated speed.

Disadvantage:

As the proposed control method may not match exactly for compensation of voltage dip effect on the dynamics of WTG with respect to the power systems, the additional design consideration is desired.

Comparison:

The comparison study is carried out by simulation study which is based on the condition in section 3.6.

As the disconnection of wind turbine during the post-fault period is mostly related to the rotor over speeding, it can be considered that the rotational speed can be used as an input to controller instead of using the magnitude of the induction generator terminal voltage. Therefore, the control system shown in Figure 4.27 is also used to compare performance of LVRT with the proposed pitch angle control. The design parameter of Kp=300, Ki=50 with the rotational speed control reference with 1.02pu is used for simulations. Then the comparison of

1) Normal mode control case

2) Proposed pitch control case and

3) Rotational speed feedback control with ω_{ref}=1.02pu cases are carried out.

The comparison of simulation results are plotted in the Figure 4.28. From this figure, it can be clearly seen that proposed pitch control can give better result in voltage recovery. In the case of speed feedback control, the voltage recovery recovers to rated level at 2.5s from simulation time. From the stability view point, as shown in the appendix C, the faster voltage recovery contributes the better transient stability performance. Moreover, if we use the rotational speed control reference with 1.04pu, the terminal voltage recovery cannot be achieve. Therefore, from the perspective of power system's transient stability, it can be considered that the proposed pitch control method is more effective and practical.

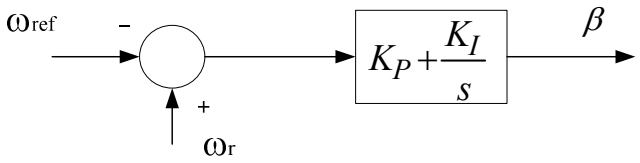

Figure 4.27: Rotational Speed Feedback Control

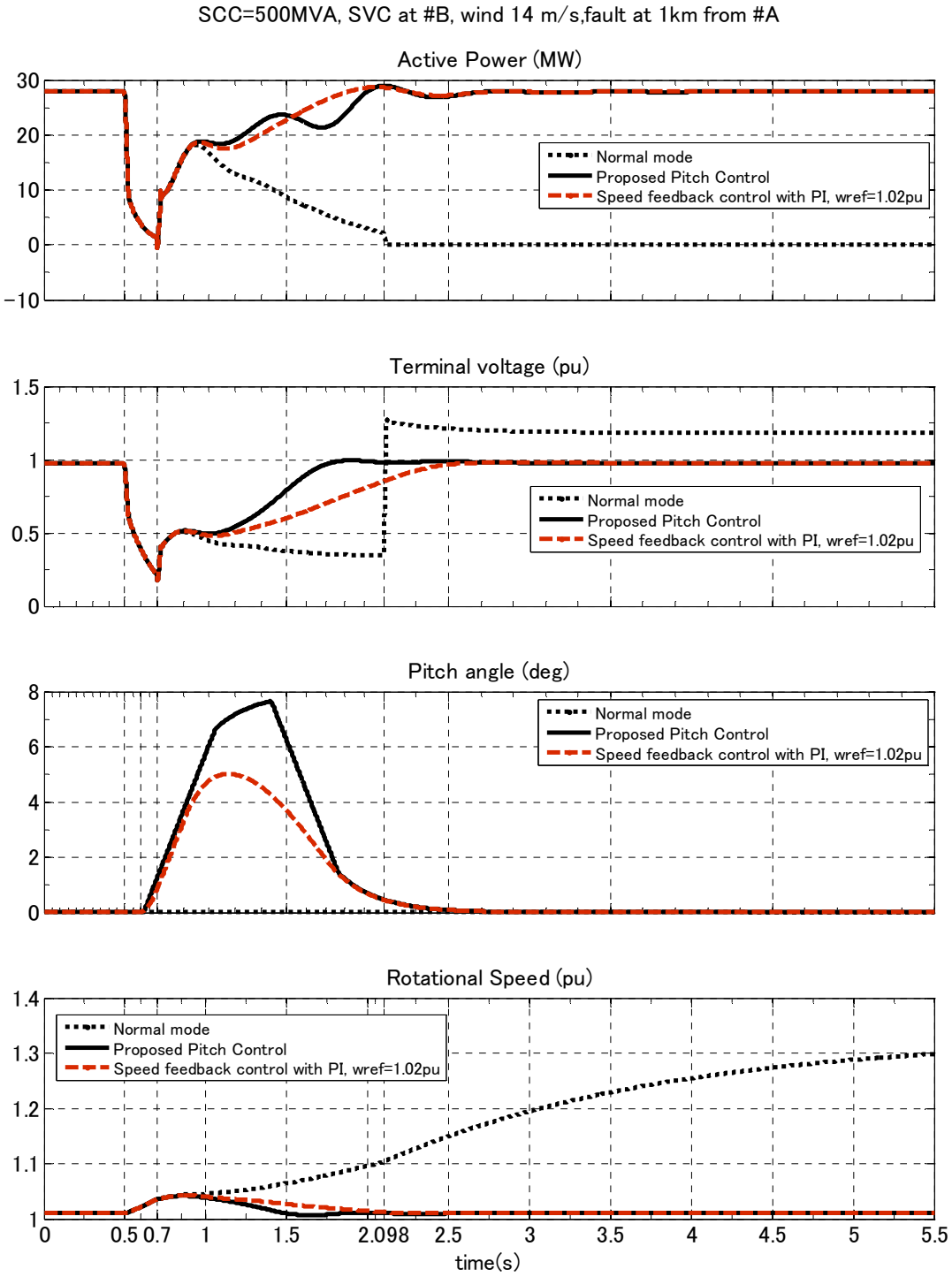

Fig. 4.28: Comparison of normal mode control, proposed pitch control and Speed feedback control with PI algorithm (ω_{ref}=1.02pu),

4.7 CONCLUSIONS

The wind farm LVRT capability can be improved by the proposed pitch control. The concept of protective relay coordination in pitch control is presented to react rapidly to the voltage dip to act during the event of fault, and use for temporary reduction of the mechanical power of wind turbine. This concept contributes the LVRT capability in cost effective way of wind farm integration as the usage frequency of the pitch control for LVRT would be expected relatively few comparing with that of pitch control in normal condition. With the expectation of advance technology development in wind turbine parts for less mechanical stress, the proposed pitch control is worthwhile to use as an additional back up counter measure for LVRT.

According to our study, the LVRT behavior is closely related to the voltage recovery after clearing the fault. Therefore, the stiffness of grid and location of reactive power source should be taken into account in LVRT studies.

There would be many ways to improve our study in this chapter. Firstly, the relationship of PI controller parameters to the grid stiffness, time delay in initiating the pitch control and the development of pitch controller parameters designing procedure are shown to be essential to study. Secondly, it would be important to take into consideration of influences on LVRT by different locations and internal network structure of wind farm in LVRT evaluations, use of instantaneous SVC model, and LVRT failure at specific wind speed range with respect to the voltage variation.

CHAPTER 5

POWER CURTAILMENT CONTROL IN VARIABLE -SPEED WIND-TURBINE GENERATOR WITH PMSG

5.1 INTRODUCTION

Among the wind turbine generators, variable-speed wind turbine (VSWT) system which employs a Permanent Magnet Synchronous Generator (PMSG) and a double conversion electronic converter to connect the turbine to grid has become increasing. PMSGs have many advantages such as the ability to work with a wide range of wind speeds, higher efficiency, and maintenance free for gear and more controllability.

This chapter presents a new control method to mitigate a faulted network impact on PMSG based wind turbine generation systems which uses back-to back frequency converter to connect the network. When a fault occurs, power imbalance causes over voltage in DC-link between the back-to-back frequency converters. To reduce the over voltage in DC-link, a new control method is proposed to balance the active power by controlling the generator side converter and pitch control. The effectiveness of the new control method is verified by analyzing the behavior of PMSG under faulted conditions with MATLAB/Simulink. Comparison study between the use of traditional approach of using the braking resistor parallel to DC-link and the presented control method is also carried out. The results show that the new control method can reduce the over voltage in

DC-link and will guarantee the Low-Voltage Ride-Through (LVRT) capability of PMSG as a back-up control system.

5.2 PROPOSAL OF POWER CURTAILMENT CONTROL

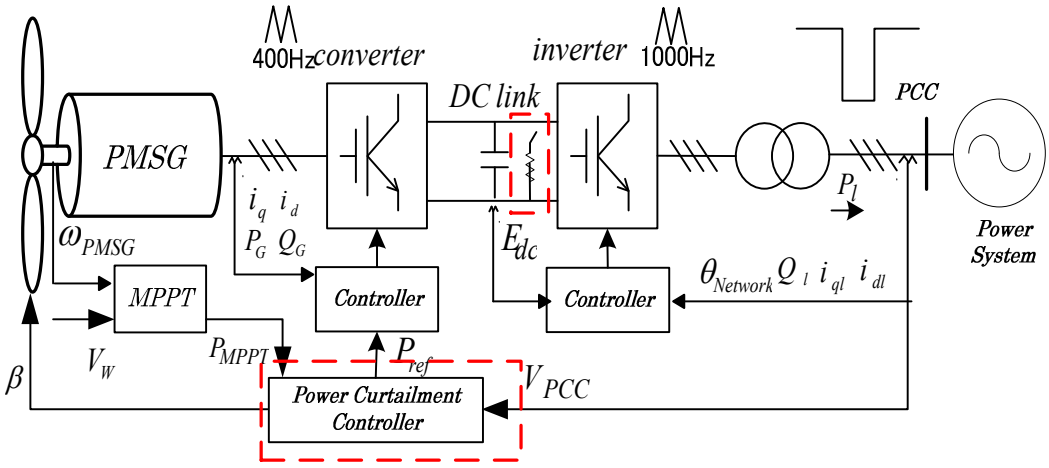

Figure 5.1: Outline diagram of PMSG including power curtailment control

The outline of the proposed power curtailment control for LVRT of PMSG wind turbine is shown in Figure 5.1. The main idea of proposed control is to release the extracted wind power by means of pitch angle (β) control and active power control (P_{ref}) at generator side converter. When the voltage dip (Vpcc) is occurred at the Point of Common Coupling (PCC), the injected power to power systems (P_l) is decreased according to the voltage dip. To improve the LVRT capability of PMSG, it is necessary to maintain the balance between generated power (P_G) and injected power to power systems (P_l) during the voltage dip. If not, the power imbalance will cause the voltage (E_{dc}) raise in DC link. This will cause the operation of protection system to protect the power electronic devices. A power curtailment control is proposed to react rapidly to the voltage dip. In the proposed control, the combination of the rotational speed is controlled by means of pitch angle (β) and generated active power is controlled (P_G) by generator side converter.

5.2.1 CONVERTER CONTROL

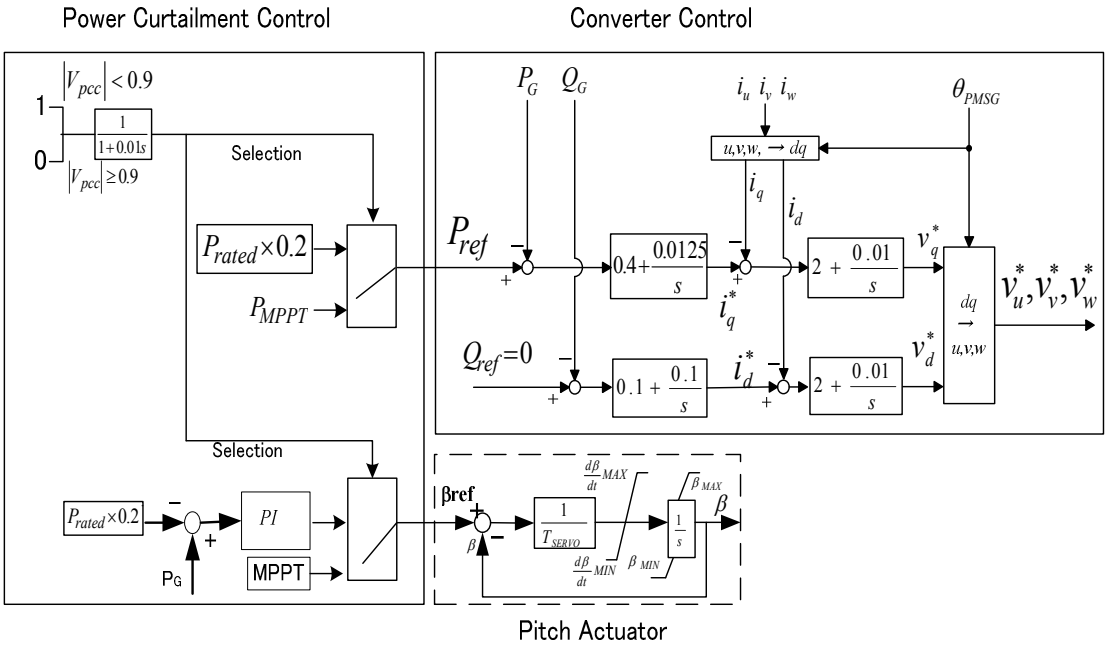

Figure 5.2: Block diagram of power curtailment control

In Figure 5.2, the block diagram of converter control is illustrated. The aim of the converter control is to set the generator terminal voltage according to the active power (P_G) and reactive power (Q_G) of PMSG. When the voltage at the PCC is detected to <0.9 (p.u.), the active power reference (P_{ref}) is switched to the 0.4MW, i.e., 20 percent of P_{rated} as the voltage dip of 0.2 p.u. is used in this study. The converter also controls to achieve the zero reactive power absorption or generation by PMSG. For normal condition, P_G is controlled by means of P_{ref} set by the Maximum Power Point Tracking (MPPT) algorithm [12, 35].

5.2.2 PITCH ANGLE CONTROL

In the Figure 5.2, the portion of pitch angle controller is illustrated. The aim of this control is to adjust the extracted power from wind and to maintain the rotational speed. When the voltage dip is detected, the reference pitch angle is switched from the MPPT mode to the Power Curtailment Control. By this way, the rotational speed can be maintained according to the generated active power condition.

5.3 DESCRIPTION OF VARIABLE-SPEED WIND-TURBINE GENERATOR MODEL

The schematic diagram of VSWT with the use of PMSG is shown in Figure 5.3. The aerodynamic rotor and generator shaft is coupled directly (i.e. without a gear box). The generator is a multi-pole synchronous generator designed for low speeds. The generator is excited by permanent magnet. To permit variable-speed operation, the synchronous generator is connected to the grid through a variable frequency power converter system which completely decouples the generator speed from the grid frequency. Therefore, the electrical frequency of the generator may vary as the wind speed changes, while the grid frequency remains unchanged.

The rating of the power converter-inverter system corresponds to the rated power of the generator plus losses. The power converter-inverter system consists of the grid-side inverter and the generator-side converter connected back-to-back through a DC link.

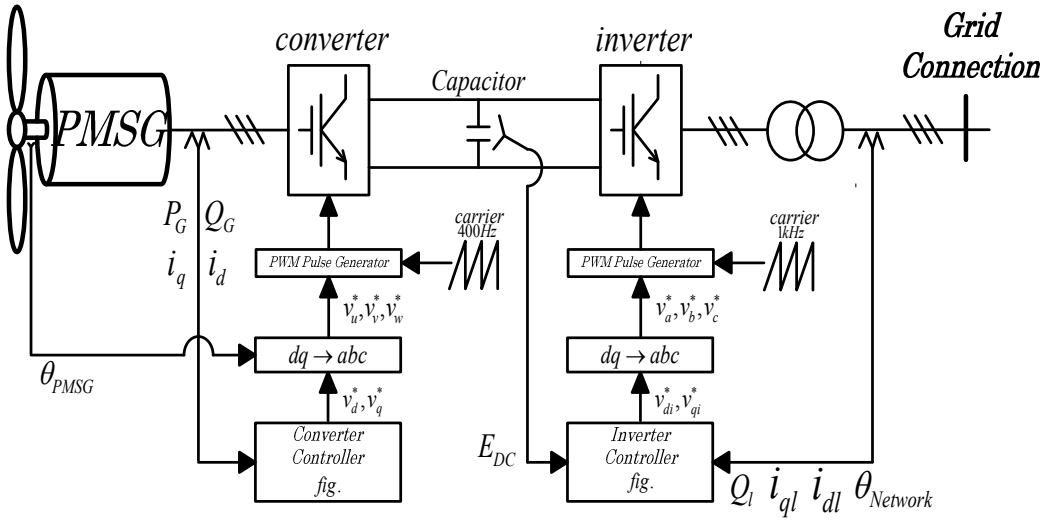

Figure.5.3: Outline of PMSG implemented wind turbine

5.3.1 GENERATOR-SIDE CONVERTER

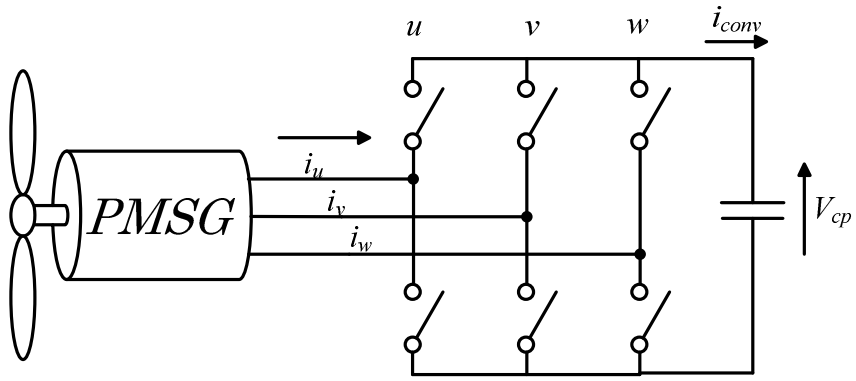

Figure.5.4: Outline of Generator-Side Converter

The grid-side converter is shown in Figure 5.4. In the grid-side converter, the two-level Pulse Width Modulated (PWM) switching method is used for each phase. PWM waveforms are constructed by triangle comparison of switching frequency. Duty ratio input is between 0 and 1. It means that either high or low level switch is to be closed. In this model, switching losses and voltage drop at diode are neglected.

In Figure 5.4, the stator currents, i_u, i_v, i_w, injected current to DC-link, i_{conv}, and DC-link voltage, V_{cp}, are illustrated. The switch states signal from the controller, 1 for closed at upper and 0 for closed at lower, can be written as

$$S(t) = \begin{bmatrix} S_u(t) \\ S_v(t) \\ S_w(t) \end{bmatrix} \tag{5.1}$$

The terminal voltage of PMSG can be calculated with the use of the DC-link voltage, V_{cp}, as follows:

$$\begin{bmatrix} v_u(t) \\ v_v(t) \\ v_w(t) \end{bmatrix} = V_{cp} \begin{bmatrix} S_u(t) \\ S_v(t) \\ S_w(t) \end{bmatrix} \tag{5.2}$$

To get the phase voltage,

$$\begin{bmatrix} v_u(t) \\ v_v(t) \\ v_w(t) \end{bmatrix} = V_{cp} \begin{bmatrix} S_u(t) \\ S_v(t) \\ S_w(t) \end{bmatrix} - \frac{n}{3} V_{cp} \begin{bmatrix} 1 \\ 1 \\ 1 \end{bmatrix} \tag{5.3}$$

where, $n = S_u(t) + S_v(t) + S_w(t)$

Then the calculated phase voltages by equation (5.3) is transformed to d-q axis which is used to calculated PMSG generated current of i_d,i_q, by equation(5.16). The stator winding is assumed as Y connected type and so natural point current, i_0, is regarded as zero. Then the calculated PMSG generated current of i_d,i_q, are inverse transformed to the stator currents, i_u,i_v,i_w,.

The injected current to DC-link, $i_{conv,}$ can be calculated by

$$i_{conv}(t) = \begin{bmatrix} i_u(t) \\ i_v(t) \\ i_w(t) \end{bmatrix}^T \begin{bmatrix} S_u(t) \\ S_v(t) \\ S_w(t) \end{bmatrix} \tag{5.4}$$

5.3.2 GRID-SIDE INVERTER

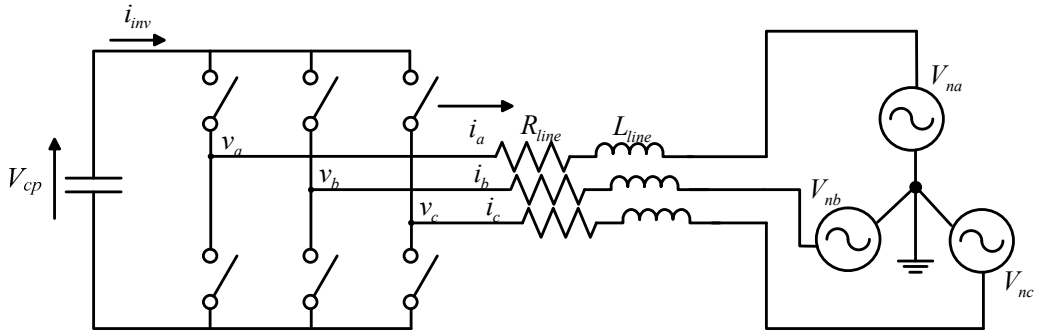

Figure.5.5: Outline of Grid-Side Inverter

In the Figure 5.5, injected current to inverter, i_{inv}, phase voltage and phase current of inverter, $v_a, v_b, v_c, i_a, i_b, i_c$, network voltage, V_{na}, V_{nb}, V_{nc}, transmission line parameters, R_{line}, L_{line}, are illustrated.

The switch states signal from the controller, 1 for closed at upper and 0 for closed at lower, can be written as

$$S_{inv}(t) = \begin{bmatrix} S_a(t) \\ S_b(t) \\ S_c(t) \end{bmatrix} \tag{5.5}$$

The inverter voltage can be calculated as

$$V_{inv}(t) = \begin{bmatrix} v_a(t) \\ v_b(t) \\ v_c(t) \end{bmatrix} = v_{cp} \begin{bmatrix} S_a(t) \\ S_b(t) \\ S_c(t) \end{bmatrix} - \frac{n(t)}{3} v_{cp} \begin{bmatrix} 1 \\ 1 \\ 1 \end{bmatrix} \tag{5.6}$$

where, $n(t) = S_a(t) + S_b(t) + S_c(t)$

Then the network voltage can be calculated as

$$v_{network}(t) = \begin{bmatrix} v_{na}(t) \\ v_{nb}(t) \\ v_{nc}(t) \end{bmatrix} = \begin{bmatrix} V_n \sin(\omega t) \\ V_n \sin(\omega t + \frac{2}{3}\pi) \\ V_n \sin(\omega t - \frac{2}{3}\pi) \end{bmatrix} \tag{5.7}$$

The injected current to network can be calculated by

$$\begin{bmatrix} v_a(t) - v_{na}(t) \\ v_b(t) - v_{nb}(t) \\ v_c(t) - v_{nc}(t) \end{bmatrix} = \left(R_{line} + L_{line} \frac{d}{dt} \right) \begin{bmatrix} i_a(t) \\ i_b(t) \\ i_c(t) \end{bmatrix} \tag{5.8}$$

$$\begin{bmatrix} \frac{d}{dt} i_a(t) \\ \frac{d}{dt} i_b(t) \\ \frac{d}{dt} i_c(t) \end{bmatrix} = \frac{1}{L_{line}} R_{line} \begin{bmatrix} i_a(t) \\ i_b(t) \\ i_c(t) \end{bmatrix} + \frac{1}{L_{line}} \begin{bmatrix} v_a(t) - v_{na}(t) \\ v_b(t) - v_{nb}(t) \\ v_c(t) - v_{nc}(t) \end{bmatrix} \tag{5.9}$$

The injected current from DC-link to inverter, i_{inv}, can be calculated by

$$i_{inv}(t) = \begin{bmatrix} i_a(t) \\ i_b(t) \\ i_c(t) \end{bmatrix}^T \begin{bmatrix} S_a(t) \\ S_b(t) \\ S_c(t) \end{bmatrix} \tag{5.10}$$

Then the calculated network voltage, $v_{network}(t)$, and injected current to network, $i_{line}(t)$, are transformed to d-q axis, v_{dn}, v_{qn} and i_{dl},i_{ql}, to calculate the active power and reactive power.

$$P_{PMSG}(t) = \frac{3}{2}\{v_{dn}(t) i_{dl}(t) + v_{qn}(t) i_{ql}(t)\} \tag{5.11}$$

$$Q_{PMSG}(t) = \frac{3}{2}\{v_{qn}(t) i_{dl}(t) - v_{dn}(t) i_{ql}(t)\} \tag{5.12}$$

5.3.3 DC-LINK

In the Figure 5.6, the outline of DC-link is illustrated. In this figure, the injected current from converter, i_{conv}, current flows into the capacitor, i_{cp}, injected current to inverter, i_{inv}, are illustrated. The current flows into the capacitor can be calculated by

$$i_{cp}(t) = i_{conv}(t) - i_{inv}(t) \tag{5.13}$$

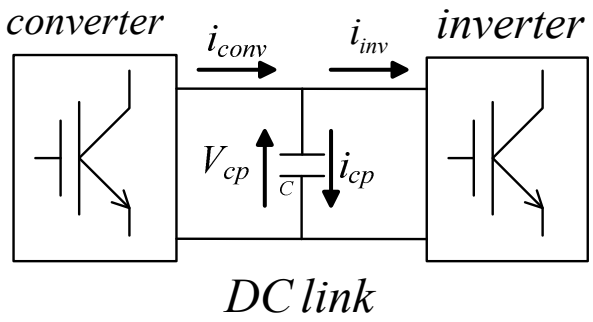

Figure.5.6: Outline of DC-link

The voltage of DC-link can be calculated by

$$V_{cp}(t) = \frac{1}{C}\int i_{cp}(t)dt \tag{5.14}$$

5.3.4 PMSG MODEL

The mathematical model of PMSG can be written as follows:

$$\begin{bmatrix} v_d(t) \\ v_q(t) \end{bmatrix} = \begin{bmatrix} -R_a - \frac{d}{dt}L_d & \omega L_q \\ -\omega L_d & -R_a - \frac{d}{dt}L_q \end{bmatrix} \begin{bmatrix} i_d(t) \\ i_q(t) \end{bmatrix} + \begin{bmatrix} 0 \\ \omega \Psi_a \end{bmatrix} \tag{5.15}$$

where $\Psi_a = \frac{3}{2}\Psi_f$, v_d, v_q : d-q axis voltage, i_d, i_q : d-q axis current, L_d, L_q : d-q axis admittance, R_a : stator resistance, Ψ_f : peak value of magnetic flux excitation ω : electrical rotation in rad/s.

Then the stator current in d-q axis can be calculated

$$\begin{bmatrix} \frac{d}{dt}i_d(t) \\ \frac{d}{dt}i_q(t) \end{bmatrix} = \begin{bmatrix} \frac{1}{L_d}\left(-R_a i_d(t) + \omega L_q i_q(t) - v_d(t)\right) \\ \frac{1}{L_q}\left(-R_a i_q(t) - \omega L_d i_d(t) + \omega \Psi_a - v_q(t)\right) \end{bmatrix} \tag{5.16}$$

From equation (5.16), the electrical torque of PMSG can be calculated as

$$Te(t) = -p_{PMSG}\{\psi_a i_q(t) + (L_d - L_q) i_d(t) i_q(t)\} \tag{5.17}$$

where P_{PMSG} is the pole pairs.

Then the calculated electrical torque is used to calculate the motion equation.

$$\frac{d}{dt}\omega_{WT} = \frac{1}{J_{WG}}(T_{WT} - T_e) \tag{5.18}$$

5.3.5 AERODYNAMIC MODEL

The power extracted from the blowing wind can be expressed by the following equation [12, 35]:

$$P_m(\lambda, \beta, u) = \omega_{wt} T_m = C_p P_w = \frac{\rho}{2} A_{wt} C_p(\lambda, \beta) v_w{}^3 \tag{5.19}$$

where ρ is the air density, λ is the tip speed ratio, β is the pitch angle, A_{wt} is the area covered by the wind turbine rotor, ω_{wt} is the wind turbine rotor angular frequency, T_m is the torque from blowing wind and u is the wind speed. The power coefficient, C_p, is approximated by the following equation [35]:

$$P_M = \frac{1}{2}\rho C_p(\lambda, \beta)\pi R^2 V_w^3, \text{ where } \lambda = \frac{\omega_m R}{V_w} \tag{5.20}$$

$$C_p(\lambda, \beta) = 0.5(\Gamma - 0.02\beta^2 - 5.6)e^{-0.17\Gamma}, \Gamma = \frac{R}{\lambda}.\frac{3600}{1609} \tag{5.21}$$

By adjusting the pitch angle, β, the power extracted from the blowing wind can be effectively controlled.

5.3.6 MAXIMUM POWER POINT TRACKING (MPPT) METHOD

Comparing to the FSWT, higher energy generation at low wind speed can be achieved in VSWT by means of MPPT control. In MPPT control, according to the characteristics of wind turbine, active power generation reference is set based on the wind speed (v_w) and associated rotational speed (ω_{m_op}) to achieve the optimal output power. For the pitch angle of zero, the optimal rotational speed can be expressed in equation (5.22) by differentiation the equation (5.21) with respect to the (ω_m) and equating to zero. According to the reference [35], optimal output power of turbine can be defined according to the wind speed and per unit of rotational speed. The following 4 operation points

1. (5.16 m/s, 0.4 p.u.),
2. (7 m/s, 0.54 p.u.),
3. (10 m/s, 0.78 p.u.),
4. (12 m/s, 0.93 p.u.) are optimal operation points of wind turbine used in this study [35].

Those optimal operation points can be tracked by the following equations:

$$\omega_{m\_op} = 0.0775 V_w \tag{5.22}$$

$$P_{REF\_1} = 0.057 V_w - 0.219 \tag{5.23}$$

$$P_{REF\_2} = 0.1133 V_w - 0.613 \tag{5.24}$$

$$P_{REF\_3} = 0.19 V_w - 1.38 \tag{5.25}$$

The method of determination in generator power control reference is shown in Figure 5.7. As shown in (A) portion, P_{G_ref} is selected from one of the equations of (5.23, 5.24,

5.25) according to the 3 operation points of wind speed. Rotational speed variation from the operation point is controlled as shown in (B) portion. P_{G_ref} is also adjusted not to decrease beyond the lower limit of rotational speed (0.4 p.u.), as shown in portion (C).

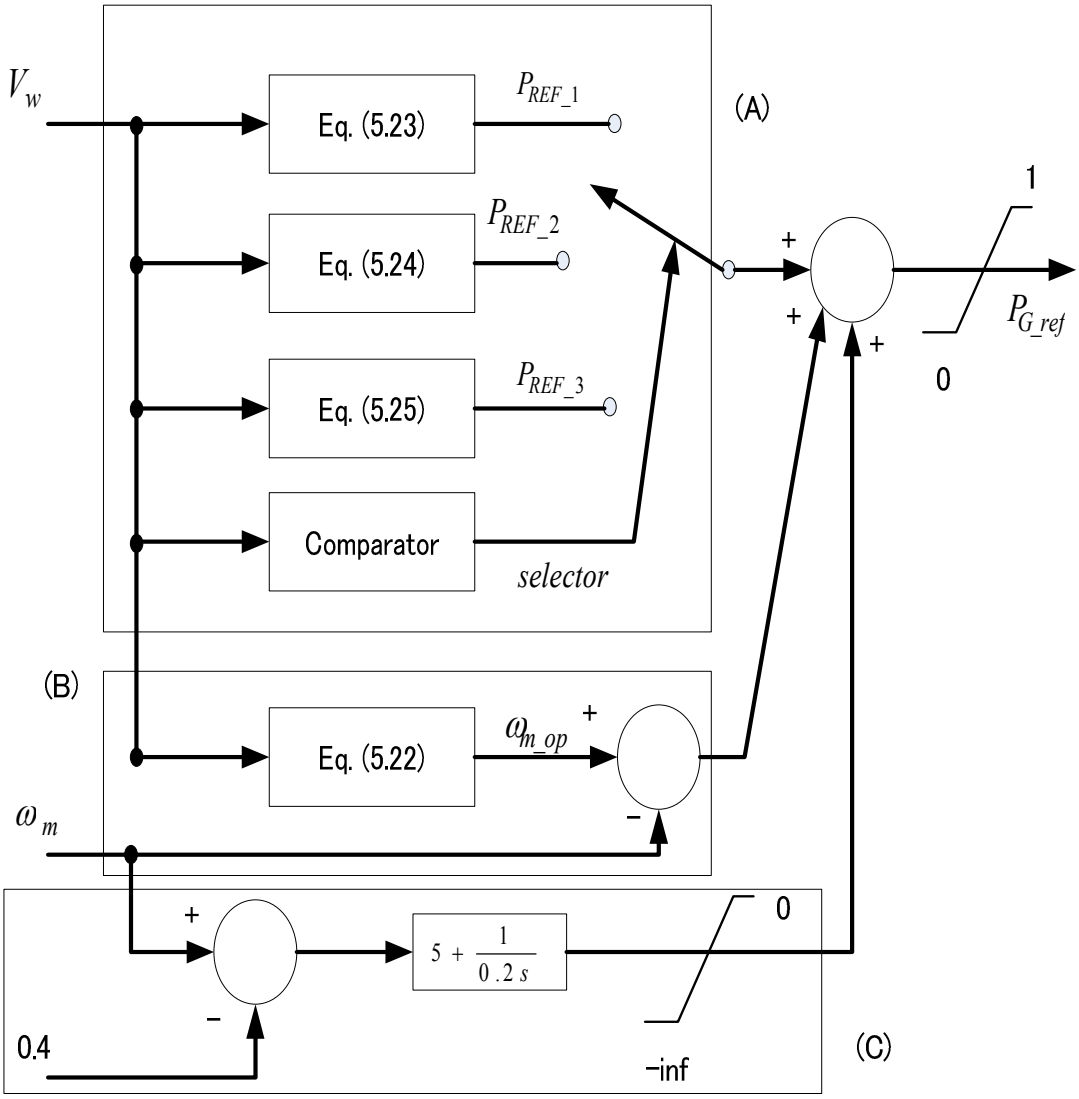

Figure.5.7: Determination method of P_{G_ref}

5.3.7 INTERFACING THE 3 PHASE TRANSMISSION SYSTEM WITH PMSG MODEL IN D-Q AXIS

The d-q-axis control systems for converter and inverter require that the phase angle of the AC voltage must be measured. This can be done using reference frame transformation or with a phase locked loop (PLL). In this study, the reference frame transformation is used. Positive sequence voltage at PCC can be transformed by

$$\dot{V}_1 = \frac{1}{3}(\dot{V}_a + \exp(j120°)\dot{V}_b + \exp(j240°)\dot{V}_c) \tag{5.26}$$

Then, based on the Euler identity and using the positive sequence as a reference voltage, real and imaginary parts of V_1 are transformed as d-axis and q-axis voltage of V_1, respectively.

The output current of PMSG in d-q axis can be transformed in to complex phase A current, $\dot{I}_a$, by using the Euler identity. Then the other phase currents can be calculated.

$$\dot{I}_b = \exp(j240^\circ)\dot{I}_a \tag{5.27}$$

$$\dot{I}_a + \dot{I}_b = -\dot{I}_c \tag{5.28}$$

5.3.8 BLOCK DIAGRAM OF GENERATOR SIDE INVERTER CONTROL

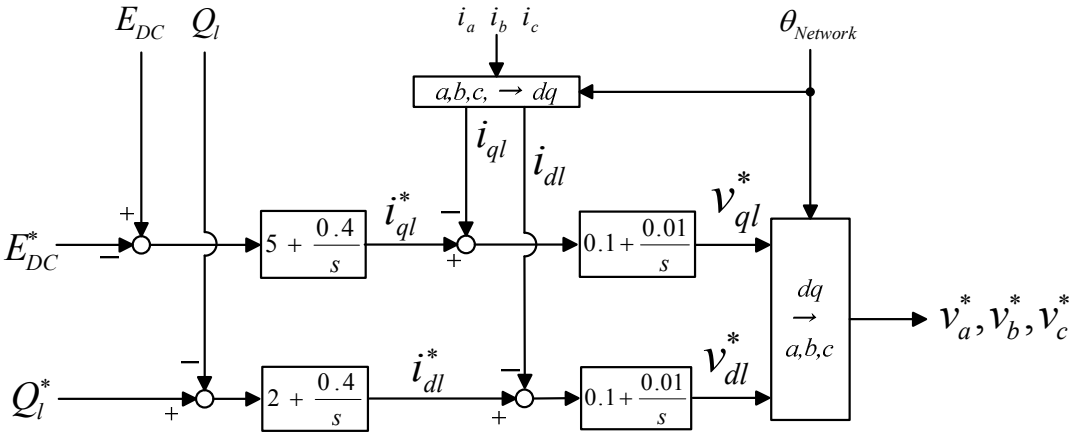

Figure 5.8: Block diagram of inverter control

In the Figure 5.8, the block diagram of inverter control is illustrated. The aim of this control is to maintain the DC link voltage and reactive power. These control parameters are adopted form the reference [12].

5.4 POWER SYSTEMS MODEL

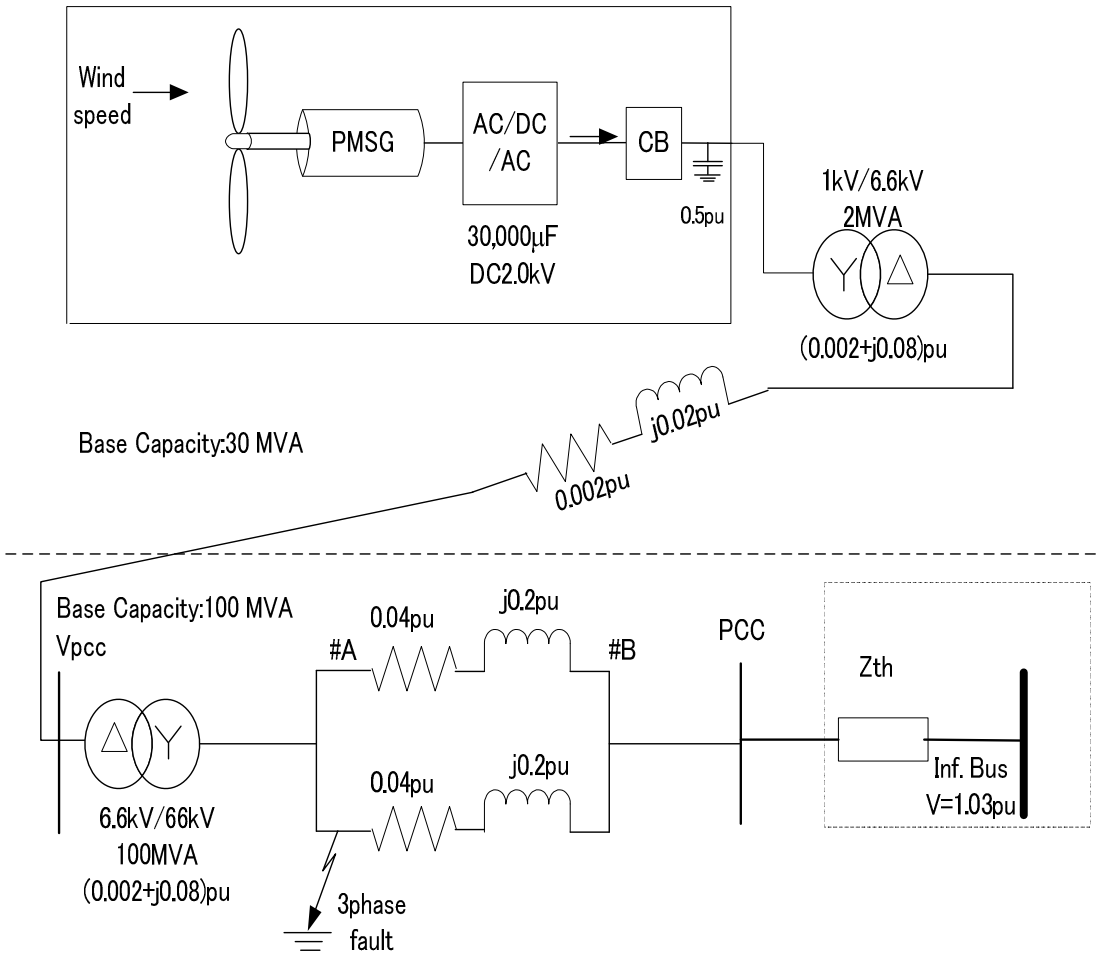

Figure 5.9: Power system model

By using Matlab/Simulink SimPowerSystem Toolbox, the behavior of PMSG and countermeasure are studied. Figure 5.9 shows the single line diagram of power system used in this study [35]. Z_{th} is chosen in order to be the Short Circuit Capacity of 100, 500, 1000(MVA) and X/R ration of 10. The transmission lines are represented by means of nominal π distributed network model. The line parameters R, L, and C are specified as positive and zero sequence parameters that take into account the inductive and capacitive couplings between the three phase conductors as well as ground parameters.

This method of specifying line parameters assumes that the three phases are balanced.

5.4.1 FAULT MODEL

Three-phase-to-ground fault model [38] is used in this study. **T**he fault in the transmission network depresses the network voltage and thereby weakens the power transfer capacity of the wind farm to power system across the network. Then the WTGs are in over speeding and trip from the network in consequence. Therefore, one of the serious network faults, three-phase-to-ground fault, is used as a worst-case for evaluating the proposed pitch control for LVRT.

5.5 VERIFICATION THE EFFECTIVENESS OF POWER CURTAILMENT CONTROL

The behavior of PMSG under faulted network condition is evaluated by simulation studies. By assuming the three-phase-to-ground fault points between node #A and #B (at 1km of 19km long sub-transmission line from the node #A) in Figure 5.9, the voltage along the sub-transmission line is depressed until the faulted line is isolated. The fault sequence used in the simulation is the three-phase-to-ground fault occurred in one of the 66kV sub-transmission lines. The fault is occurred at 500 ms and the faulted line is isolated at 700 ms from the start point of simulation. Due to the relatively short duration of fault continuation, the rated wind speed of 12 m/s is used throughout the study.

5.5.1 EFFECTS OF DIFFERENT SCC

To examine the effects of different SCC, voltage at PCC and DC-link voltage of PMSG without countermeasure are studied. The Figure 5.10 shows the comparison of voltage dip behavior at PCC with the SCC of 100MVA, 500MVA and 1000MVA. The voltage at PCC is started to depress at 500 ms. The magnitude of voltage at PCC is depressed to the 0.2 p.u. level. Then the voltage is recovered at 700 ms.

The transient recovery voltage is found in all cases. In the case of 100MVA SCC, and this transient recovery voltage is raised around 1.2 p.u. In generally, all the voltage dip behaviors are similar in all cases; 100 MVA, 500MVA and 1000MVA.

In Figure 5.11, the comparison of DC link voltage is shown. Voltage rise in all cases

show the similar trend. Once the fault is occurred at 500 ms, the DC link voltage starts to rise until the fault is cleared at 700 ms. For the lesser the SCC, the larger the DC link voltage rise is observed.

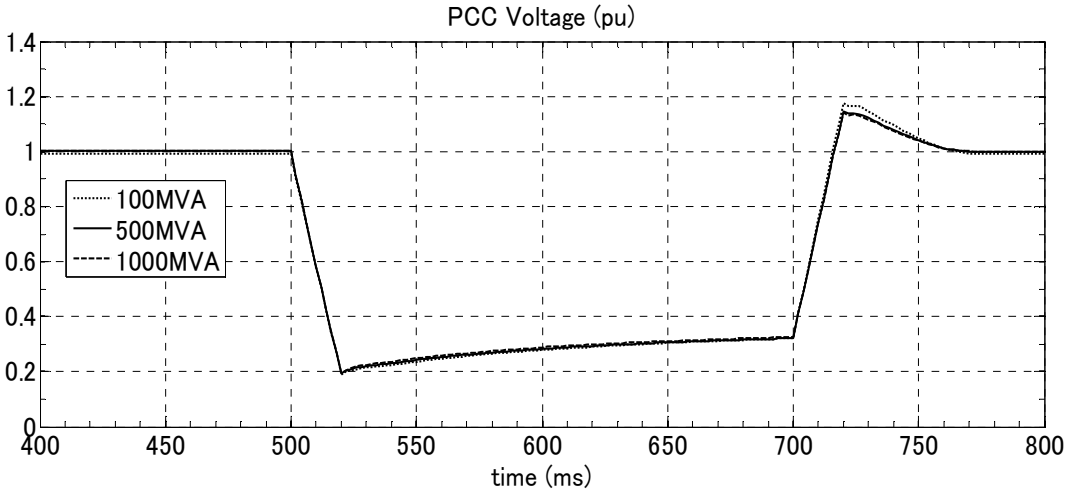

Figure 5.10: Comparison of voltage at PCC

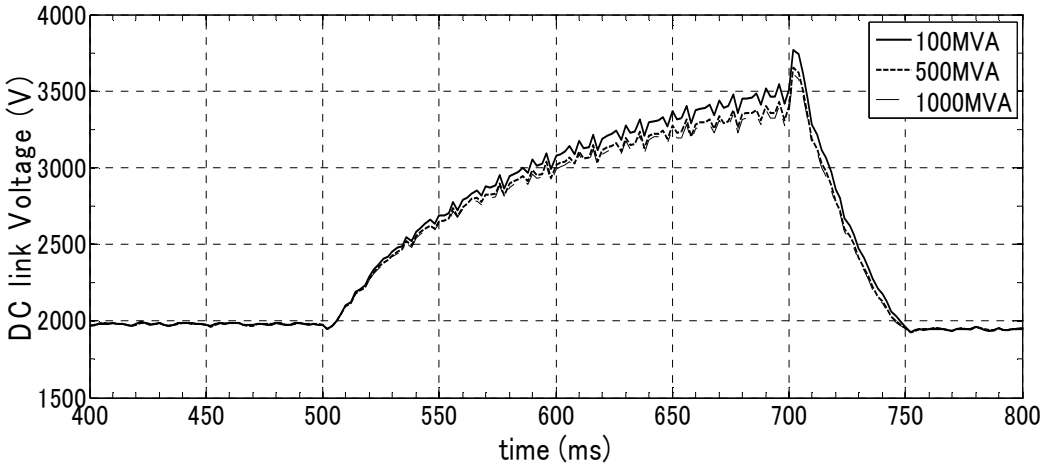

Figure 5.11: Comparison of DC link voltage

5.5.2 EVALUATION WITH DIFFERENT SHORT CIRCUIT CAPACITY

PMSG Behavior with the 100MVA SCC

PMSG behaviors with the short circuit capacity of 100MVA are shown in this section. The Figure 5.12 shows the DC-link voltage, active power, reactive power and rotation speed of the PMSG in the case of no countermeasure for fault impact. The DC-link voltage raises continuously during fault period, from 500 ms to 700 ms. Due to the voltage dip at PCC, the active power cannot inject during fault period. However, the reactive power injection is observed due to the energy exchanged by the DC capacitor at DC link, behaving like STATCOM. Rotational speed increases around 0.5 rpm.

By using the PC control, the voltage rise in DC-link can be reduced only up to 3200V. As the PC control starts to initiate at 600 ms, the voltage rise is start to reduce at 610 ms until the 730 ms. This is shown in figure 5.13.

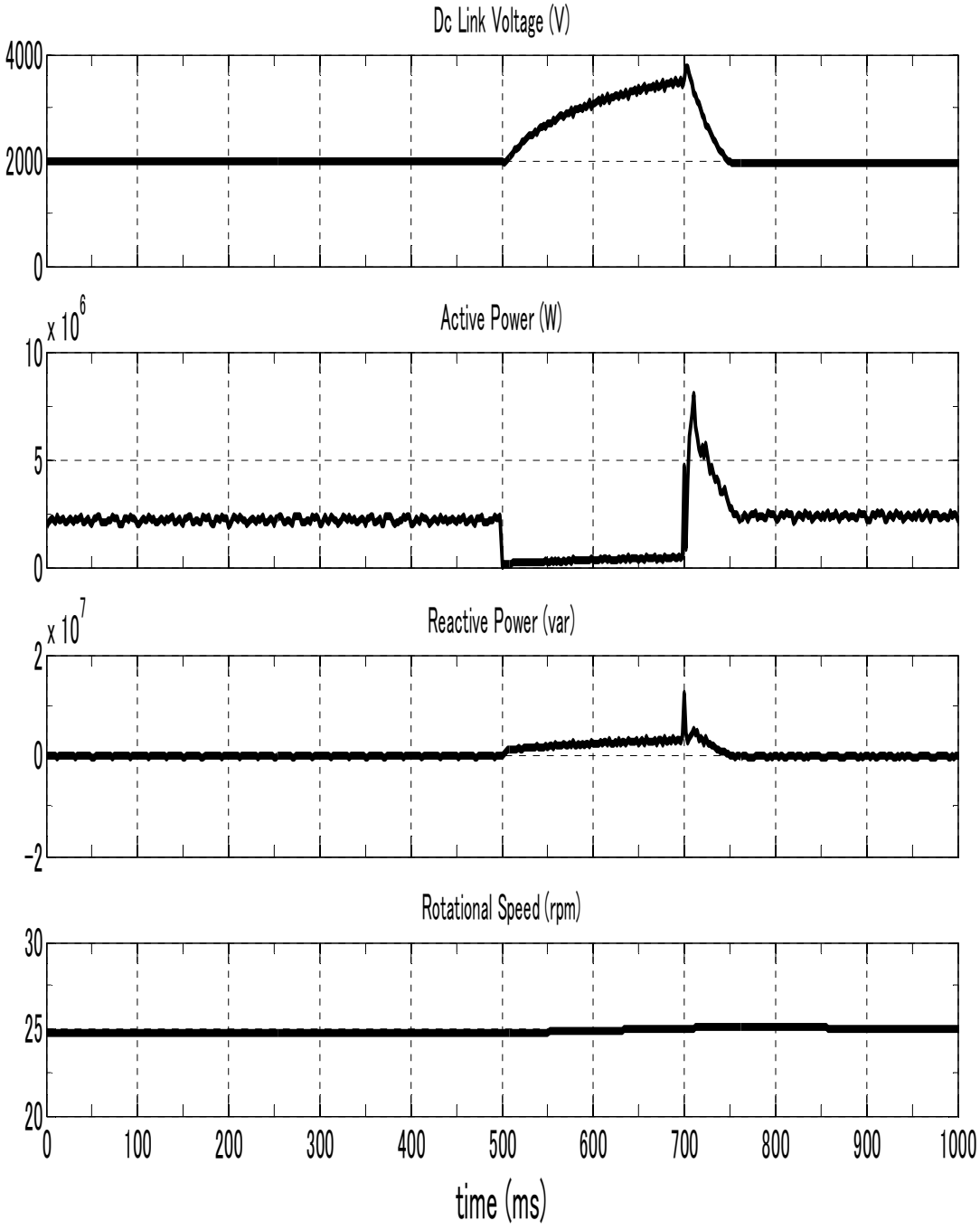

Figure 5.12: PMSG behavior (100MVA SCC, without PC control)

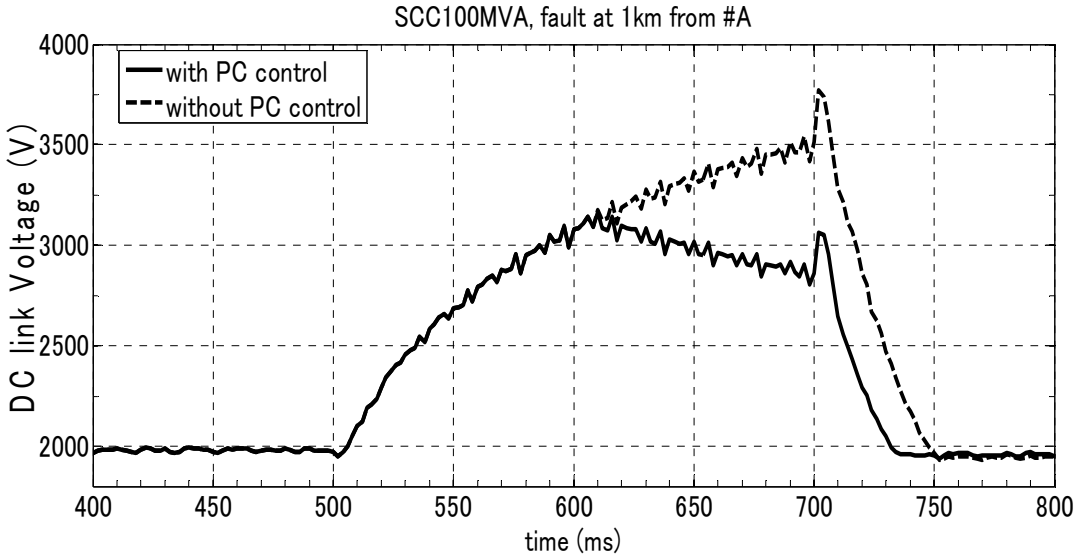

Figure 5.13: Comparison between the DC link voltage with PC control and without PC control

PMSG Behavior with the 500MVA SCC

PMSG behaviors with the short circuit capacity of 500MVA are shown in this section. The Figure 5.14 shows the DC-link voltage, active power, reactive power and rotation speed of the PMSG in the case of no countermeasure for fault impact. The DC-link voltage raises continuously during fault period, from 500 ms to 700 ms. Due to the voltage dip at PCC, the active power cannot inject during fault period. However, the reactive power injection is observed due to the energy exchanged by the DC capacitor at DC-link, behaving like STATCOM. Rotational speed increases around 0.5 rpm.

By using the Power Curtailment control, the voltage rise in DC-link can be reduced up to 3100V. As the PC control starts to initiate at 600 ms, the voltage rise is then start to reduce at 610 ms until the 730 ms, as shown in Figure 5.15.

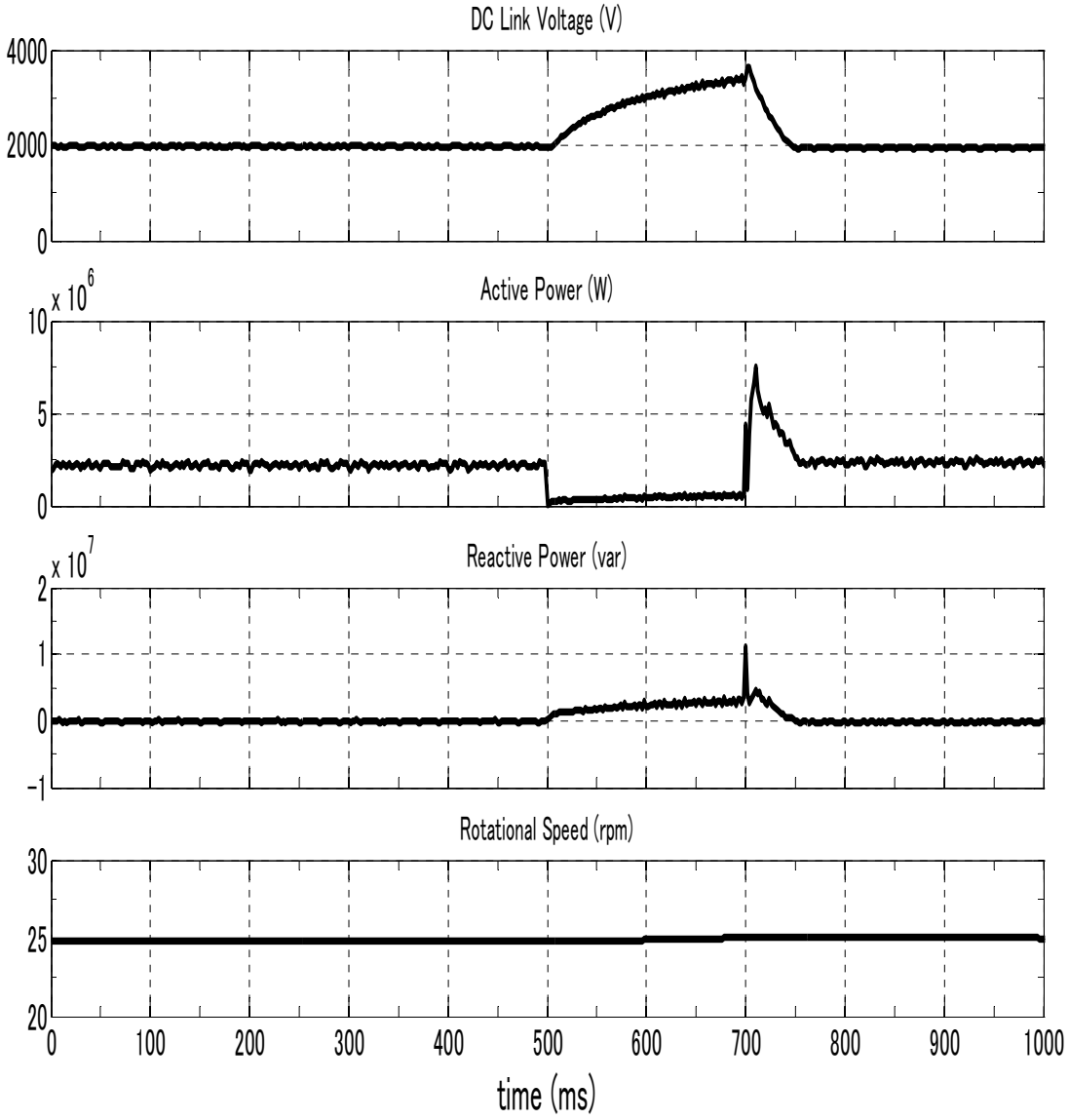

Figure 5.14: PMSG behavior (500MVA SCC, without PC control)

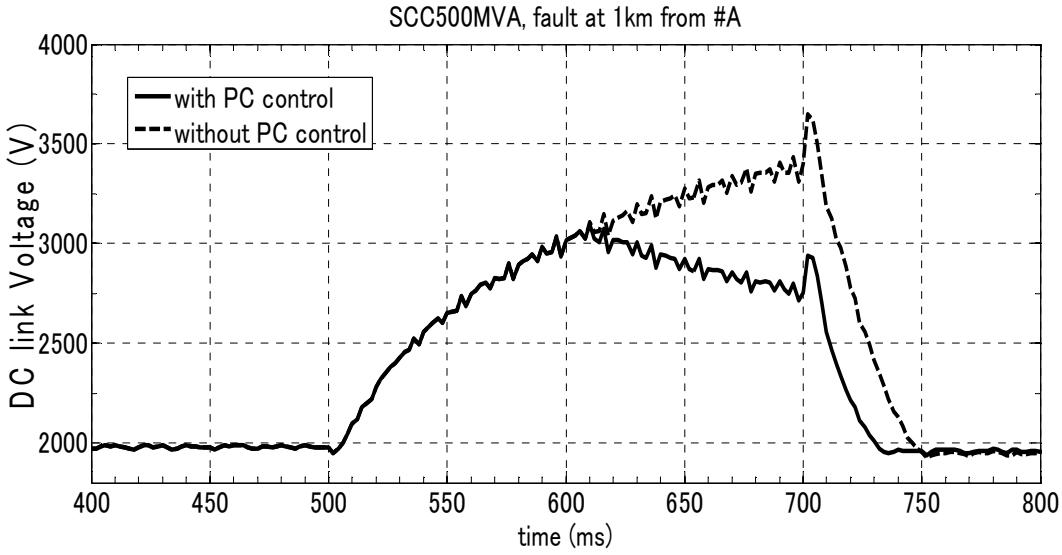

Figure 5.15: Comparison between the DC link voltage with PC Control and without PC control

PMSG Behavior with the 1000MVA SCC

PMSG behaviors with the short circuit capacity of 500MVA are shown in this section. The Figure 5.16 shows the DC link voltage, active power, reactive power and rotation speed of the PMSG in the case of no countermeasure for fault impact. The DC-link voltage raises continuously during fault period, from 500 ms to 700 ms. Due to the voltage dip at PCC, the active power cannot inject during fault period. However, the reactive power injection is also observed due to the energy exchanged by the DC capacitor at DC-link, behaving like STATCOM. Rotational speed increases around 0.5 rpm.

By using the Power Curtailment control, the voltage rise in DC-link can be reduced only up to 3000V. As the PC control starts to initiate at 600 ms, the voltage rise is then start to reduce at 610 ms until the 730 ms. This is shown in Figure 5.17.

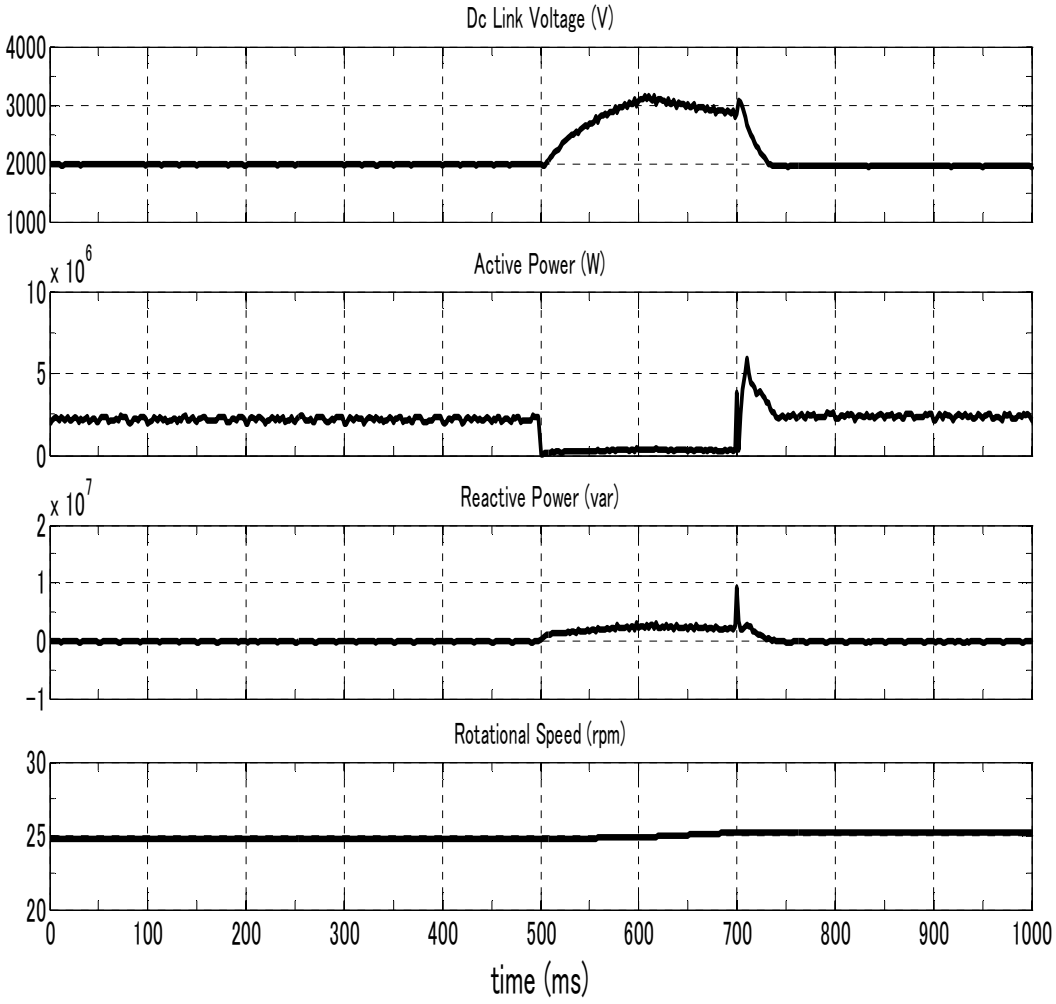

Figure 5.16: PMSG behavior (1000MVA SCC, without PC control)

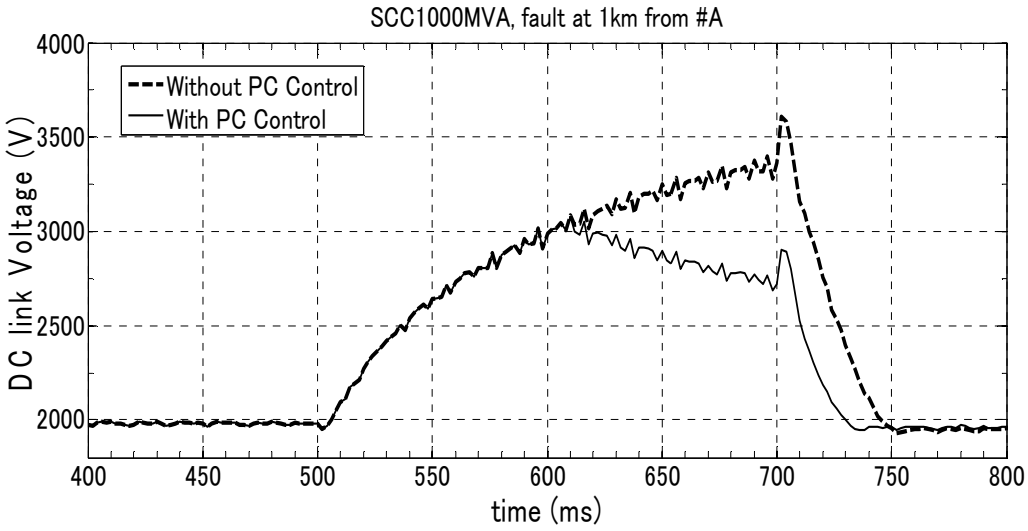

Figure 5.17: Comparison of the DC link voltage with PC Control and without PC control

5.5.3 COMPARISON STUDY WITH BRAKING RESISTOR

By using the BR, the voltage rise in DC-link can be reduced at the designed voltage level. In this section, for 1000MVA SCC, the simulation results of PMSG with the use of BR, with the use of PC and without any use of countermeasure are compared.

To compare the BR and PC control in PMSG, the simulation of PMSG under faulted network condition results are shown in Figure 5.18 and 5.19. The simulation studies are based on the SCC of 1000MVA. In this study, BR is designed to reduce the over voltage in DC-link at 3000V. As choosing the proper BR resistor size is not the main objective of this study, we did not include size and switching cycle of BR in consideration. The figure 5.18 shows the DC-link voltage, active power, reactive power and rotation speed of the PMSG with the use of BR. The continuous voltage rise in DC-link up to 3000V level is observed from 500 ms to 700 ms. Due to the voltage dip at PCC, the active

power cannot inject during fault continuation time. However, the reactive power injection can be also observed due to the energy exchanged by the DC capacitor at DC-link, behaving like STATCOM. Increase in rotational speed of around 0.5 rpm is also observed.

The Figure 5.19 shows the DC-link voltage, active power, reactive power and rotation speed of the PMSG with the use of PC. The continuous voltage rise in DC link up to 3000V level is observed from 500 ms to 600 ms. This voltage rise can be reduced by PC control from 610 ms to 700 ms. The PC control method only tries to balance the extracting power from the wind by means of pitch control and converter control. Therefore, there is no reduction of the reactive power injection during the voltage dip which is necessary for system voltage recovery. Rotational speed increases around 0.5 rpm.

The comparison of DC-link voltages are shown in Figure 5.20. Without any countermeasure case, the DC-link voltage continuously increases during fault period; from 500ms to 700ms. Once the fault is clear, the transient in voltage recovery is occurred. Then the DC-link voltage is returned back to nominal voltage level of 2000V at 750ms. By using BR, the voltage rise in DC-link can be kept constant at 3000V during fault period. Once the fault is isolated, the voltage transient is observed at 700 ms. Then the DC-link voltage is returned back to nominal voltage level of 2000V at 740ms. By using PC, the voltage rise in DC-link can be reduced until 2750V during fault period. As the PC control starts to initiate at 600ms; i.e. with the 100ms delay after the voltage dip detection, the DC-link voltage is continuously increased up to 3000V. Once the fault is isolated, the voltage transient is observed at 700 ms. Then the DC-link voltage is returned back to nominal voltage level of 2000V at 730ms.

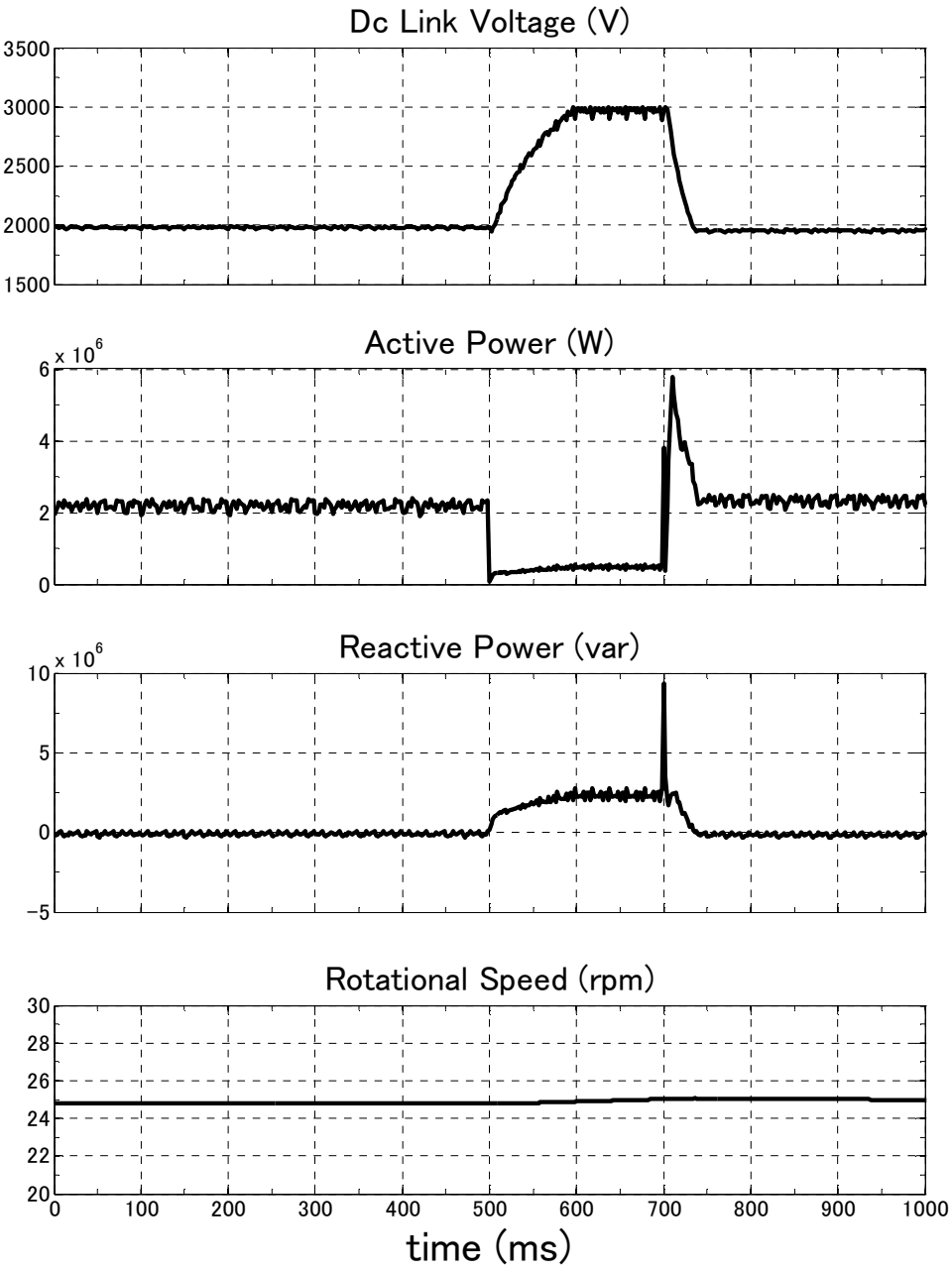

Figure 5.18: PMSG behavior (100MVA SCC, use of braking resistor case)

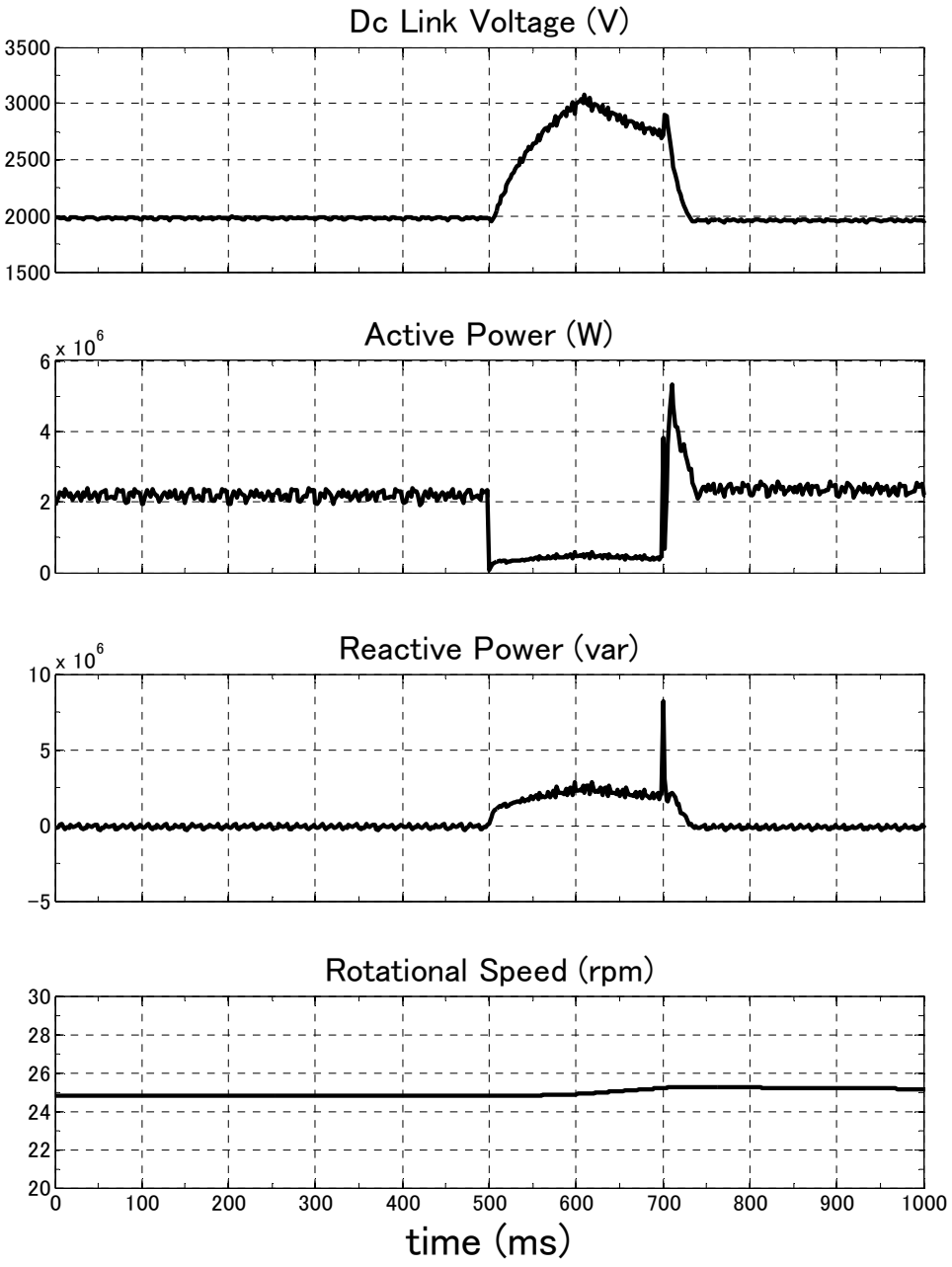

Figure 5.19: PMSG behavior (1000MVA SCC, with PC control)

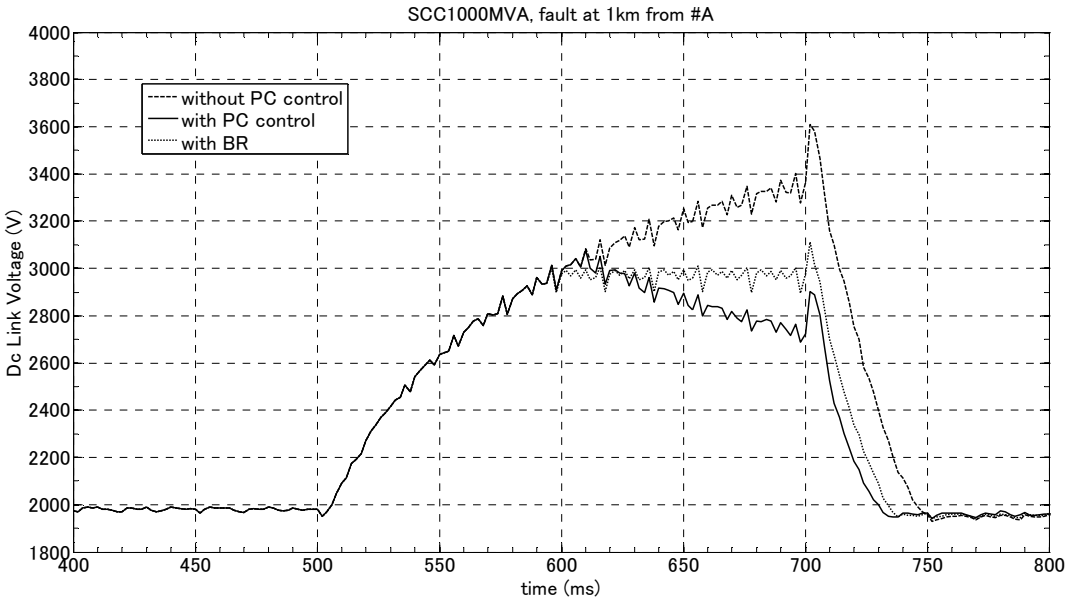

Figure 5.20: Comparison of the DC link voltage with BR, with and without of PC control

5.6. Effect of Pitch Angle Control

The reason of using pitch control is explained in the section. To illustrate the role of pitch control, the simulation studies is carried out under 4 situations; 1) with MPPT control, 2) with PC control, 3) with PC control by using only converter, 4) with PC control by using only pitch control. The simulation results in this section are considering in the case of SCC is 500MVA and fault is occurred at 1km from #A. Comparing to the converter control, pitch angle control is less effective in reduction of DC-link voltage rise due to the slower response than that of converter control, as shown in Figure 5.21. However, co-ordination with pitch control to converter control can reduce over speed as shown in Figure 5.22 and 5.23. Therefore, co-ordination of pitch control is also desired.

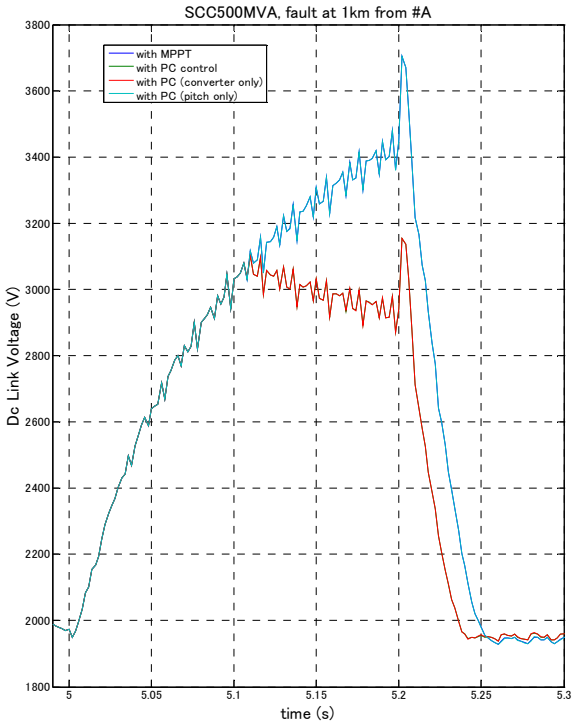

Figure 5.21: DC-link Voltage

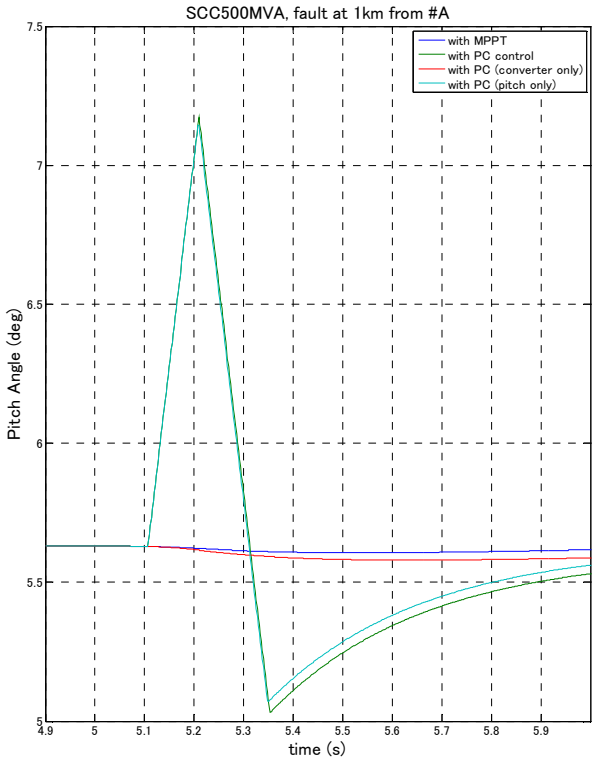

Figure 5.22: Pitch Angle

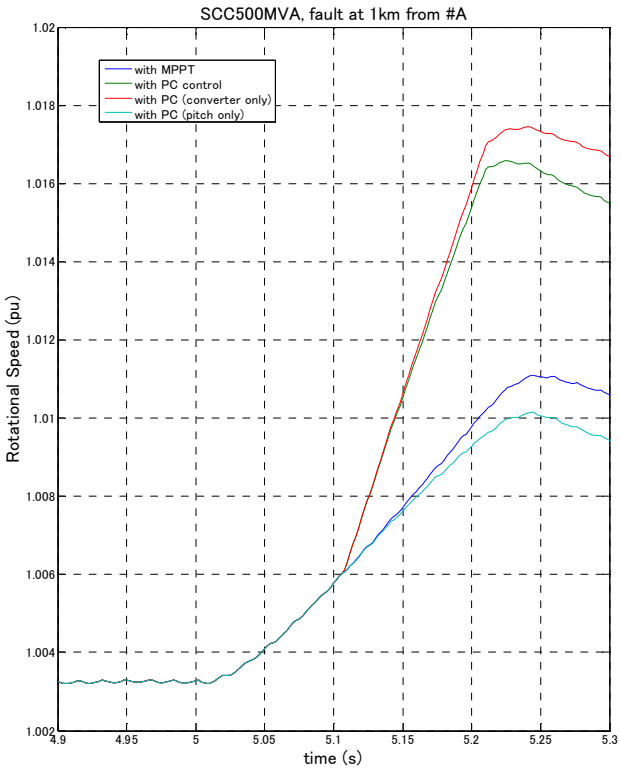

Figure 5.23: Rotational Speed

5.7. CONCLUSIONS

The use of Power Curtailment is effective to mitigate the faulted network impact on PMSG. The effectiveness of proposed PC control is compared with that of braking resistor. Although the use braking resistor gives more flexible and simple in control of voltage level, the Power Curtailment Control can be used as an additional countermeasure. Therefore, we can conclude that the additional use of PC control can give the guarantee for LVRT capability of PMSG as a backup control system in the case of BR failure.

There are many ways to improve our study in this chapter. Firstly, it should be taken in to account of converter blocking, which may be occurred to avoid the damage of power electronic device due to over current. Secondly, loss of synchronism phenomena of energy conversion systems during the post-fault period is desired to study as a future work.

CHAPTER 6

SUMMARY AND CONCLUDING REMARKS

In this dissertation, we discussed wind energy integration impacts of stability of power system and proposed the control method for LVRT improvement of wind energy generation systems which is one of the requirements in high wind energy integration to power systems. The conclusions of each chapter are summarized at the end of associated chapter. In order to study the effectiveness of proposed control method, we did simulation studies in which the dynamics of wind turbine generators and power systems are modeled in fundamental frequency. Then the LVRT behaviors of wind generation systems are discussed with respect to the three-phase short circuit fault under different locations of fault and stiffness of power system. Based on the type wind energy generation systems, this dissertation can be categorized into two parts, generally.

In the first part, we have used the fixed-speed wind turbine (FSWT) model including a Squirrel-Cage Induction Generator (SCIG). As the LVRT behavior is related to short-term transient stability, we used the instantaneous time domain models of wind turbine generators and three-phase power transmission network which are relevant to the phenomenon of short-term transients.

In the second part, we have used the variable-speed wind turbine (VSWT) model including a Permanent Magnet Synchronous Generator (PMSG). In order to analyze the LVRT behavior, the instantaneous time domain models of PMSG, converter, inverter and three-phase power transmission network are used.

The simulation results shown in both parts confirmed that the LVRT requirements can be achieved by the proposed control method. In the case of FSWT, it is obvious that the proposed control method can mitigate the local impact on the system voltage; improvement of voltage recovery during the post fault period. However, the proposed control method is based on the feed-forward control method approach which has disadvantage in output power oscillations during the post-fault period. According to the power system size and generation mix, there is a possibility to propagate through the system causing synchronous generator to exhibit speed oscillations phenomenon. In the case of VSWT, confirmation of proposed control method with Doubly Fed Induction Generator (DFIG) is not yet included. Moreover, the phenomenon of the rising inrush current in power electronic devices and blocking the inverter/converter are not considered as they are not the scope of this dissertation.

There would be many ways to improve our proposed method presented in this dissertation as follows:

1) Considering as a co-operate control system with the FACT devices and/or control systems with conventional generators in power systems.
2) Designing in such a way of the adaptive control according to the operation states of wind farm with respect to power systems.
3) Development of detailed design approach of control system to get the least output power oscillations during the post-fault period.
4) Consideration the influence of wind farm internal structure for performance evaluation.
5) The study for unbalance fault condition.

In conclusion, we have proposed the conceptual consideration of controlling the wind power generation systems for LVRT capability improvement. The analysis of the LVRT behavior of wind farm is presented. To achieve the low-carbon and green society, electricity generation from wind energy is the one of the key players in all over the world. LVRT requirement is the most challenging issues of high wind energy penetration into the power systems. The proposed method contributes not only the fulfillment of LVRT requirements in wind energy integration but also in improvement of the transient stability of conventional synchronous generator in power systems. In any case, the studies presented in this dissertation provide a good starting point to consider the grid stiffness and carry out the operation coordination with WTGs' protection systems for LVRT capability of wind farm.

REFERENCES

[1] P. Kundur, *Power System Stability and Contro*l. New York: McGraw-Hill, 1994.

[2]http://www.windenergy.org.vn/uploads/246/worldwindenergyreport2010_s-pdf/, retrieved on 2011-11-01.

[3]Söder, L., Hofmann, L., Orths, A., Holttinen, H., Wan, Y.H., Tuohy, A.2007. Experience from wind integration in some high penetration. IEEE Transactions on Energy Conversion, vol. 22, 2, pp. 4–12.

[4] Wind Report 2005, http://www.wind-watch.org/docviewer.php?doc=eonwindreport2005.pdf, (available 2008)

[5]W.L.Kling, L. Söder, I. Erlich, P. Sorensen, M. Power, H.Holttinen, J. Hidalgo, B.G. Rawn, "Wind Power Grid Integration: The European Experience", 17th Power Systems Computation Conference, Stockholm Sweden- August 22-26, 2011

[6]G. Fulli, A.R. Ciupuliga, A. L'Abbaté, M. Gibescu."Review of existing methods for transmission planning and for grid connection of wind power plants". Realisegrid Deliverable,http://realisegrid.rse-web.it/content/files/File/Publications%20and%20results/Deliverable_REALISEGRID_3.1.1.pdf, retrieved on 2011-11-01

[7]IEEE Standard for Distributed Resources Interconnected With Electric Power Systems, IEEE P1547 Std., 2004.

[8]B. Fox, D. Flynn, L. Bryans, N.Jenkins, D. Milborrow, M.O'Malley, R. Waston, O. Anaya-Lara, *Wind power integration: Connection and system operational aspects*, IET Power and Energy Series, ISBN 978-0-86341-449-7.

[9]H. Holttinen, P. Meibom, A. Orths, B. Lange, M. O'Malley, J.O. Tande, A. Estanquerio, E. Gomez, L. Söder, G. Strbac, J.C. Smith, F. V. Hulle, "*Impacts of large amounts of wind power on design and operation of power systems, results of IEA collaboration"*, 8th International Workshop on Large-Scale Integration of Wind Power into Power Systems as well as on Transmission Networks of Offshore Wind Farms, 14-15 Oct. 2009, Bremen.

[10]J.G. Slootweg, W.L. Kling, "*The Impact of Large Wind Power Generation on Power System Oscillations"*, Electric Power Systems Research 67 (2003) 9-20.

[11]Y. Hori, H. Saitoh: "*Disconnection Control of Wind Power Generators for the Purpose of Reducing Frequency Fluctuation"*, IEEJ Trans. PE vol. 128, No.1, pp. 721-727, 2008. (In Japanese)

[12]Sato, D., Saitoh, H.:"*Smoothing Control of Wind Farm Output by using Kinetic Energy of Variable Speed Wind Power generators*." IEEJ Trans. PE. Vol. 129, No.5, pp.580-590. 2009. (in Japanese)

[13]Sørensen P., Unnikrishnan A.K., and Mathew S.A. *Wind Farms Connected to WeakGrids in India*. Wind Energy, VOL: 4, ISSUE: 3, pp. 137-149, 2001

[14]Jauch, C., Islam S.M., Sørensen, P., and Bak-Jensen, B. *Design of a Wind Turbine Pitch Angle Controller for Power System Stabilisation*. Renewable Energy 32 (2007) 2334-2349.

[15]Isao Aoki, Ryoichi Tanikawa, Nobuyuki Hayasaki, Mitsuhiro Matsumoto, Shigero Enomoto, "*Development and operational status of wind power forecasting system*." The Papers of Technical Meeting on Power Systems Engineering, IEE Japan, PSE-12-6, pp.31-36 (2012-01-27) (in Japanese)

[16]P. Kunder, J.Paserba, V. Ajjarapu, G. Andersson, A. Bose, C. Canizares, N. Hatziargyriou, D. Hill, A. Stankovic, C. Taylor, T. Van Custem, V. Vittal. "*Definition and Classification of Power System Stability IEEE/CIGRE joint task force on stability terms and definitions". Power Systems, IEEE Trans.* Vol. 19.2004; pp. 1387-1401.

[17]Tande J.O.G. *Applying Power Quality Characteristics of Wind Turbines for Assessing Impact on Voltage Quality*. Wind Energy, VOL: 5, ISSUE: 1, pp. 37-52, 2002,

[18]Bronzeado H.S., Feitosa E.A.N., Rosas P.A.C., Miranda M.S., de Barros M.E.M., and Rohatgi J. *Investigation of the Behaviour of Wind Turbines Under Low Turbulence Wind Conditions and Their Interaction With the Distribution Grid*. WIND ENGINEERING , VOL: 24, ISSUE: 2, pp. 101-109, 2000,

[19]Akhmatov V., Knudsen H., and Nielsen A.H. *Advanced Simulation of Windmills in the Electric Power Supply*. International Journal of Electrical Power & Energy Systems ,VOL: 22, ISSUE: 6, pp. 421-434, 2000,

[20]Palsson, M.P.; Tande, J.O.G.; Toftevaag, T.; Uhlen, K.; "Large-scale wind power integration and voltage stability limits in regional networks" *Power Engineering Society Summer Meeting, 2002 IEEE,* Volume: 2, 2002 Page(s): 762 –769.

[21]Erlich, I.; Rensch, K. and Shewarega, F. , "Impact of Large Wind Power Generation on Frequency Stability", *Power* Engineering *Society General Meeting* , June 2006 IEEE, Montreal, Canada.

[22]Vladislav Akhmatov: *"System Stability of Large Wind Power Networks: A Danish study case"*, Electrical Power and Energy Systems 28 (2006) 48-57.

[23]Strbac, G. & Bopp, T. 2007. *Value of fault ride through capability for wind farms*.

Report to Ofgem (http://www.sedg.ac.uk), July 2004

[24]Marta Molinas, Jon Are Suul, and Tore Undeland: *"Low Voltage Ride Through of Wind Farms with Cage Generators: STATCOM Versus SVC"*, *Power Electronics, IEEE Trans.* Vol. 23, No. 3, May 2008; pp. 1104-11117

[25]Andrew Causebrook, David J. Atkinson, and Alan G. Jack: *"Fault Ride-Through of Large Wind Farms Using Series Dynamic Barking Resistors"*, *Power Systems, IEEE Trans.* Vol. 22, No. 3, August 2007; pp. 966-975

[26]Vladislav Akhmatov, "Induction Generators for Wind Power", Multi-Science Publishing Co. Ltd, ISBN 0 906522.

[27]T. Sun, Z. Chen and F. Blaabjerg, "*Transient Stability of DFIG Wind Turbines at an External Short-Circuit Fault",* Wind Energy, 2005; 8:345-360, John Wiley & Sons, 2005.

[28]Y. Liao, H. Li, J. Yao,*"Unbalance-Grid Fault Ride-Through Control for a Doubly Fed Induction Generator Wind Turbine with Series Grid-Side Converter"*, WSEAS Transaction on circuits and systems, issue 2, vol. 10, Feb. 2001.

[29]G. Michalke, A. D. Hansen, T. Hartkopf,*"Variable speed wind turbines-fault ride-through and grid support capabilities"*, European Wind Energy Conference EWEC, Brussels-Belgium, 31 March-3 April. 2008.

[30]Conroy, J.F. and Waston, R., 2007, Low-Voltage Ride-Through of a Full Converter Wind Turbine with Permanent Magnet Generator, *IET Renew. Power Gener.*,2007, 1(s) p182-189.

[31]Mittal, R., Sandhu, K.S. , Jain, D.K., 2009, Low Voltage Ride Through of Grid Interfaced Wind Driven PMSG, *ARPN Journal of Engineering and Applied Sciences,* Vol.4, No.5, July.

[32]Hguyen, T.H., LEE, D.C, Song, S.H., Kim, E.H., 2010, Improvement of Power Quality for PMSG Wind Turbine Systems, *Energy Conversion Congress and Exposition (ECCE),* 12-16 Sept, 2010, IEEE.

[33]Hu, W, Chen, Z., Wang, Y., Wang, Z., 2009, Low Voltage Ride Through of Variable Speed Wind Turbines with Permanent Magnet Synchronous Generator, *Ecologic Vehicles Renewable Energies,* Monaco, March 26-29, 2009.

[34]J.G. Slootweg, H. Polinder, W.L. Kling, *Representing Wind Turbine Electrical Generating Systems in Fundamental Frequency Simulations*. IEEE Transactions on energy conversion, vol. 18, pp516-524, No.4, December 2003: 516-524.

[35]R. Takhashi, J. Tamura, Y. Tomaki, A. Sakahara, E. Sasano, *Wind Farm Stabilization by Variable Speed Wind Energy Conversion System using Permanent Magnet Synchronous Generator*. IEEJ, RM-05-114 (in Japanese).

[36]http://www.benderrelay.com/voltage%20relays%20table.htm, SUR 353Z-71, 3 AC 690V, 0.7-0.95 Un, 50-60 Hz, download on 2008-July-1.

[37]S. Heier, *Grid Integration of Wind Energy Conversion Systems*. Chicester, U.K.: Wiley, 2006,2nd edn.

[38]MATLAB R2009a, Manual, MathWorks, Inc., 2009.

[39]T. V. Cutsem, C. Vournas, *Voltage Stability of Electric Power Systems*:Kluwer Academic Publishers, Massachusetts, U.S.A , 1998.

[40]N.G. Hingorani, L. Gyugyi, "Understanding FACTS; Concepts and Technology of Flexible AC Transmission Systems," IEEE Press book, 2000.

[41]Claudio L.Souza et. Al., "Power System Transient Stability Analysis Including Synchronous and Induction Generator," IEEE Porto Power Tech Proceeding, Vol. 2, pp.6, 2001.

[42]P. M Anderson, A.A. Fouad, *Power System Control and Stability*. New York: IEEE Press, 1994.

Appendix

A Simulation Models Parameters

A.1. Proposed pitch controller parameters: K_P=8, K_I=50

A.2 Synchronous Generator Parameters

Rated Power (Base MVA for impedances) =100MVA

Rated kV (line-to-line voltage) = 13.8kV

Unsaturated d-axis sub-transient reactance: x_d"=0.145 (pu)

Unsaturated d-axis transient reactance: x_d'=0.220 (pu)

Unsaturated d-axis synchronous reactance: x_d=1.180 (pu)

Unsaturated q-axis sub-transient reactance: x_q"=0.145 (pu)

Unsaturated q-axis synchronous reactance: x_q=1.050 (pu)

Armature resistance: r_a=0.0035 (pu)

Leakage reactance: x_l= 0.075 (pu)

d-axis sub-transient open circuit time constant: T_{d0}"=0.042 (s)

d-axis transient open circuit time constant: T_{d0}'=5.9 (s)

q-axis sub-transient open circuit time constant: T_{q0}"=0.092(s)

d-axis sub-transient short circuit time constant: T_d"=0.023 (s)

d-axis transient short circuit time constant: T_d'=1.28 (s)

q-axis sub-transient short circuit time constant: T_q"=0.023 (s)

A.3 Parameters of wind turbine model:

Nominal rotor speed: 17 RPM, Shaft stiffness:0.3pu/el.rad,

Rotor diameter: 75m, Area covered by rotor: 4418m^2,

Nominal power: 2 MW, Nominal wind speed: 14m/s,

Gear box ratio: 1:89, Inertia constant: 2.5s,

Approximation in Aerodynamic Power:

$$P_m = C_p P_w = \frac{\rho}{2} A_{wt} C_p(\lambda,\theta) u^3 \; C_p(\lambda,\beta) = c_1(\frac{c_2}{\lambda_i} - c_3\beta - c_4\beta^{c5} - c_6)e^{-\frac{c7}{\lambda_i}} \;, \quad \lambda_i = 1/(\frac{1}{\lambda + c_8\beta} - \frac{c_9}{\beta^3 + 1})$$

C_1=0.73, C_2=151, C_3=0.58, C_4=0.002, C_5=2.14, C_6=13.2, C_7=18.4, C_8=-0.02, C_9=-0.003,

A.4. Parameters of induction generator model:

Number of poles: 4, Generator speed: 1500 RPM,

Mutual inductance: 3.0p.u, Stator leakage inductance: 0.1p.u, Rotor leakage inductance: 0.08p.u, Stator resistance: 0.01p.u, Rotor resistance,: 0.01p.u.

A.5. Parameters of permanent magnet synchronous generator model:

Number of poles: 48, Stator Winding Resistance R_a: 0.002887 [Ω],

d-axis Exicitation Inductance L_d:0.002393 [H], Flux Linkage of Rotor ψ_f:9.4755 [Wb]

q-axis Exicitation Inductance L_q:0.001675 [H], Inertia J_{WG}: 1899980 [kg/m2]

A.6. Parameters of power converter and transmission line

Capacity of DC-Capacitor: 3000 [μF], Switching Frequency of Converter: 400 [Hz],

Switching Frequency of Inverter: 1000 [Hz], Cable Resistance R_{lins}: 7.96×10^{-3}[Ω]

Cable Inductance L_{lins}: 7.63×10^{-5}[H]

B. LVRT Impact on Frequency Stability of Power System (based on the Generation Mix of Hokkaido Power System)

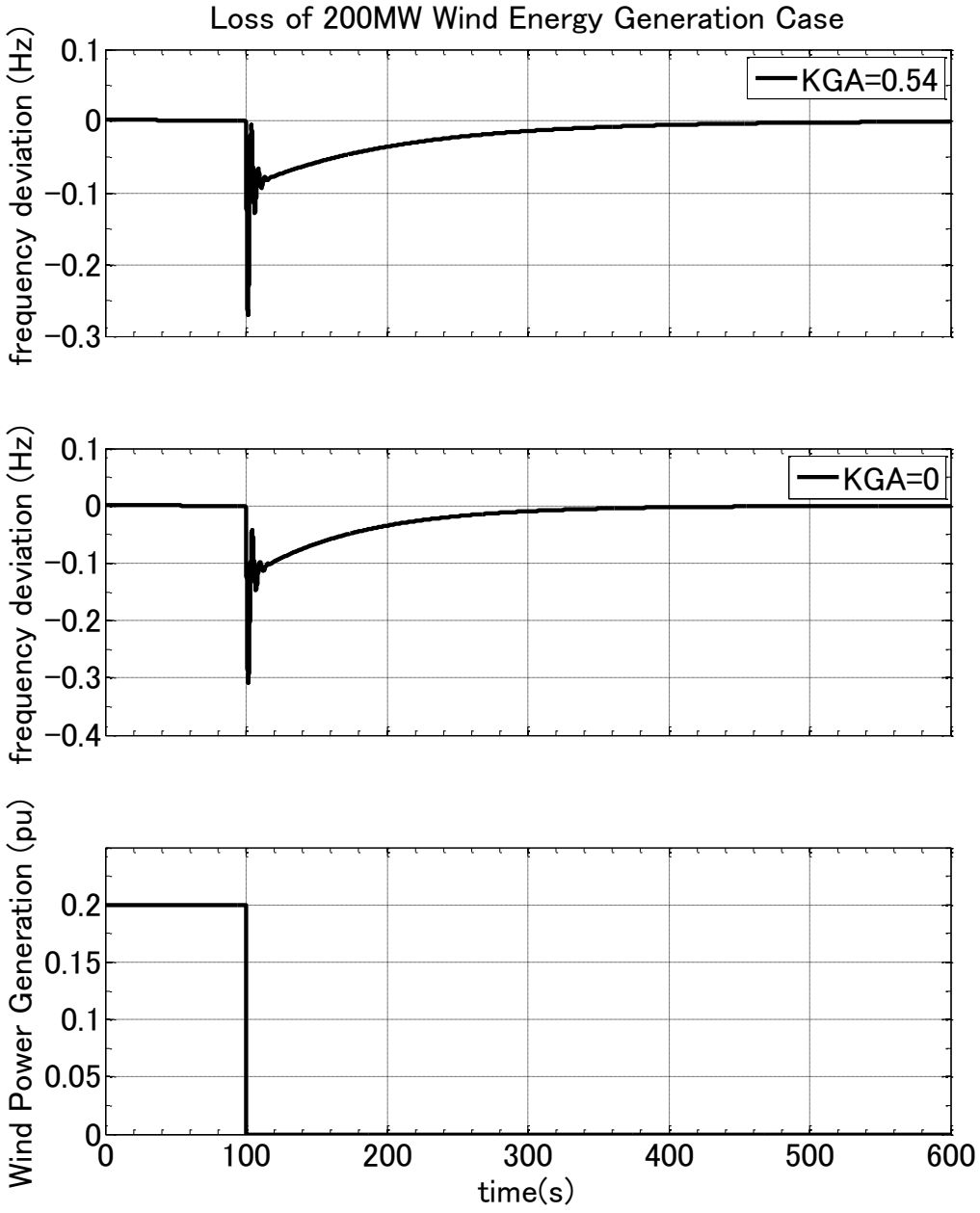

Fig. B.1 Frequency deviation due to the loss of wind power generation (Impact of loss of 200MW generation (e..g due to the lack of wind power LVRT) in power system (based on the Hokkaido Power System Generation Mix))

Model and Parameters in simulation study

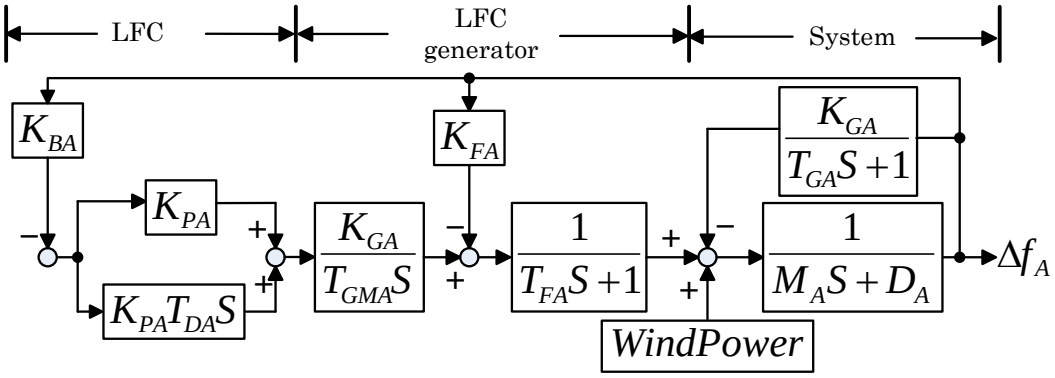

Fig.B.2 LFC Control Block Diagram for Power System with Wind Power Generation

Δf_A : frequency deviation from nominal value $[Hz]$,

M_A : System Inertia Constant $[puMW \cdot s / Hz]$,

K_{GA} : Speed Regulation of Generator with Governor Free Operation $[puMW / Hz]$,

T_{GA} : Time Constant of Governor Free (without LFC)Generator $[s]$,

K_{FA} : Speed Regulation of Generator with LFC$[puMW / Hz]$,

T_{FA} : Time Constant of Governor with LFC Control $[s]$,

K_{CA} / T_{GMA} : LFC Ramp Rate Factor ,

K_{PA} : LFC Proportional Gain ,

T_{DA} : Time Constant for Derivative Gain $[s]$,

D_A : Percent Change in Load divided by Percent Change in Frequency$[puMW / Hz]$,

K_{BA} : Area Composite Frequency Response Characteristic $[puMW / Hz]$,

TableB.1. Parameters for Power System with 200MW Wind Energy Generation

Base Frequency	50	*[Hz]*
Installed Capacity	4	*[puMW]*
Installed Capacity of Thermal Plants with LFC	2.92	*[puMW]*
Installed Capacity of Thermal Power Plants without LFC	1.08	*[puMW]*
Based Capacity	1000	*[MW]*

TableB.2. Parameters for Block Diagram

K_{GA}	0	[*puMW/Hz*]
T_{GA}	2.5	[*s*]
K_{FA}	1.46	[*puMW/Hz*]
T_{FA}	2	[*s*]
K_{CA}/T_{GMA}	2.0	
K_{PA}	0.01	
T_{DA}	1	[*s*]
D_A	0.08	[*puMW/Hz*]
K_{BA}	1	
M_A	0.56	[*puMWs/Hz*]

Percent Change in Load divided by Percent Change in Frequency for 1.0%

$$D_A = \frac{0.01}{0.01 \times 50} \times 4 = 0.08 \ [puMW / Hz] \tag{B.1}$$

Speed Regulation of Generator for 4.0%

$$K_{GA} = 1.08 \times \frac{1}{50 \times 0.04} = 0.54 \ [puMW / Hz] \quad \text{(with Gov. Free Operation Case)} \tag{B.2}$$

$$K_{FA} = 2.92 \times \frac{1}{50 \times 0.04} = 1.46 \ [puMW / Hz] \tag{B.3}$$

System Inertia Constant

Assume Single Generator Inertia Constant= 3.5[s]

$$M_A = 2 \times 3.5 \times 4 \times \frac{1}{50} = 0.56 \ [puMW \cdot s / Hz] \tag{B.4}$$

C. Influence of Proposed Pitch Control on Conventional Generation in Power System

The LVRT behavior of WTG is closely related to the rotor over-speeding during the voltage dip. The rotational speed of the WTG with a directly grid-connected SCIG is considered to operate at fixed speed. Therefore, the wind turbine rotor over-speeding behavior can be figured out by means of the power imbalance between mechanical input power and electrical output power which is proportional to a square of its terminal voltage. SCIG requires large reactive power to recover the air gap flux when a short circuit fault occurs in the power systems [41]. Therefore, the reactive power supply is necessary for voltage recovery of SCIG. Moreover, the rate of voltage recovery after the fault is closely related to the voltage controllability of power network.

In this regard, by considering the influence of Auto Voltage Regulator (AVR) of Synchronous Generator (SG) and SVC at different locations in power systems, we can evaluate the performance of proposed pitch control in more practical perspective. In this paper, the effects of AVR and SVC locations on performance of pitch control for wind farm's LVRT is investigated by simulation studies. The comparison of the LVRT behaviors with the different SG and SVC locations in power systems are included.

C.1 Power Systems with Synchronous Generator Model

In order to evaluate the performance of the proposed pitch control for LVRT, simulation studies were performed. The single line diagram of a power system including a wind farm, as shown in Figure C.1, is modeled in simulation tools of MATLAB/Simulink, in which the wind farm of 30MW installed capacity is supplying

power to power systems represented by the infinite bus. The wind farm consists of 15 FSWTs of which each has 2MW rated power capacity. The wind farm is connected to the 66kV bus at which SVC of 30Mvar capacity is installed for bus voltage stabilization. The parameters of wind turbine transformers, cables and grid transformers are taken from the reference [35]. The length of sub-transmission line between the node #A and #B, and that of node #B and #C is 19km each.

The SVC model used in this study is shown in Figure C.2. This model only considers observing the impact on voltage stability at the fundamental frequency [38, 40]. The SVC has the dynamic performance of ±30 MVar, with the average thyristor valves firing time delay, T_d, of 4ms and the V-I characteristics slope or droop reactance, K_{SL}, of 0.03 p.u. at 30 MVA base. The reference voltage (V_{ref}) of the voltage regulator with PI controller is set at 1.03 p.u. to stabilize the voltage at the Point of Common Coupling (Vpcc). In this block diagram, V_T is the terminal voltage of SVC.

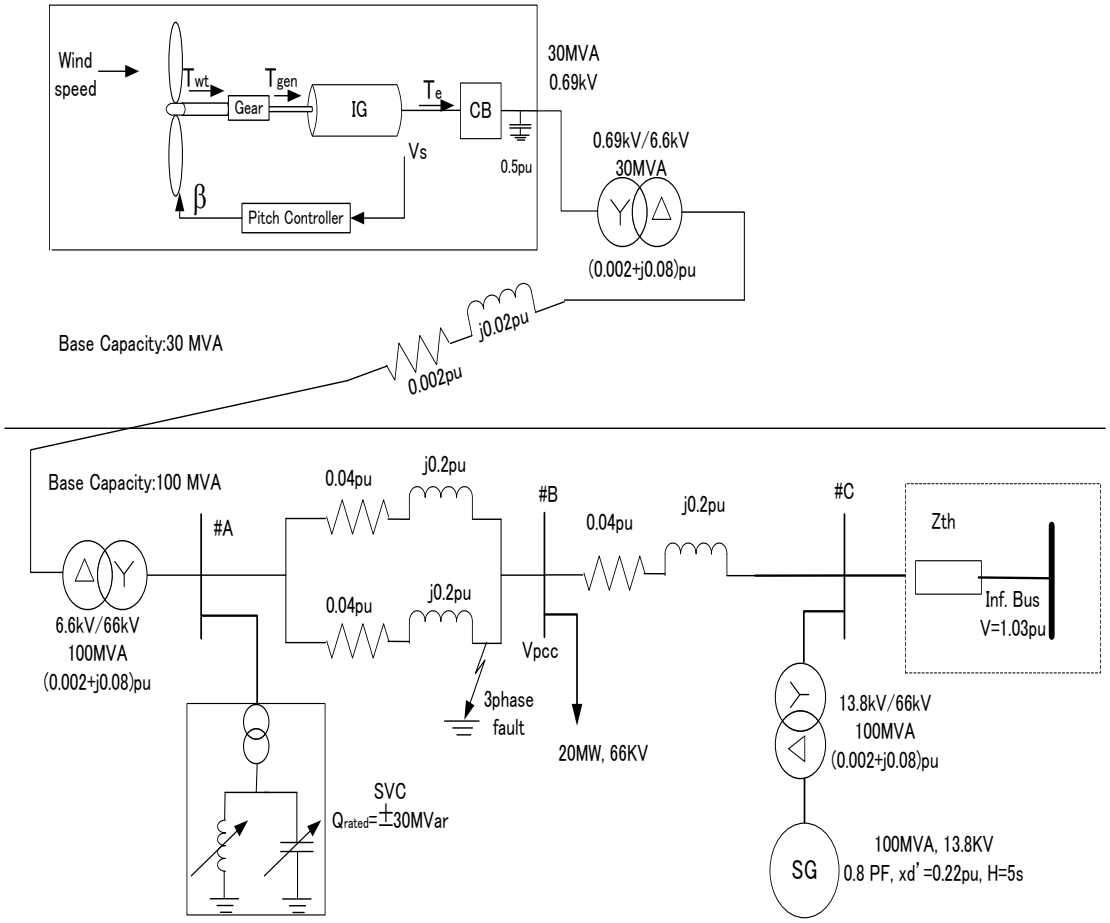

Figure C.1 Power system model including synchronous generator

C.2 Synchronous Generator with AVR Model

The synchronous generator model is based on the reference [38, 40]. The electrical part of the machine is represented by a sixth-order state-space model, and the mechanical part is described by the swing equation. All the rotor parameters and electrical quantities shown in Appendix A.2 are referred to the stator and the mechanical part is described by the following swing equation.

$$\Delta\omega(t) = \frac{1}{2H}\int_0^t (T_m - T_e)dt - Kd\Delta\omega(t) \tag{C.1}$$

$$\omega(t) = \Delta\omega(t) + \omega_0 \tag{C.2}$$

where

$\Delta\omega$=Speed variation with respect to speed of operation

H= Constant of inertia

T_m=Mechanical torque

T_e=Electromagnetic torque

K_d=Damping factor representing the effect of damper windings

$\omega(t)$=Mechanical speed of the rotor

ω_0=Speed of operation (1pu)

The model takes into account the dynamics of the stator, field, and damper windings. The equivalent circuit of the model is represented in the rotor reference frame (dq frame). All rotor parameters and electrical quantities are viewed from the stator. They are identified by primed variables. The subscripts are defined as follows:

d,*q*: d and q axis quantity

r,*s*: rotor and stator quantity

l,*m*: leakage and magnetizing inductance

f,*k*: field and damper winding quantity

The electrical model of the machine is represented by the following equations:

$$
\begin{aligned}
V_d &= R_s i_d + \frac{d}{dt}\Phi_d - \omega_r \Phi_q \\
V_q &= R_s i_q + \frac{d}{dt}\Phi_q + \omega_r \Phi_d \\
V'_{fd} &= R'_{fd} i'_{fd} + \frac{d}{dt}\Phi'_{fd} \\
V'_{kd} &= R'_{kd} i'_{kd} + \frac{d}{dt}\Phi'_{kd} \\
V'_{kq1} &= R'_{kq1} i'_{kq1} + \frac{d}{dt}\Phi'_{kq1} \\
V'_{kq2} &= R'_{kq2} i'_{kq2} + \frac{d}{dt}\Phi'_{kq2}
\end{aligned}
\tag{C.3}
$$

where

$$
\begin{aligned}
\Phi_d &= L_d i_d + L_{md}(i'_{fd} + i'_{kd}) \\
\Phi_q &= L_q i_q + L_{mq} i'_{kq} \\
\Phi'_{fd} &= L'_{fd} i'_{fd} + L_{md}(i_d + i'_{kd}) \\
\Phi'_{kd} &= L'_{kd} i'_{kd} + L_{md}(i_d + i'_{fd}) \\
\Phi'_{kq1} &= L'_{kq1} i'_{kq1} + L_{mq} i_q \\
\Phi'_{kq2} &= L'_{kq2} i'_{kq2} + L_{mq} i_q
\end{aligned}
$$

$$
T_e = \frac{3}{2} P(\varphi_d i_d - \varphi_q i_d) \tag{C.4}
$$

The AVR model used in this study is shown in Figure 4.19. This model is based on the excitation control systems with potential-source-rectifier exciter. The static voltage regulator generates a control signal by which the SCR gating in the excitation system is controlled. This type of control is very fast since there is no time delay in shifting the firing angle of the SCR's [42].

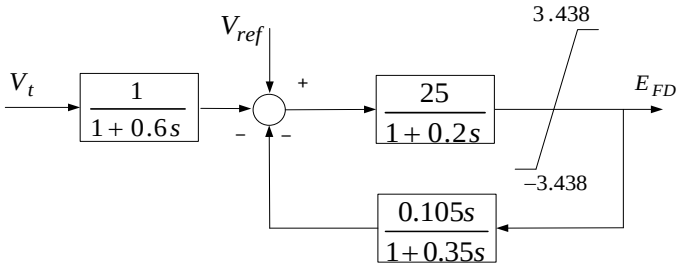

Figure C.2 AVR model

C.3 Simulation Results

The LVRT behavior is evaluated by means of simulation studies. By assuming the fault points at 18 km from the node #A in 19km long double-circuit sub-transmission line in Figure C.1, the voltage along the sub-transmission lines is depressed until the faulted line is isolated. The fault sequence used in the simulation is the three-phase-to-ground fault occurred in one of the 66kV sub-transmission lines. The fault is occurred at 500 *ms* and the faulted line is isolated at 700 *ms* from the start point of simulation. In addition to these, LVRT behaviors of wind farm are explored by considering the different locations of SVC (whether at node #A, node #B or node #C) and SG (whether at node #B or node #C).

C.3.1 SG at node #C

The LVRT behaviors of wind farm are checked for the far location of SG to wind farm.

C.3.1.1 Case 1 (without SVC)

The LVRT behavior of wind farm in this case is shown in Figure C.3. The associated SG behavior is also shown in Fig. C.4. In Figure C.3, the generated active power of wind farm is lost at 5.68s from the start point of simulation due to the wind farm disconnection after isolating the faulted line. When the fault is occurred at the distance of 18km from node #A, the generator terminal voltage is depressed suddenly to 0.5 p.u

at the 500 ms. The generator terminal voltage continues depressing to the 0.05 p.u. until the faulted line is isolated at 700 ms. As explained in section 2, the imbalance between mechanical input and electrical output is occurred, which causes the rotor over speeding.

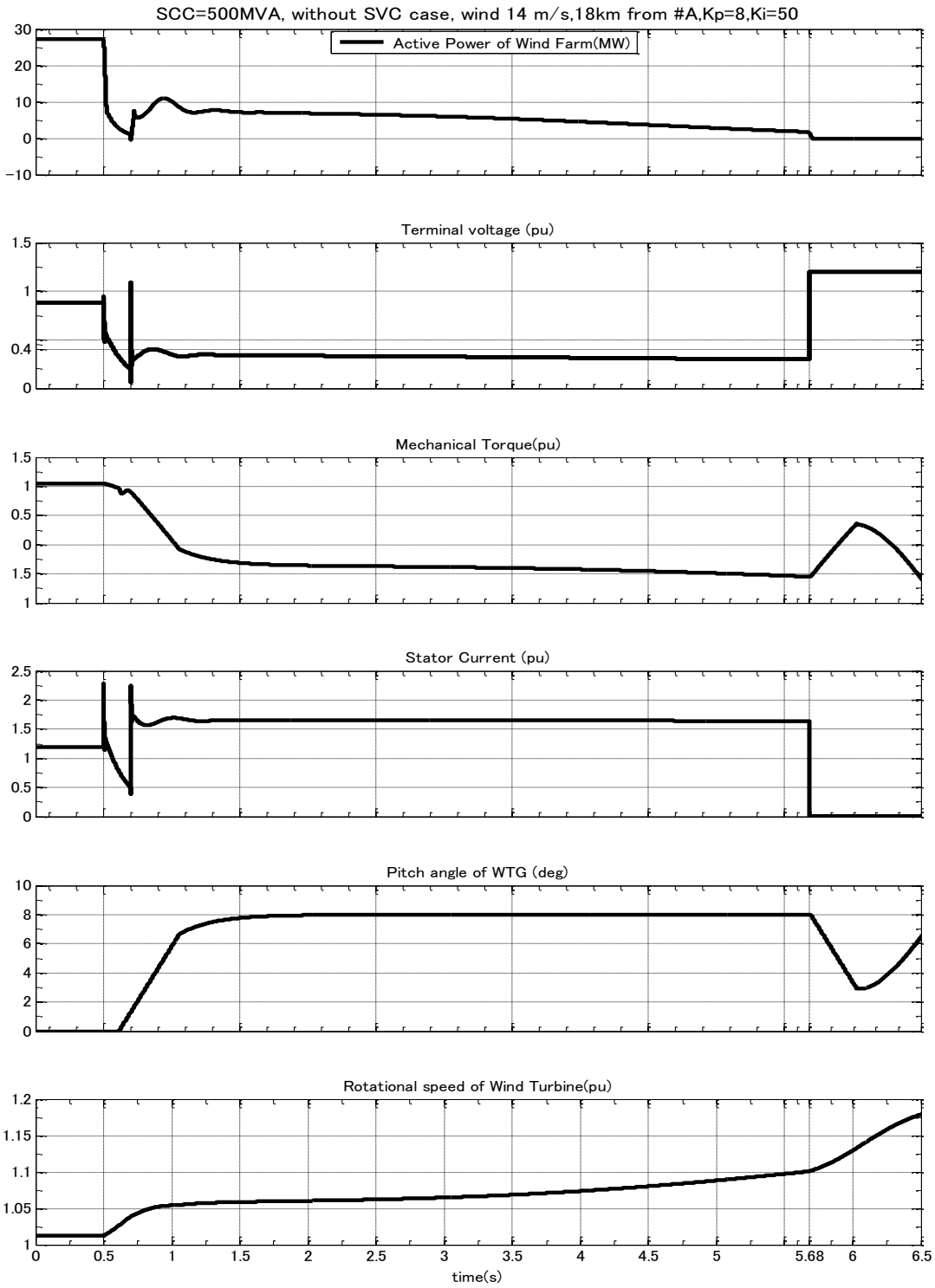

Figure C.3 Behavior of wind farm (case 1: without SVC)

Once the faulted line is isolated at 700 *ms*, the terminal voltage tends to recover back. Consequently, SCIG absorbs more reactive power due to over speeding (not reached to the protection system limit of 1.1 p.u. at that instance), and this causes over current in the stator of SCIG (not reached to the protection system limit of 2 p.u. for 40*ms* at that instance) as shown in Figure 4.18. However, the terminal voltage of SCIG is collapsed and cannot recover back above the 0.4 p.u. level. Due to the continuous over speeding, the rotor unfortunately reached to over speed protective relay limits for 40 *ms* at the time of 5.68s from the start point of simulation. Therefore, WTG is disconnected from the grid by over speed protection in order to avoid the damaging.

The behavior of SG is shown in Figure C.4. Due to the fault, the terminal voltage is depressed suddenly to the 0.52 p.u. until the fault is isolated. According to the exciter field voltage controlled by AVR, SG injected the reactive power during and after the voltage dip period. The rotor speed oscillation is decayed at 2.5s and backswing is observed due to the decelerating. Although the SG fed the reactive power absorbed by the wind farm during and after the fault, the continuous power supply of wind farm is cannot be achieved in this case.

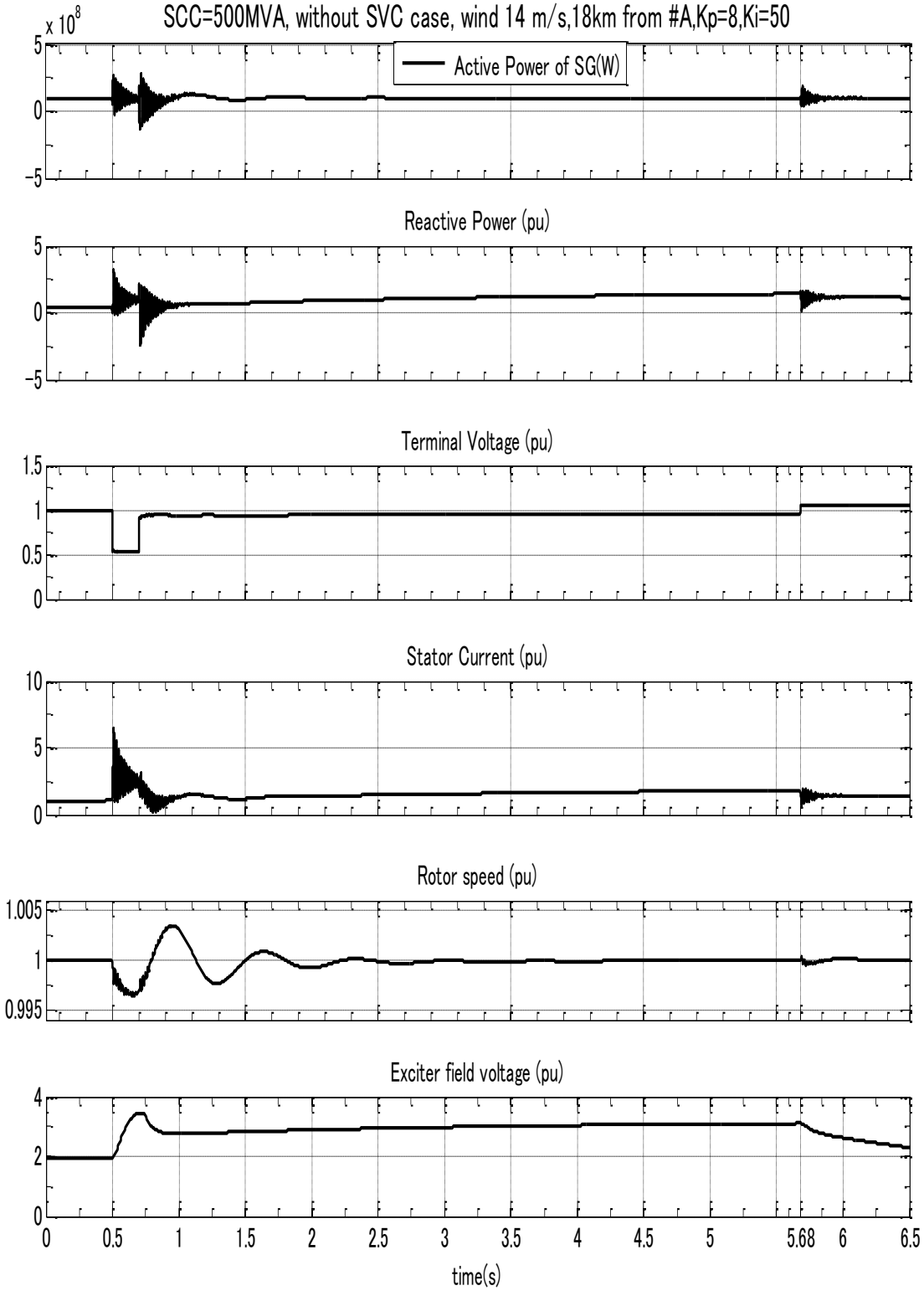

Figure. C.4. SG Behavior (case 1: without SVC)

C.3.2 Case 2 (SVC at node #A)

The LVRT behavior of wind farm for this case is shown in Figure C.5. The associated SG and SVC behavior are also shown in Figure C.6 and C.7. With the use of proposed pitch control, the LVRT can be improved. By comparing Figure C.3 with C.5, the over speeding of rotor can be reduced during the post-fault period in case 2. The terminal voltage of SCIG is gradually recovered from the 0.5 p.u. level. The rotor speed returns to pre-fault level (around 1p.u.) at 2.5s. Consequently, the proposed pitch control contributes to voltage recovery of SCIG after the fault is isolated as shown in Figure C.5.

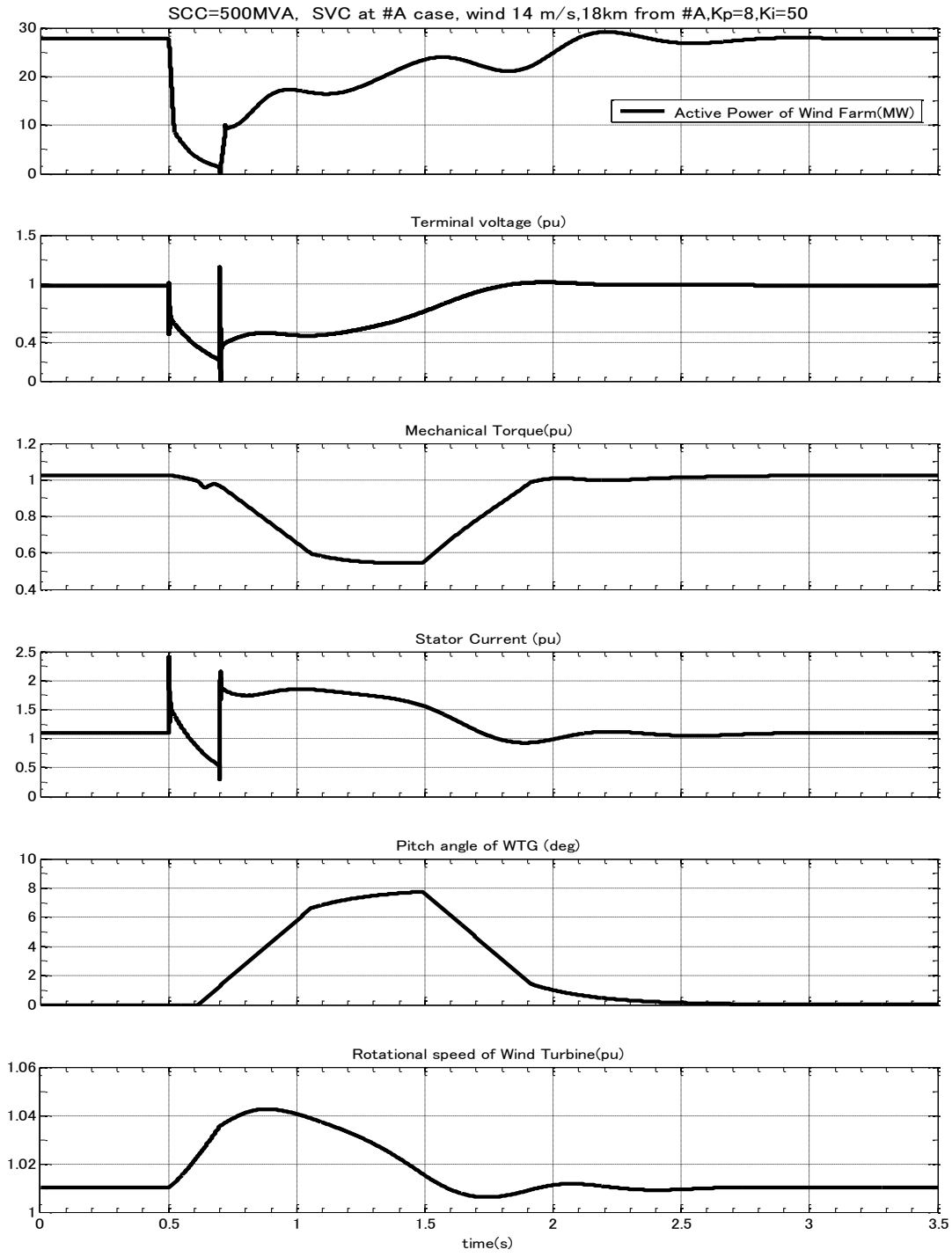

Fig. C.5. Wind Farm Behavior (case 2: SVC at #A)

The behavior of SG is shown in Fig. C.6. Due to the fault, the terminal voltage is depressed suddenly to the around 0.52 p.u. until the fault is isolated. According to the exciter field voltage controlled by AVR, SG injected the reactive power during the voltage dip period. The rotor speed oscillation is decayed at 2.5s and backswing due to the decelerating is improved by means of SVC and proposed pitch control.

The behavior of SVC is shown in Figure C.7. Due to the fault, the bus voltage controlled by SVC at node #A is depressed to almost 0 p.u. until the fault is isolated. According to the reference voltage setting of voltage regulator, SVC injected the reactive power of 30Mvar once the voltage at node #A is recovered. The SVC fed the reactive power absorbed by the wind farm after the fault until the terminal voltage recovers back to the nominal voltage of 1 p.u. Due to the close location to fault, SVC cannot feed reactive power during the voltage dip.

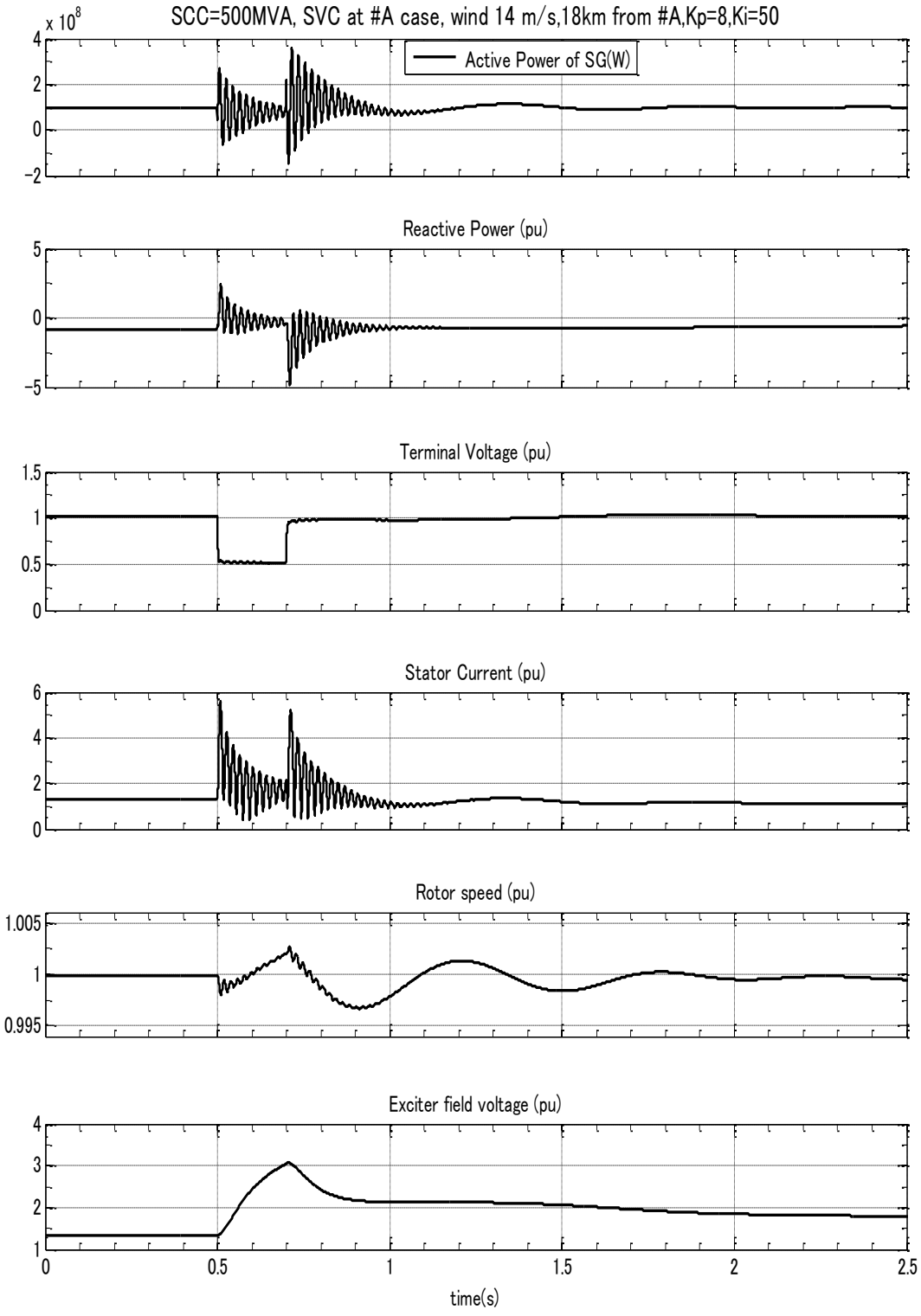

Fig. C.6. SG Behavior (case 2: SVC at #A)

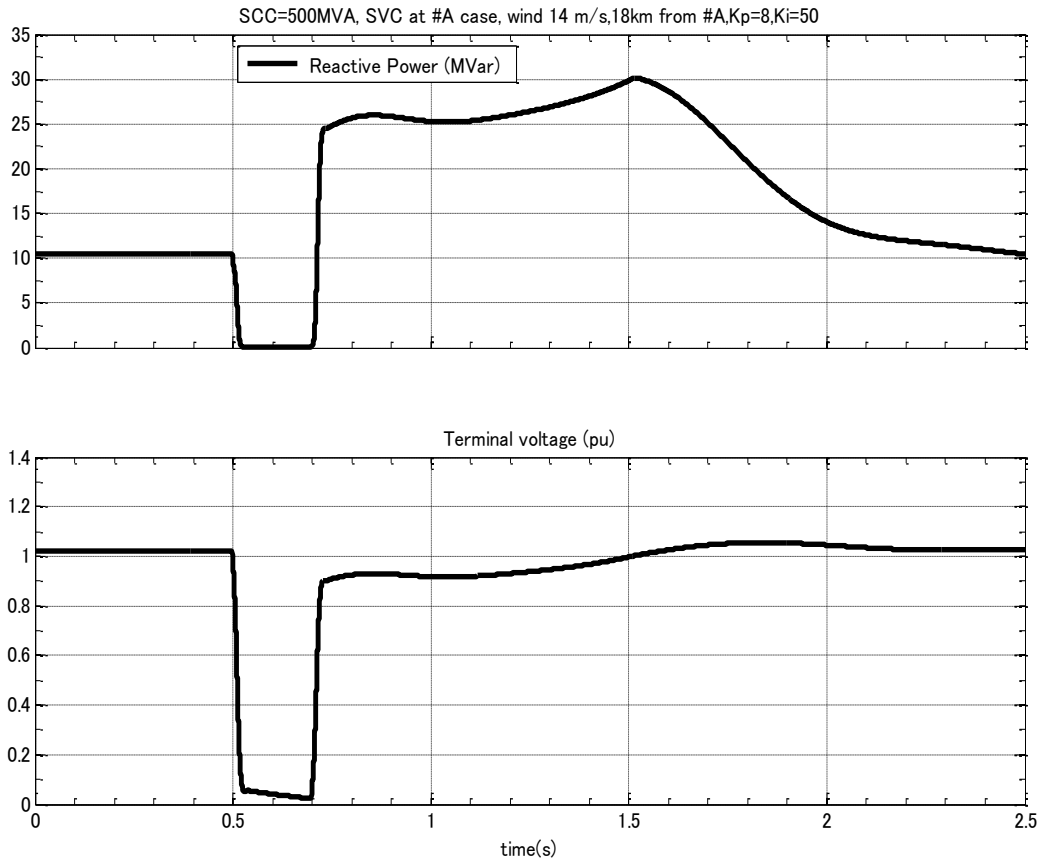

Fig. C.7. SVC Behavior (case 2: SVC at #A)

C.3.3 Case 3 (SVC at node #B)

The LVRT behavior of wind farm in this scenario is shown in Figure C.8. The associated SG and SVC behavior are also shown in Figure C.9 and C.10. With the use of proposed pitch control, the LVRT can be improved. By comparing Figure C.3 with C.8, the over speeding of a rotor can be reduced during the post-fault period in case 3. The terminal voltage of SCIG is gradually recovered from the 0.5 p.u. level. The rotor speed returns to pre-fault level (around 1p.u.) at 2.5s. Consequently, the proposed pitch control contributes to voltage recovery of SCIG after the fault is isolated as shown in Figure C.8.

The behavior of SG is shown in Figure C.9. Due to the fault, the terminal voltage is depressed suddenly to the around 0.52 p.u. until the fault is isolated. According to the exciter field voltage controlled by AVR, SG injected the reactive power during the voltage dip period. The rotor speed oscillation is decayed at 2.5s and backswing due to the decelerating is improved by means of SVC and proposed pitch control.

The behavior of SVC is shown in Figure C.10. Due to the fault, the bus voltage controlled by SVC at node #B is depressed to around 0 p.u. until the fault is isolated. According to the reference voltage setting of voltage regulator, SVC injected the reactive power of 30Mvar once the voltage at node #B is recovered. The SVC fed the reactive power absorbed by the wind farm after the fault until the terminal voltage recovers back to the nominal voltage of 1 p.u. Due to the close location to fault, SVC cannot feed reactive power during the voltage dip.

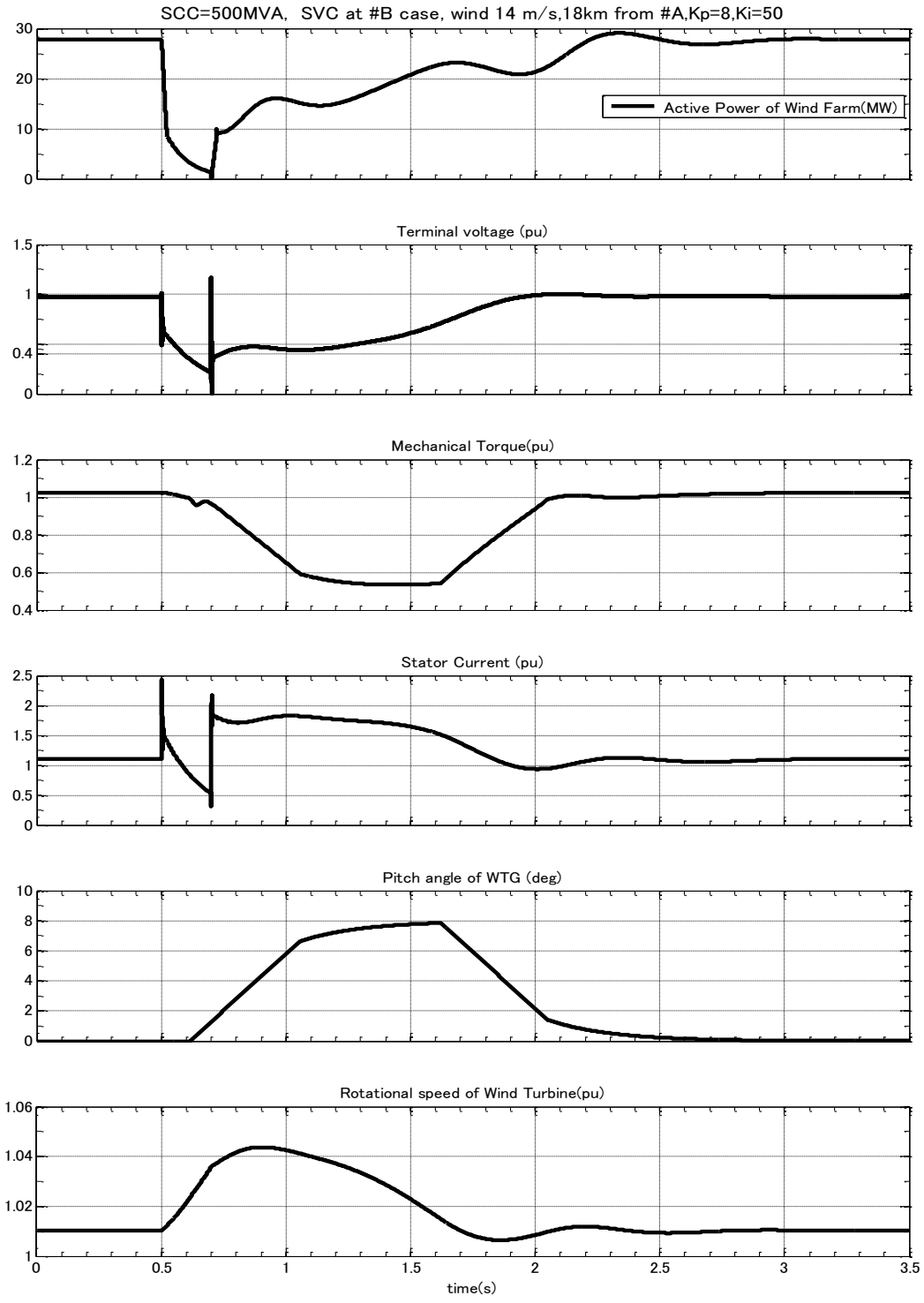

Fig. C.8 Wind Farm Behavior (case 3: SVC at #B)

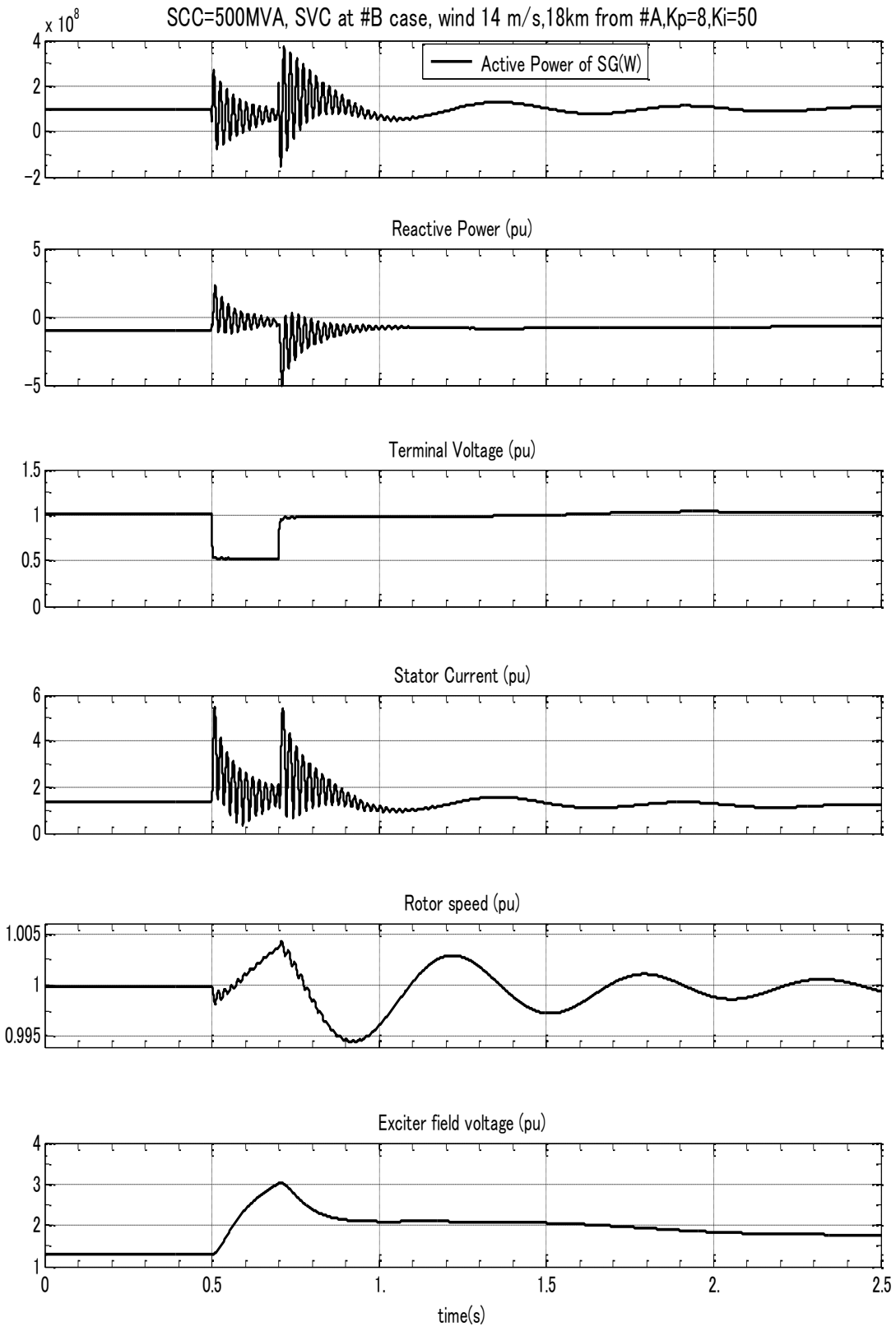

Fig. C.9 SG Behavior (case 3: SVC at #B)

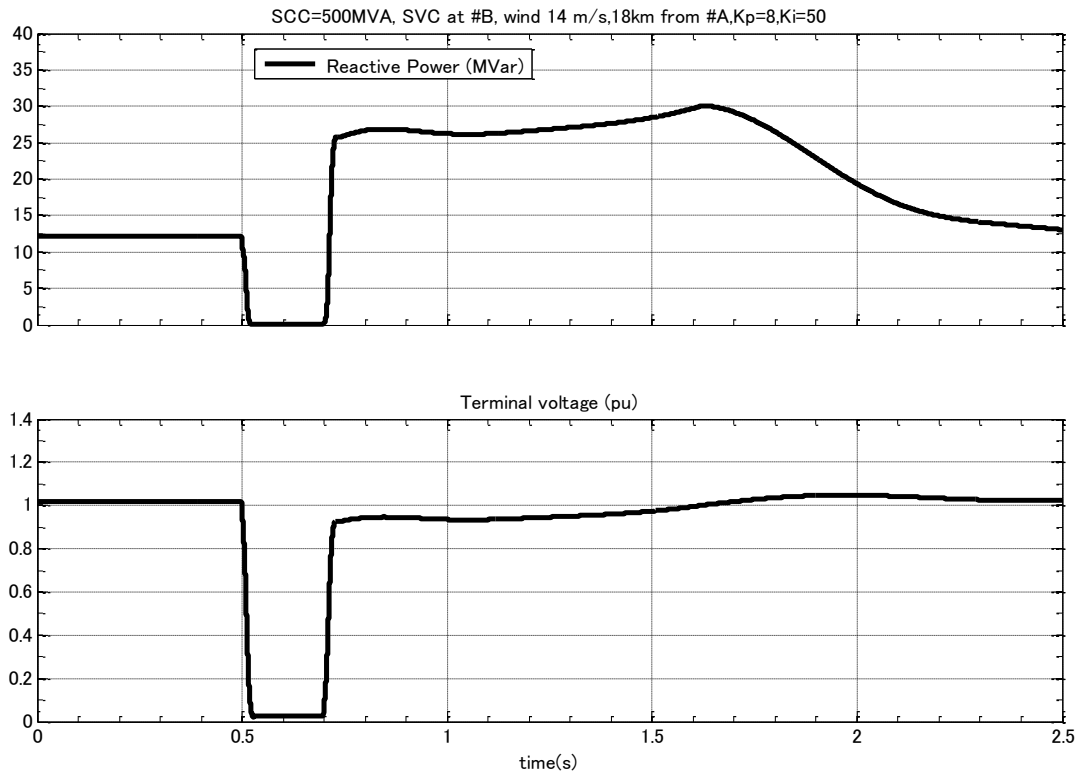

Fig. 10 SVC Behavior (case 3: SVC at #B)

C.3.4 SG at Node #B

The LVRT behaviors of wind farm are checked for the near location of SG to wind farm. Table C.1 summarizes the LVRT behaviors of wind farm for these cases in which the SG is supposed to be connected at the node #B and #C. In this table, the disconnection reason with corresponding time and SVC locations are shown. The proposed pitch control is effective with the use of SVC at node #A and #C. For without SVC case, the proposed pitch control is not effective for LVRT. Comparing to the far location of SG cases, WTG can stay connected longer time until to reach it's over speed limit in the close location of SG case. Therefore, we can say that the electrical distance between the wind farm and SG has influence on LVRT of wind farm.

Table C.1. LVRT Behaviors for SVC at node #B case

	SG at node #B (about 19km far from wind farm)	SG at node #C (about 38km to wind farm)
SVC at node #A (close to wind farm)	Success for LVRT	Success for LVRT
SVC at node #B (about 19km far from wind farm)	Not considered	Success for LVRT
SVC at node #C (about 38km to wind farm)	Success for LVRT	Not considered
Without SVC	Fail for LVRT at 6.1s (over speed)	Fail for LVRT at 5.68s (over speed)

C.4 Conclusions

We show the influence of synchronous generator and static var compensator locations on the performance of proposed pitch control for LVRT. The performance of proposed pitch control is satisfied in the case of existing reactive power source in local area. According to our study, the LVRT behavior is closely related to the voltage recovery after clearing the fault. Therefore, the influence of AVR during the post-fault period and location of reactive power source should be taken into account in LVRT studies. In this study, we also observed that the back swing phenomenon of SG is improved by the use of SVC and proposed pitch control.

D Comparison study with control strategy of back-to-back frequency converter system from literature [32]

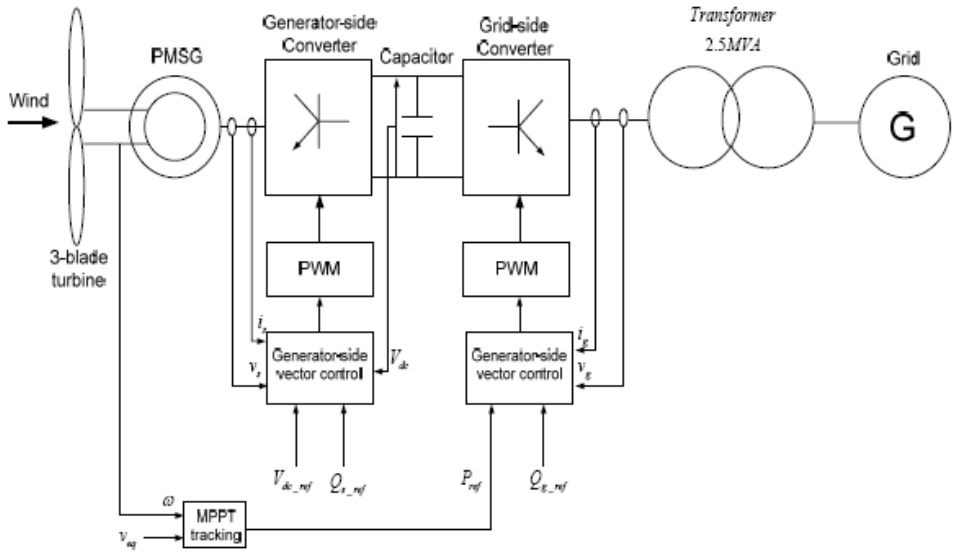

Fig.D.1. Control scheme in the literature [32]

The countermeasure of LVRT for PMSG is proposed in literature [32].As shown in the Fig.5.1, in the conventional control schemes in PMSG, the objective of the vector-control scheme for the generator-side PWM converter is to control the optimal power tracking for maximum energy capture from the wind by adjusting the speed of the wind turbine. The objective of the vector-control scheme for the grid-side PWM inverter is to keep the DC-link voltage constant regardless of the magnitude of the generator power. To maintain the power factor, the reactive power output is kept to be zero. In literature [32], the authors paid special focus on the regulation of the DC-link voltage. A new control scheme of is suggested as shown in Fig.D.1. The objective of vector-control scheme for the generator-side converter is to maintain the DC-link voltage to be constant. At the same time, the grid-side converter controls the optimal power tracking for maximum energy capture. The energy imbalance during the voltage dip is stored in the kinetic energy of the large rotating masses. To maintain the power

factor, the reactive power output is kept to be zero. **However, the controllability of Grid-side converter is doubtful and the graph of reactive power output is not shown in this paper.** Therefore, simulation study is carried out by this approach and compared to the proposed power curtailment control.

D.1 Simulation Model and Results

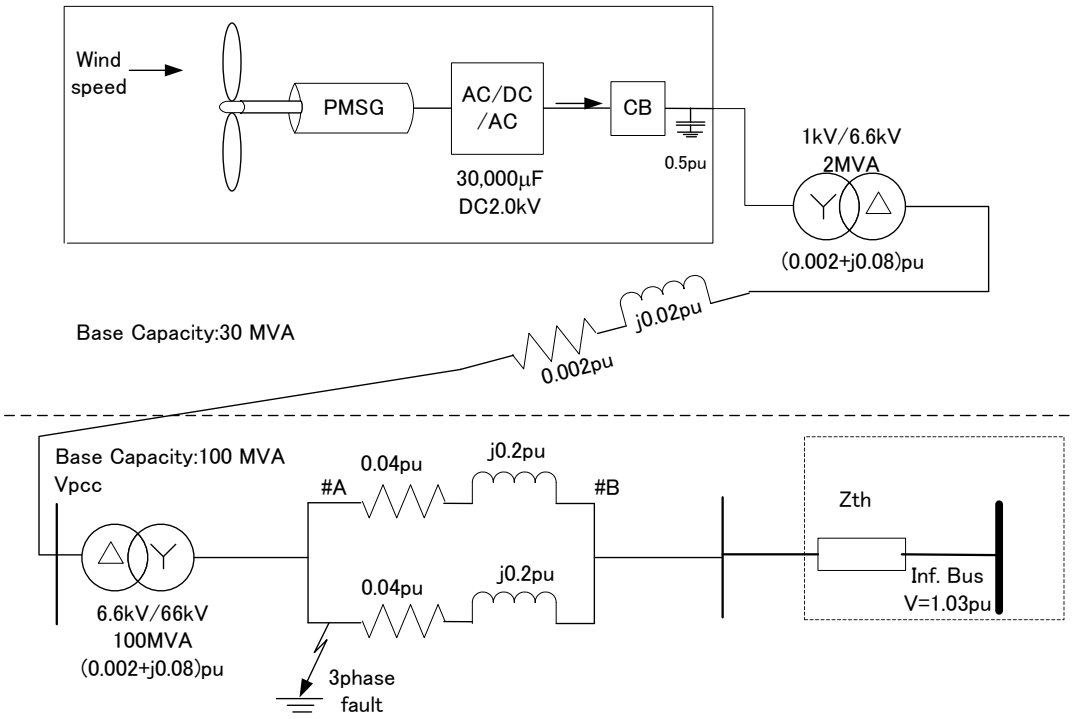

Fig.D.2. Power System Model

Fig.D.2. shows the single line diagram of power system used in this study. Z_{th} is chosen in order to be the Short Circuit Capacity of 500MVA and X/R ration of 10. Based on the network and PMSG parameters from reference paper, simulation study is carried out. Three phase short circuit fault is assumed to be occurred at 9s and isolated at 9.2s.

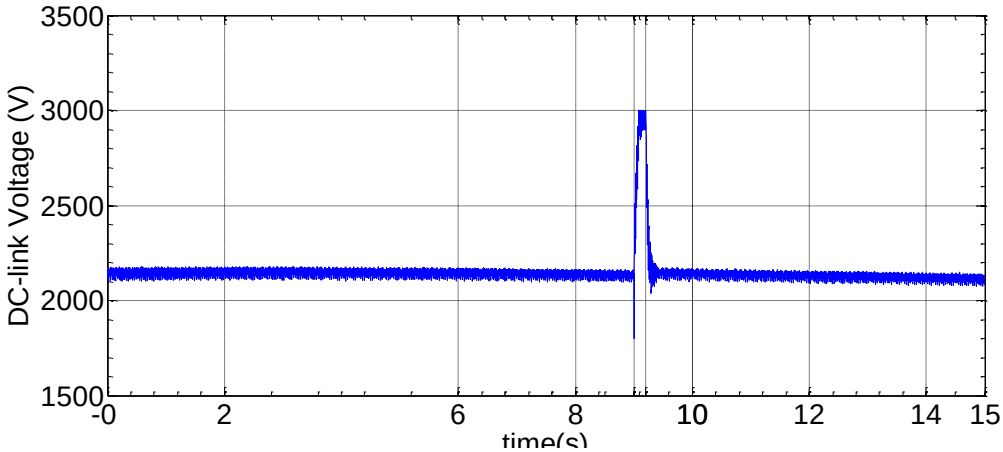

Fig.D.3 DC-link voltage by using the control scheme in literature [32]

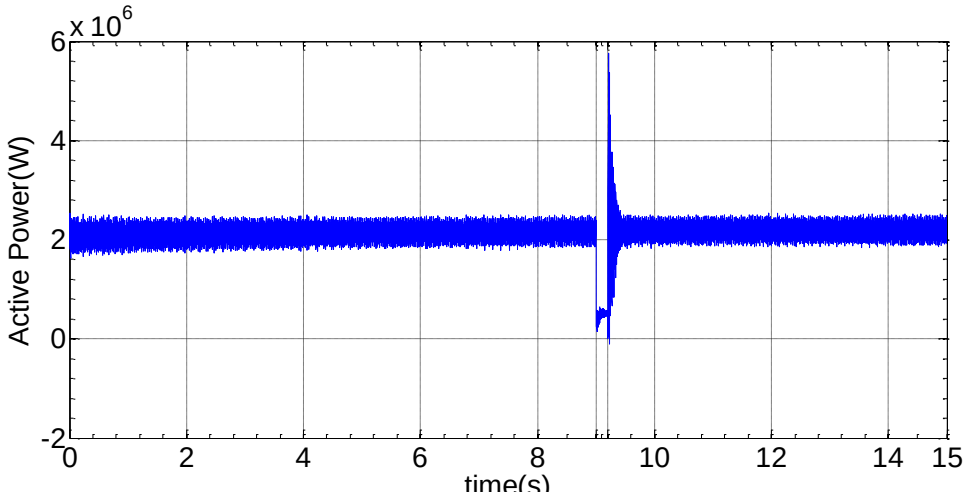

Fig.D.4 Active power output by using the control scheme in literature [32]

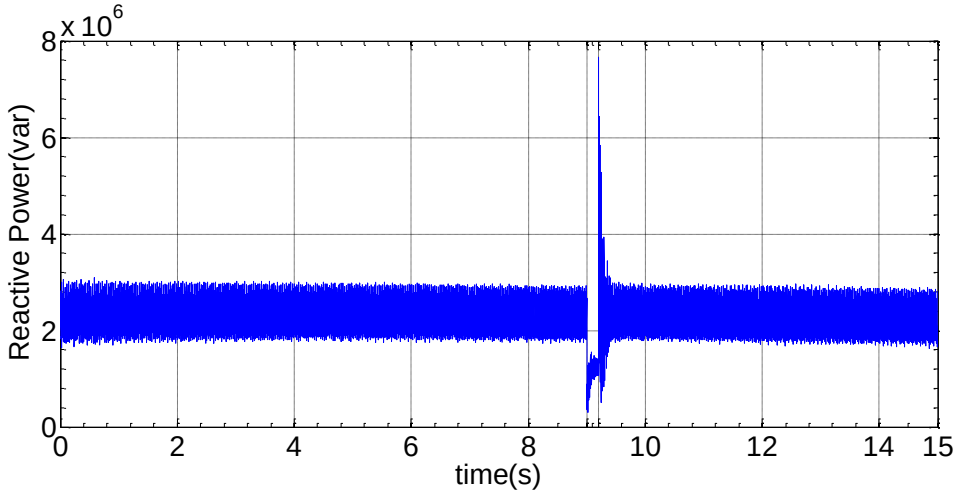

Fig.D.5 Reactive power output by using the control scheme in literature [32]

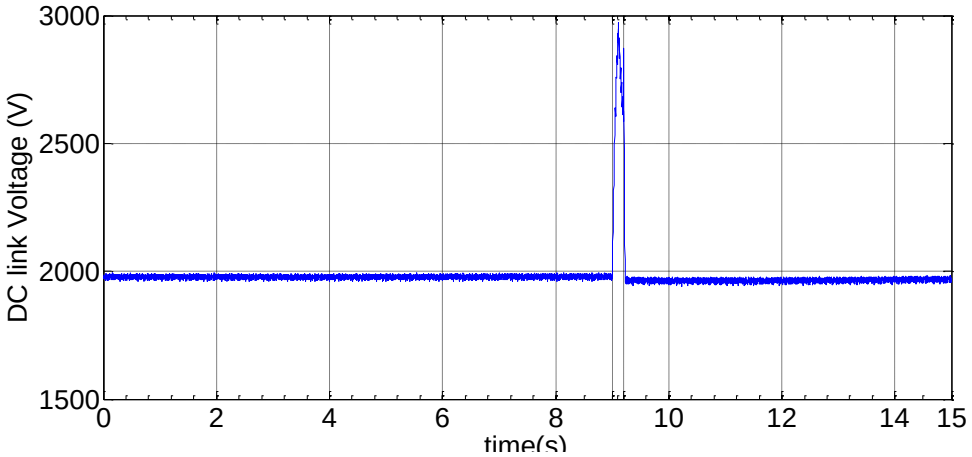

Fig.D.6 DC-link voltage by using Power Curtailment Control

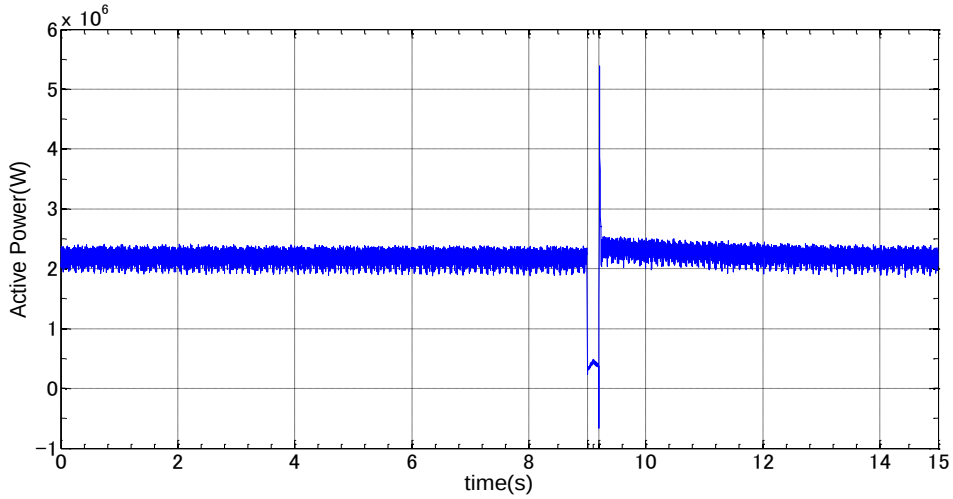

Fig.D.7 Active power output by using Power Curtailment Control

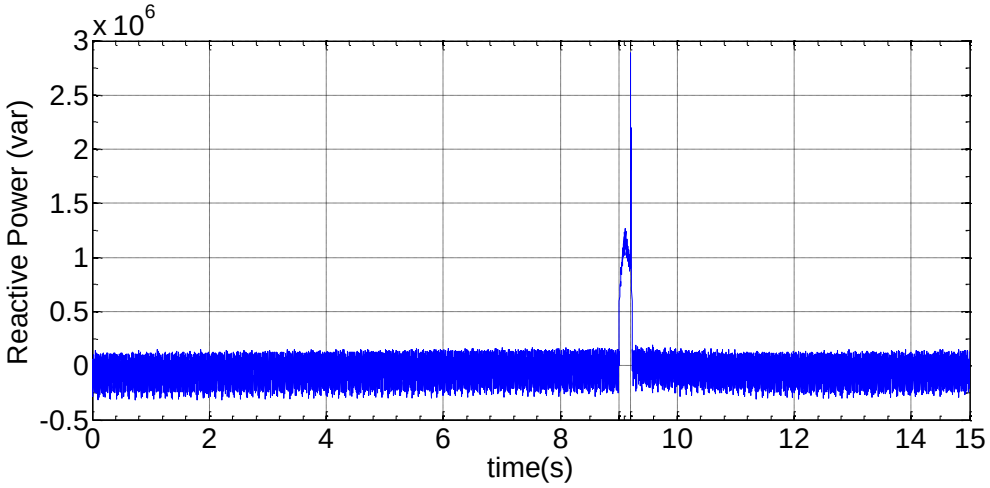

Fig.D.8 Reactive power output by using Power Curtailment Control

By comparing the Figure (D.3~8), the following points can be summarized.

1) The reactive power and active power control cannot be achieved by the control method in literature [32]. As the controller parameters are not shown in this literature, the more detailed studies are necessary to achieve reactive power output to be zero.
2) Better performance can be observed by using the power curtailment control in reducing the DC-link voltage rise and injecting the reactive power to power system during the fault.

D.2 Conclusions

The comparison of power curtailment control and control scheme in literature [32] is presented by using simulation study. Due to this study, the proposed power curtailment control is effective for reducing the DC-link voltage while injecting the reactive power to power systems for system voltage stability improvement.

List of Tables

List of Figures